AD-A034 129 CALIFORNIA UNIV SAN DIEGO LA JOLLA F/G 4/1
THE RELATION BETWEEN IONOSPHERIC PROFILES AND ELF PROPAGATION I--ETC(U)
NOV 76 H G BOOKER N00014-75-C-0959
UNCLASSIFIED NL

1 OF 2
ADA034129

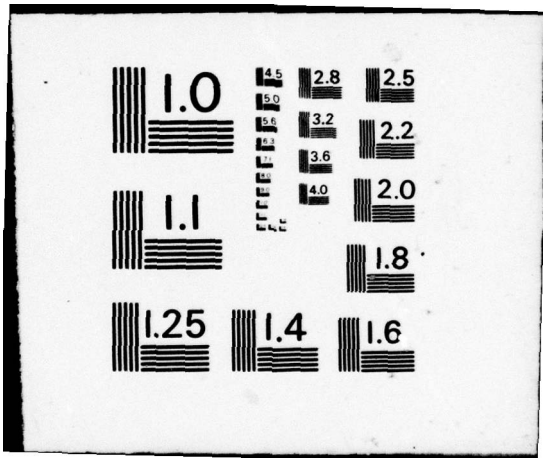
1.0
1.1
1.25
1.4
1.6
1.8
2.0
2.2
2.5
2.8
3.2
3.6
4.0
4.5
5.0
5.6

(12) FG.

Report N00014-75-C-0959-0001

The relation between ionospheric profiles and ELF propagation in the earth-ionosphere transmission line

Henry G. Booker
Professor of Applied Physics
University of California, San Diego
La Jolla, California 92093

30 November 1976

Final report for period 1 April 1975 - 30 November 1976

For public release; distribution unlimited

Prepared for
Office of Naval Research
800 North Quincy St.
Arlington, Virginia 22217

Unclassified

SECURITY CLASSIFICATION OF THIS PAGE (When Data Entered)

REPORT DOCUMENTATION PAGE

READ INSTRUCTIONS BEFORE COMPLETING FORM

1. REPORT NUMBER: N00014-75-C-0959-0001

2. GOVT ACCESSION NO.

3. RECIPIENT'S CATALOG NUMBER

4. TITLE (and Subtitle): THE RELATION BETWEEN IONOSPHERIC PROFILES AND ELF PROPAGATION IN THE EARTH-IONOSPHERE TRANSMISSION LINE

5. TYPE OF REPORT & PERIOD COVERED: Final Report, 1 April 1975 to 30 November 1976

6. PERFORMING ORG. REPORT NUMBER

7. AUTHOR(s): Henry G. Booker

8. CONTRACT OR GRANT NUMBER(s): N00014-75-C-0959

9. PERFORMING ORGANIZATION NAME AND ADDRESS: University of California, San Diego, La Jolla, California 92093

10. PROGRAM ELEMENT, PROJECT, TASK AREA & WORK UNIT NUMBERS

11. CONTROLLING OFFICE NAME AND ADDRESS: Director, Field Projects, Earth Sciences Division, ONR, 800 N. Quincy St., Arlington, VA 22217

12. REPORT DATE: 30 November 1976

13. NUMBER OF PAGES: 151

14. MONITORING AGENCY NAME & ADDRESS (if different from Controlling Office)

15. SECURITY CLASS. (of this report): Unclassified

15a. DECLASSIFICATION/DOWNGRADING SCHEDULE

16. DISTRIBUTION STATEMENT (of this Report)

For public release, distribution unlimited

17. DISTRIBUTION STATEMENT (of the abstract entered in Block 20, if different from Report)

18. SUPPLEMENTARY NOTES

19. KEY WORDS (Continue on reverse side if necessary and identify by block number)

ELF propagation
Earth-ionosphere wave-guide
Earth-ionosphere cavity
Shumann resonances
Ionospheric D region
Ionospheric E region

20. ABSTRACT (Continue on reverse side if necessary and identify by block number)

An approximate method, based on a wave-solution, is used to sketch the dependence of ELF propagation in the earth-ionosphere transmission line on time of day, latitude, season of the year, epoch in the sunspot cycle, and occurrence of sudden ionospheric disturbances and polar cap absorption events. As the frequency descends through the ELF band, penetration of the D region occurs in succession for the O and X waves, leading to next page

DD FORM 1 JAN 73 1473 EDITION OF 1 NOV 65 IS OBSOLETE S/N 0102-LF-014-6601

Unclassified

SECURITY CLASSIFICATION OF THIS PAGE (When Data Entered)

072380

cont.

reflexion from the E region at the Schumann resonant frequency. Under quiet day-time ionospheric conditions the penetration frequency-band is around 20-60 hz in middle and high latitudes, but around 75-150 hz near the equator. At a frequency low enough to be reflected primarily from the E region under quiet ionospheric conditions, an increase in D region ionization that is just sufficient to transfer primary reflexion from the E region to the D region results in an increase in the rate of attenuation. On the other hand, when once reflexion is firmly established at the lower level, further increase of ionization in the D region causes a reduction in the rate of attenuation. Similar effects are expected to occur at night in association with a sub-E region ledge of ionization. Small variations in the ionization profile of such a ledge are the likely cause of night-time fluctuations of transmission at 45 and 75 hz.

There is a need to improve the theory in order to handle properly situations involving more than one major reflecting stratum. There is also a need to check the method against other methods. The results of all methods should be so presented that the levels principally responsible for reflexion are located and the specific causes of the reflexion are identified.

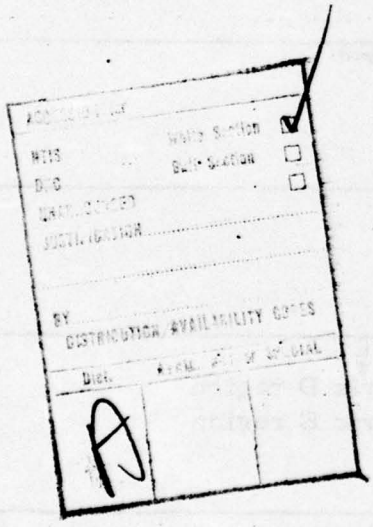

1. Introduction

The work summarized in this report is aimed at describing and applying, for the frequency range 7.5 to 300 hz, a relatively inexpensive approximate method for calculating propagation in the earth-ionosphere transmission line taking into account the profiles of electron density and of other ionospheric parameters. The method used is described in Appendix A, and application of the method is presented in Appendix B.

In the course of the work it was found necessary to devise a scheme whereby realistic ionospheric profiles could be represented by a single analytic function of height. This is important in order to have profiles free of mathematical singularities such as discontinuities of slope that cause spurious partial reflexions. It is also important in order to be able to change from one profile to the next merely by changing the numerical values of a few parameters in the computer program. The method of profile specification developed for this purpose is described in Appendix C. It is understood that URSI and COSPAR plan to make some use of this method in connection with the International Reference Ionosphere that these organizations are jointly preparing.

2. Theory

The theory described in Appendix A is based on a wave-solution, but nevertheless substantial approximations are involved. The basic wave-solution is the well-known one for an exponential increase of ionization density. At ELF, $1/(2\pi)$ times the wavelength λ_o in free space is large compared with the scale-height. Approximations on this basis are feasible, and they greatly simplify the handling of propagation at ELF. There is a reflecting stratum the thickness of which is about one scale-height h, defined in terms of the profile of the square of refractive index. The center of the reflecting stratum occurs where $1/(2\pi)$ times the local wavelength λ is equal to γ times the local scale-height h, where γ is a factor (between 2 and 3) for which a method of successive approximation is devised.

Above the reflecting stratum the medium can be assumed to be slowly varying, and here the direction of phase propagation can nearly always be assumed to be approximately vertical regardless of the directions of propagation of the incident and reflected waves below the ionosphere. Almost the same complex reflexion coefficient is obtained if the ionosphere below the center of the reflecting stratum is abolished and the ionosphere above the center of the reflecting stratum is treated as a slowly varying medium.

On this basis the mode-transmission problem in the earth-ionosphere transmission line is solved taking into account the effect of the earth's magnetic field. A mode consists, not of two crossing plane waves, but of four. There are a pair of upgoing waves and a pair of downcoming waves, the members of each pair having the elliptic polarizations corresponding to ordinary and extraordinary waves propagating vertically in the ionosphere. In terms of the refractive indices and polarization ratios at the levels of reflexion of the ordinary and extraordinary waves, expressions are obtained for the phase-velocity and attenuation rate in the earth-ionosphere transmission line due to leakage of energy into the region above the level of reflexion.

There is also attenuation in the earth-ionosphere transmission line due to collisional absorption below the level of reflexion. A method for estimating this contribution to the attenuation rate is devised similar to that used for dielectric loss in an engineering transmission line.

3. Calculations

The theory described in Appendix A has been applied numerically to explore propagation in the earth-ionosphere transmission line in the frequency band 7.5 to 300 hz under a wide range of circumstances. This covers dependence on time of day, latitude, season of the year, epoch in the sunspot cycle and occurrence of sudden ionospheric disturbances and polar cap absorption events. The most intense ionospheric

disburbance considered is probably comparable with the situation that would be likely to ensue after a high altitude nuclear explosion.

During the past decade, major progress has been made in the extent to which the day-time profile of ionospheric electron density below 100 km is understood. This has arisen largely through the application of *in situ* rocket techniques, and is in process of culminating in the day-time profiles currently being proposed for the URSI-COSPAR International Reference Ionosphere. These profiles differ substantially from those used in previous studies of day-time ELF propagation in the earth-ionosphere transmission line, and they lead in Appendix B to substantially different results.

While the day-time profile of electron density below 100 km has been the subject of intensive studies during the past decade, the same is not true for the night-time profile. The profiles of electron density for the night-time ionosphere being proposed for the URSI-COSPAR International Reference Ionosphere are based on a Russian compilation of data. However, it is shown in Appendix B that these night-time profiles lead to the unacceptable conclusion that the Schumann resonance in the earth-ionosphere cavity would not be observable. A modified night-time profile of electron density more acceptable for describing ELF phenomena is therefore devised. This involves an E region with a rather sharp under boundary at about 90 km, and with a sub-E region ledge of ionization below 90 km. Small variations in the profile of this ledge are the likely cause of the night-time fluctuations of transmission that have been observed at frequencies of 45 and 75 hz.

Over the entire radio spectrum, the frequency where the height of reflexion from the ionosphere has its lowest value occurs in the VLF band. As the frequency is shifted either upwards or downwards from the VLF band, a radio wave penetrates further into the ionosphere, and it ultimately pierces the ionosphere at VHF on the high frequency side and at micropulsation frequencies on the low frequency side. In

consequence, as the frequency descends through the ELF band during the day-time, penetration of the D region occurs, leading to reflexion from the E region at the Schumann resonant frequency.

Transfer of the primary reflecting stratum from the D region to the E region is not sudden. Reflexion from the D region weakens as reflexion from the E region strengthens. The ordinary and extra-ordinary waves each possess a band of frequencies over which reflecting strata in both the D and E regions are simultaneously important, and this band is at somewhat higher frequencies for the ordinary wave than for the extraordinary wave.

The calculations in Appendix B indicate that, under quiet ionospheric conditions, the penetration frequency-band for the day-time D region is around 20-60 hz in middle and high latitudes, but around 75-150 hz near the equator. Under quiet night-time conditions, the penetration frequency-band for the sub-E region ledge of ionization is about the same, if the ionization density in the ledge is taken to be about the same as for the day-time D region. The night-time calculations in Appendix B suggest, however, that the ionization density in the ledge should probably be somewhat less, and this would shift the penetration wave-band for the ledge to somewhat higher frequencies.

Penetration of the D region (day-time), or of the sub-E region ledge (night-time), as the frequency descends through the ELF band causes a rise in the velocity of phase propagation in the earth-ionosphere transmission line, and a drop in the attenuation rate. Moreover, this occurs in two stages because penetration of the ordinary and extra-ordinary waves occurs in succession.

For a given frequency in the band 7.5 to 300 hz, attenuation rates at low latitudes are less than they are at high latitides, especially during the day-time. It follows that, for the same transmitter arrangements (including the same site geology), the latitude at which an ELF communications transmitter is located has an important bearing on the degree of world-wide coverage that it achieves.

During the day-time, the attenuation rates are higher in winter than they are at the equinoxes, and higher at the equinoxes than they are in summer. Attenuation rates are lower during an epoch of high sunspot number than they are when the sunspot number is low, except near the equator. At a frequency such as 75 hz the effect of sunspot number is reversed at the equator because penetration of the D region occurs as one approaches the equator during an epoch of low sunspot number, whereas this does not occur when the sunspot number is high.

At a frequency low enough to be reflected from the E region under quiet day-time ionospheric conditions, an increase in D region ionization that is just sufficient to transfer primary reflexion from the E region to the D region results in an increase in the rate of attenuation in the earth-ionospheric transmission line. On the other hand, when once reflexion is firmly established at the lower level, a further increase of ionization in the D region causes a reduction in the rate of attenuation. A large increase in the ionization density at low levels in the ionosphere results in a low rate of attenuation.

At a frequency such as 75 hz, the effect of an enhancement in the ionization density of the day-time D region by a factor of ten reduces the attenuation rate in the earth-ionosphere transmission line in middle and high latitudes, but increases it at the equator. This is because, as one approaches the equator, penetration of the D region occurs under quiet ionospheric conditions but not under disturbed conditions.

4. Further work needed

The calculations in Appendix B have revealed the fact that, as the frequency descends from 300 hz to 7.5 hz, penetration of the D region occurs by day, and of a sub-E region ledge by night. This behavior constitutes a major factor in understanding day-time propagation in the earth-ionosphere transmission line in the frequency range 20-60 hz in middle and high latitudes. The corresponding penetration frequency-range

is somewhat higher near the equator, and in all probability it is also somewhat higher at night.

The D region penetration phenomenon was not anticipated when the theory described in Appendix A was developed. Consequently, it is now necessary to extend the theory to deal with a situation in which simultaneous reflexion from strata in the D and E regions is important. Development of such an extended theory will be required before detailed agreement between theory and observation can be expected at frequencies such as 45 and 75 hz. On the other hand, when such a theory is available in convenient form, and when the profiles for the International Reference Ionosphere are sufficiently comprehensive and reliable, there seems to be no reason why useful propagation curves for ELF communications should not be prepared covering most ionospheric conditions.

It will also be desirable to compare the extended version of the theory in Appendix A with theories based on dividing the ionosphere up into a large number of thin horizontal homogeneous non-isotropic steps. The latter theories constitute relatively expensive methods of calculation if applied over a wide range of ionospheric conditions, but they are quite reasonable for checking a number of selected cases.

Methods that involve, directly or indirectly, dividing up the ionosphere into steps are often described as giving the "exact" or "full" wave solution to the problem. This is true provided that the size of each step is allowed to tend to zero, and the number of steps is allowed to tend to infinity. In practice, however, a finite number of steps with non-zero sizes have to be used. Moreover, to keep the cost of calculation down, the number of steps is sometimes reduced undesirably. In this way it can happen that an "exact" numerical solution is less accurate than a frankly approximate analytical solution. Experience shows that, when an "exact" numerical solution disagrees unexpectedly with a reasonable analytical approximation for which the details can be fully understood, it is a good idea to suspect the "exact" solution.

In approximating a continuous ionospheric profile by means of a staircase profile, the sizes of the steps must be arranged so that the step in the natural logarithm of the magnitude of the refractive index is everywhere quite small. This means that a large number of steps must be used at levels where the gradient of the ionization density is high -- for example, at the under edge of the day-time E region just above 80 km. But it also means that a large number of steps must be used near the bottom of the ionosphere where the refractive index has not departed radically from unity. It must not be argued that little reflexion can be expected near the bottom of the ionosphere and that consequently there is no need to model the ionosphere carefully at this level. On the contrary a substantial part of the cost of the calculation has to be devoted to low levels in order to avoid creating reflexion that does not exist. Unless these precautions are taken, it may actually be better to replace the "exact" calculation by an approximation of the type presented in Appendix A.

There is a need to improve the approximate theory described in Appendix A in order to handle situations involving more than one major reflecting stratum. There is also a need to check the method against other methods and, in so doing, to take adequate cognizance of precautions such as those described in the previous paragraph. The results for all methods should be so presented that the levels principally responsible for reflexion are located and the specific causes of the reflexion are identified.

Appendix A

Theory

30 November 1976

The relation between ionospheric profiles and ELF propagation in the earth-ionosphere transmission line (1) theory

by

Henry G. Booker*

University of California, San Diego

La Jolla, California 92093

and

F. Lefeuvre

Centre de Recherches en Physique de L'Environnement

Avenue de la Recherche Scientifique, Orléans, France

Abstract

It is shown approximately that, for reflexion of ELF waves from a given ionosphere described by a simple profile of ionization density, the phase-integral method may be used above a certain level, and the ionosphere may be abolished below this level. The height of ELF reflexion thus determined is independent of angle of incidence, but not of frequency. The height of reflexion increases as the frequency decreases in the ELF

---

*This author was supported partly by the UCSD Department of Applied Physics and Information Science and the Groupe de Recherches Ionosphériques during sabbatical leave in 1972, and partly through the UCSD Institute for Pure and Applied Physical Sciences, using funds provided through the Advanced Research Projects Agency and monitored by the U. S. Army Research Office under Contract No. DAHC04-72-C-0037. The work was completed in 1976 using funds provided by the Office of Naval Research under Contract No. N00014-75-C-0959.

band until penetration of the ionosphere occurs at micropulsation frequencies.

An approximate solution is obtained to the mode problem in the earth-ionosphere transmission-line in terms of four crossing plane waves, one pair having O wave polarization and the other X wave polarization. If, for the O and X waves, respectively, the heights of reflexion are z_O and z_X and the scale heights of the ionospheric profile at these heights are h_O and h_X, then for a simple ionosphere the phase velocity is decreased below c by the fraction $0.50\, h_O/z_O$ and the attention rate at frequency f hertz due to leakage into the ionosphere above the level of reflexion is $0.117\, f\, h_X/z_X$ decibels per megameter approximately. A method for calculating the attenuation rate due to collisional absorption below the level of reflexion is also devised similar to that used for dielectric loss in an engineering transmission line.

1. Introduction

Propagation of the transmission-line mode in the wave-guide between the conducting earth and the conducting ionosphere was first studied by Watson (1919), and the theory has since been developed, particularly for application in the ELF band. It is summarized in books by Budden (1961b), Wait (1962) and Galejs (1972), and also in a special issue of the IEEE Transactions on Communications edited by Wait (1974). The earth, the atmosphere and the ionosphere are often regarded as three media that are homogeneous and isotropic. More elaborate versions of the theory take the ionosphere to involve two or more homogeneous isotropic layers (Wait, 1958;

Chapman and Jones, 1964; Jones, 1967). Theories involving a more-or-less continuously stratified ionosphere, isotropic or non-isotropic, have been developed mainly for VLF and higher frequencies, but they have also been used at ELF (Cole, 1965; Madden and Thompson, 1965; Hughes and Theisen, 1970; Barr, 1972; Pappert and Moler, 1974).

Even if it is agreed that a homogeneous ionosphere with a discontinuous under boundary is an adequate model at ELF, we need to know at what height to place the discontinuity and what parameters to assign to the ionosphere above this height. Furthermore, from experience at higher frequencies, one would expect the height of reflexion and the other relevant parameters to depend on angle of incidence and frequency. Konrad and Poverlein (1958) have conjectured that the level of reflexion should be higher at ELF than at VLF. Nevertheless, it is frequently assumed that the same ionospheric discontinuity is satisfactory for all angles of incidence and all frequencies in the ELF band. If so, then it should be possible to give theoretical reasons for this result. At the Schumann resonance frequencies, this matter has been considered by Large and Wait (1968).

It is the objective of this paper to start with a simple but reasonably realistic profile of ionization density, and to derive a method, suitable for use at ELF, for ascertaining at what level the ionosphere may best be cut off at the bottom and be replaced by a discontinuity. We shall also ascertain the dependence of this discontinuity-level on angle of incidence and frequency, and go on to assess the rate of attenuation in the earth-ionosphere transmission line due to leakage of energy into the ionosphere above the level of reflexion.

We shall do this taking into account the effect of the earth's magnetic field, but neglecting coupling between the ordinary and extraordinary waves (the O and X waves). It will be necessary to solve the mode transmission problem in the earth-ionosphere transmission line taking the ionospheric conductor as a non-isotropic medium. It should be noted that, in such circumstances, a mode involves, not two crossing plane waves, but four. There are a pair of upgoing waves and a pair of downgoing waves, the members of each pair having the elliptic polarization corresponding to the O and X waves in the ionosphere. We shall assess the attenuation rate in the earth-ionosphere transmission line not only due to leakage of energy into the region above the level of reflexion but also due to collisional absorption below the level of reflexion.

2. The Level of Reflexion in the Ionosphere at ELF

We shall base our discussion of the level of reflexion in the ionosphere at ELF on an ionospheric model for which the index of refraction n varies with height z according to the formula

$$n^2 = 1 - (b\exp j\psi)\exp\{(z-a)/h\} \qquad (1)$$

where b and ψ are real constants, h is a scale height, and a is a reference height. Such a profile of refractive index is not ideal, but gives a reasonable representation of the underside of the ionosphere in circumstances when the increase of ionization density with height is roughly exponential. The profile does not represent properly the variation of collisional frequency with height, as a result of which there is a tendency to

underestimate absorption just below the level of reflexion and overestimate it just above this level.

For a plane wave incident upon a plane stratified ionosphere with the profile (1) there is an exact wave solution for horizontal polarization. We shall assume that this solution gives a reasonable clue to determination of the level of reflexion in a practical ionosphere for the O and X waves. The solution is given by Budden (1961a, pp. 354-357) and by Wait (1962, pp. 72-74). It involves a Bessel function of an argument that is small at the bottom of the ionosphere and large well inside the ionosphere, with reflection occurring in the transition region between the two. For an angle of incidence θ ($S = \sin\theta$, $C = \cos\theta$), possibly complex, the change in complex phase between the incident wave (measured at the reference height a and the reflected wave (also measured at $z = a$) is

$$\Phi = \pi - \frac{4\pi hC}{\lambda_o} \ln \left\{ (\text{bexpj}\psi) \left(\frac{2\pi h}{\lambda_o}\right)^2 \right\} - 2 \arg \Gamma \left(1 - j \frac{4\pi hC}{\lambda_o}\right) \qquad (2)$$

where λ_o is the wavelength in free space. When $2\pi h/\lambda_o$ is large, Equation (2) corresponds to the phase-integral (or WKB) approximation (Budden, 1961a). On the other hand, at ELF $2\pi h/\lambda_o$ is small, and we may then write approximately

$$\Gamma \left(1 - j \frac{4\pi hC}{\lambda_o}\right) = \Gamma(1) - j\Gamma'(1) \frac{4\pi hC}{\lambda_o} \qquad (3)$$

so that

$$2 \arg \Gamma \left(1 - j \frac{4\pi hC}{\lambda_o}\right) = -2 \frac{\Gamma'(1)}{\Gamma(1)} \frac{4\pi hC}{\lambda_o} \tag{4}$$

Let us define

$$\delta = -2 \frac{\Gamma'(1)}{\Gamma(1)} = 1.1544 \quad . \tag{5}$$

Then Equation (2) may be written at ELF

$$\Phi = \pi + \frac{4\pi hC}{\lambda_o} \left[\ln \left\{ \frac{1}{b \exp j\Psi} \left(\frac{\lambda_o}{2\pi h}\right)^2 \right\} - \delta \right]$$

or

$$\Phi = \pi + \frac{4\pi hC}{\lambda_o} \left[\ln \left\{ \frac{1}{b} \left(\frac{\lambda_o}{2\pi h}\right)^2 \right\} - (\delta + j\Psi) \right] \tag{6}$$

For the ionospheric profile in Equation (1) the phase-integral approximation always applies at sufficiently large heights. A sufficiently large height is one for which the argument of the Bessel wave-function is appreciably greater than unity. Any height above the zone of transition from small argument to large argument satisfies this condition, and this zone is the reflecting stratum. Consequently we may simply say that the phase-integral approximation applies above the reflecting stratum.

Let us compare the result in Equation (6) with that for an ionosphere in which (i) the same refractive index profile is maintained above a certain level z_1, (ii) the phase integral approximation is applied for $z > z_1$, and (iii) the refractive index is taken as unity for $z < z_1$. Let us see whether it is possible to adjust the level z_1 of the resulting discontinuity in

refractive index so that, well below the level z_1, the phase-change Φ between an incident wave (measured at the reference height a) and the reflected wave (measured also at $z = a$) is nearly the same as the right hand side of Equation (6).

Just above the level z_1 the square of the refractive index is

$$n_1^2 = 1 - (b\exp j\psi) \exp\{(z_1 - a)/h\} \tag{7}$$

and if we assume that this level is sufficiently far into the ionosphere to make $|n| >> 1$, we may write approximately

$$n_1^2 = -(b\exp j\psi) \exp\{(z_1 - a)/h\} \tag{8}$$

For an angle of incidence whose cosine is C, the Fresnel reflection coefficient at the discontinuity at level z_1 is

$$\rho = \frac{C - (C^2 - n_1^2)^{1/2}}{C + (C^2 - n_1^2)^{1/2}} \quad . \tag{9}$$

Assuming that $|n_1| >> C$, this becomes

$$\rho = -\left(1 - \frac{2C}{n_1}\right) \tag{10}$$

which is equivalent to a complex phase-change on reflection of

$$j \ln \rho = \pi - j\frac{2C}{n_1} \tag{11}$$

and does not differ much from π. This is the phase-change referred to z_1 as reference height. If a is used as the reference height, the complex phase-change between the incident and reflected waves is

$$\Phi' = \pi + \frac{4\pi C}{\lambda_o}(z_1 - a) - j\frac{2C}{n_1} \quad . \tag{12}$$

To put this result in approximately the same form as Equation (6), we note that Equation (8) may be rewritten

$$z_1 - a = h \ln\left(-\frac{n_1^2}{b\exp j\psi}\right) \tag{13}$$

so that Equation (12) becomes

$$\Phi' = \pi + \frac{4\pi hC}{\lambda_o} \ln\left(-\frac{n_1^2}{b\exp j\psi}\right) - j\frac{2C}{n_1}$$

or, again using Equation (8),

$$\Phi' = \pi + \frac{4\pi hC}{\lambda_o} \ln\frac{|n_1|^2}{b} + \frac{2C}{|n_1|}\left(\cos\frac{\psi}{2} - j\sin\frac{\psi}{2}\right) \tag{14}$$

We are now in a position to deduce from Equations (6) and (14) whether it is possible to choose z_1 (i.e. n_1) so as to make the complex phase-change Φ' for the discontinuity profile approximately the same as that for the original exponential profile. We see that it is not possible to do so precisely because of the terms following the logarithms in Equations (6) and (14). On the other hand we also see that these terms are small compared with the logarithmic terms when $\lambda_o/(2\pi h)$ and $|n_1|$ are large, that is, at ELF. To make the dominant logarithmic terms

equal we require that

$$|n_1| = \frac{\lambda_o}{2\pi h} \tag{15}$$

This means that the reflecting stratum in the ELF band occurs close to where the local reduced wavelength $\lambda_o/(2\pi|n_1|)$ is equal to the scale height h of the profile. Appreciably below the level corresponding to Equation (15) the local wavelength is large compared with the structure-scale of the ionization profile which is therefore largely ignored by the waves. Appreciably above the level corresponding to Equation (15) the local wavelength is small compared with the structure-scale of the ionization profile and the phase-integral approximation is applicable. It is in the neighborhood of the level given by Equation (15) that the bulk of the reflexion takes place.

Let us now examine the small terms following the logarithms in Equations (6) and (14). While it is not in general possible to adjust the level z_1 so as to make these terms exactly equal, it is possible to adjust the level in such a way as to minimize the difference between Φ and Φ'. From Equations (6) and (14) we deduce that

$$\Phi - \Phi' = \left(\frac{4\pi hC}{\lambda_o}\right)\left[\left\{2\ln\left(\frac{1}{|n_1|}\,\frac{\lambda_o}{2\pi h}\right) - \delta - \frac{1}{|n_1|}\,\frac{\lambda_o}{2\pi h}\cos\frac{\psi}{2}\right\} - j\left\{\psi - \frac{1}{|n_1|}\,\frac{\lambda_o}{2\pi h}\sin\frac{\psi}{2}\right\}\right] \tag{16}$$

Hence

$$|\Phi - \Phi'|^2 = \left(\frac{4\pi hC}{\lambda_o}\right)^2 \left\{\left(2 \ln \gamma - \delta - \gamma \cos \frac{\psi}{2}\right)^2 + \left(\psi - \gamma \sin \frac{\psi}{2}\right)^2\right\} \qquad (17)$$

where

$$|n_1| = \frac{1}{\gamma} \frac{\lambda_o}{2\pi h} \qquad (18)$$

For a value of γ differing somewhat from unity, Equation (18) determines a height a little different from that given by Equation (15). We select γ so as to minimize the expression for $|\Phi - \Phi'|^2$ given in Equation (17). This value of γ turns out to be independent of frequency, of scale height and of angle of incidence, but to be dependent on the phase-angle ψ of the refractive index profile in Equation (1). The value of γ varies between the extreme values 2.00 and 2.65 as shown in Figure 1, and even less in practice. With the value of γ chosen in this way, the error in $|\Phi - \Phi'|$ has magnitude

$$\frac{4\pi hC}{\lambda_o} \beta \qquad (19)$$

where β is as shown in Figure 1. This expression has to be compared with the logarithmic term in Equations (6) or (14), and therefore with the term

$$\frac{4\pi C}{\lambda_o} (z_1 - a) \qquad (20)$$

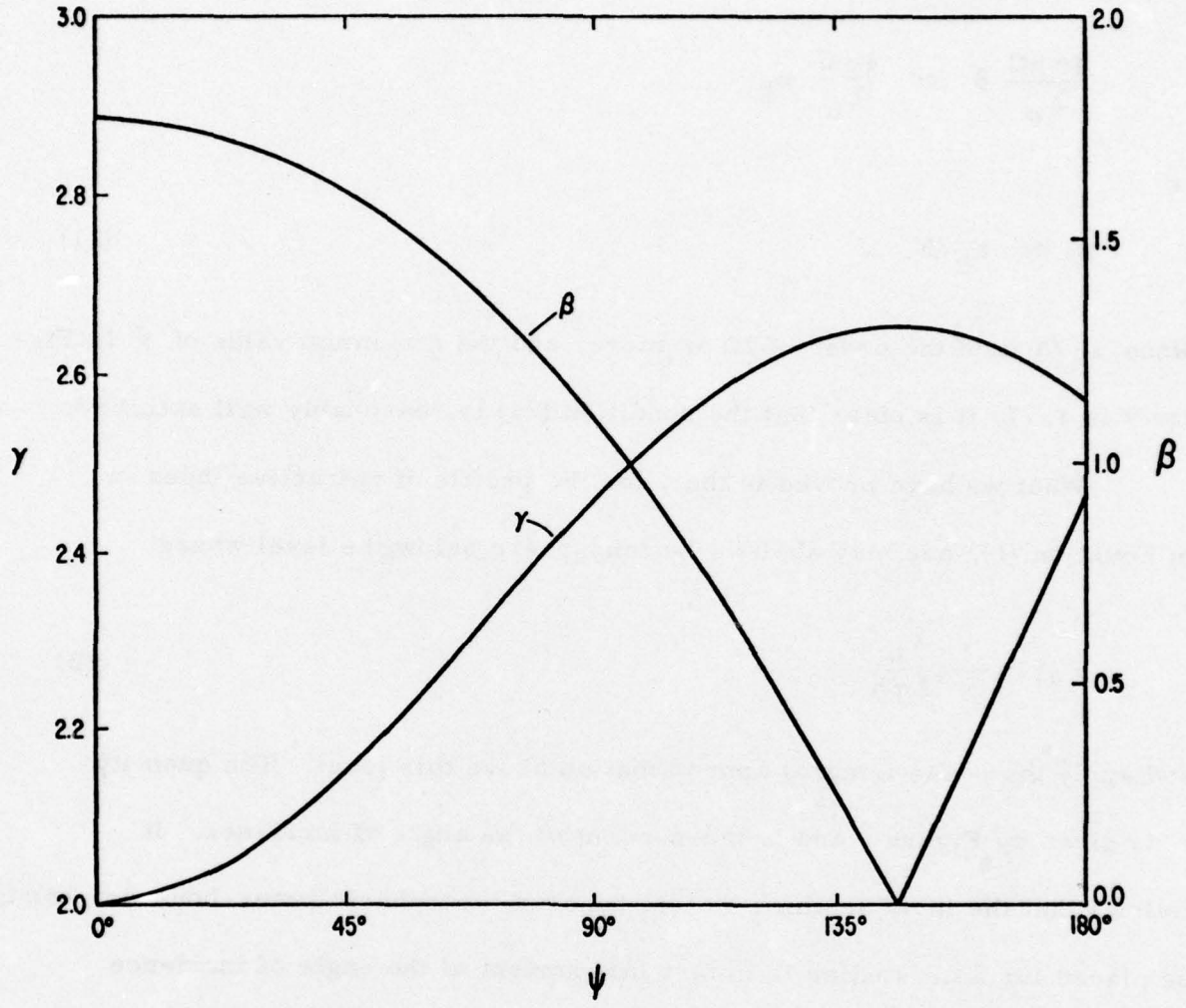

Figure 1. Illustrating (i) the value of γ required to minimize error in the complex phase-change on reflexion, and (ii) the value of β to be used in expression (19) for estimating the resulting error.

in Equation (12). The condition that Φ may be replaced by Φ' in a mode calculation involving ionospheric reflexion at a height z_R above the surface of the earth is therefore

$$\frac{4\pi hC}{\lambda_o}\beta \ll \frac{4\pi C}{\lambda_o} z_R$$

or

$$\beta \ll z_R/h \quad . \tag{21}$$

Since z_R/h is of the order of 20 or more, and the maximum value of β in Figure 1 is 1.77, it is clear that the condition (21) is reasonably well satisfied.

What we have proved is that, for the profile of refractive index n in Equation (1), one may abolish the ionosphere below the level where

$$|n| = \frac{1}{\gamma} \frac{\lambda_o}{2\pi h} \tag{22}$$

and apply the phase integral approximation above this level. The quantity γ is given by Figure 1 and is independent of the angle of incidence. It follows that the level at which a discontinuous ionospheric lower-boundary should be placed for ELF studies is in fact independent of the angle of incidence (including complex angles of incidence). On the other hand, the discontinuity-level does depend on frequency: not only does λ_o appear explicitly in Equation (22), but the refractive index n is also frequency dependent. Hence it is not advisable to use the same discontinuity-level throughout the ELF band, although at each frequency it is satisfactory to use the same

discontinuity-level for all angles of incidence.

While the above deductions apply strictly to the refractive index profile in Equation (1), it is not difficult to devise a way to apply the results to more practical ionospheric profiles. For such a profile a scale height can be defined at each height for each frequency by means of the equation

$$h = \left| \frac{1}{n^2 - 1} \frac{d}{dz} (n^2 - 1) \right|^{-1} \tag{23}$$

and it is then simple to ascertain the height where this is equal to the local reduced wavelength $\lambda_o / |2\pi n|$. This height is roughly the ELF height of reflexion in accordance with Equation (15). At this height one can ascertain the value of the complex refractive index n_1 for the given profile and hence the quantity

$$\psi = \pi + 2 \arg n_1 \quad . \tag{24}$$

In accordance with Equation (8), this is approximately the value of ψ to be used in Figure 1 in order to deduce a value for γ. We can now ascertain the level where the scale height given by Equation (23) is equal to the corrected local reduced wavelength $\lambda_o / |2\pi \gamma n|$. In accordance with Equation (22) this height is a reasonable approximation to the ELF height of reflexion for the selected frequency and for any angle of incidence. Substitution from Equation (23) into Equation (22) shows that the ELF height of

reflexion, defined in this way, is given approximately by

$$\left| \frac{1}{n^3} \frac{dn^2}{dz} \right| = \frac{2\pi\gamma}{\lambda_o} \qquad (25)$$

In the presence of the earth's magnetic field, the above technique may be applied to the refractive index profiles for O and X waves, provided that one neglects coupling between these waves. The refractive indices at the levels given by Equation (25) always turn out to be large compared with unity. Hence the ELF waves transmitted into the ionosphere may be assumed to travel almost vertically upwards regardless of the direction of the incident and reflected waves below the ionosphere. This greatly simplifies the handling of the earth's magnetic field. The refractive indices to be used in Equation (25) for the O and X waves are simply those for vertical propagation in the ionosphere.

3. The Mode Theory at ELF

We derive the mode theory in the earth-ionosphere wave-guide at ELF on the assumption that curvature of the earth may be neglected, that the height of reflexion is given by Equation (22), that the phase-integral approximation may be applied above this level, and that the ionosphere may be abolished below this level. Reflexion at the resulting discontinuity is then determined by the refractive index immediately above the discontinuity.

We derive separate heights of reflexion z_O and z_X for the O and X waves from Equation (22) using the refractive indices for the O and X waves for vertical propagation. Just above the associated discontinuities,

let n_O and n_X be the refractive indices for the O and X waves, so that the impedances looking vertically upwards at the location of the discontinuities are ζ_o / n_O and ζ_o / n_X, where ζ_o is the impedance of free space (377 ohms). If we take axes as shown in Figure 2, with z vertically upwards and the yz plane as the vertical plane of propagation of the mode, then we have, in terms of the components of the complex electromagnetic fields E^O, H^O for the O wave and E^X, H^X for the X wave at their respective levels of reflexion,

$$-\frac{E_y^O}{H_x^O} = \frac{E_x^O}{H_y^O} = \frac{1}{n_O}\zeta_o , \quad z = z_O \tag{26}$$

$$-\frac{E_y^X}{H_x^X} = \frac{E_x^X}{H_y^X} = \frac{1}{n_X}\zeta_o , \quad z = z_X \tag{27}$$

Also, if Q_O and Q_X are the polarization ratios for the O and X waves at their respective levels of reflexion, we have

$$-\frac{E_x^O}{E_y^O} = \frac{H_y^O}{H_x^O} = Q_O , \quad z = z_O \tag{28}$$

$$-\frac{E_x^X}{E_y^X} = \frac{H_y^X}{H_x^X} = Q_X , \quad z = z_X \tag{29}$$

A mode in the earth-ionosphere wave-guide consists of a pair of crossing plane waves at an angle θ to the vertical ($S = \sin\theta$, $C = \cos\theta$) having an elliptic polarization whose horizontal projection corresponds to

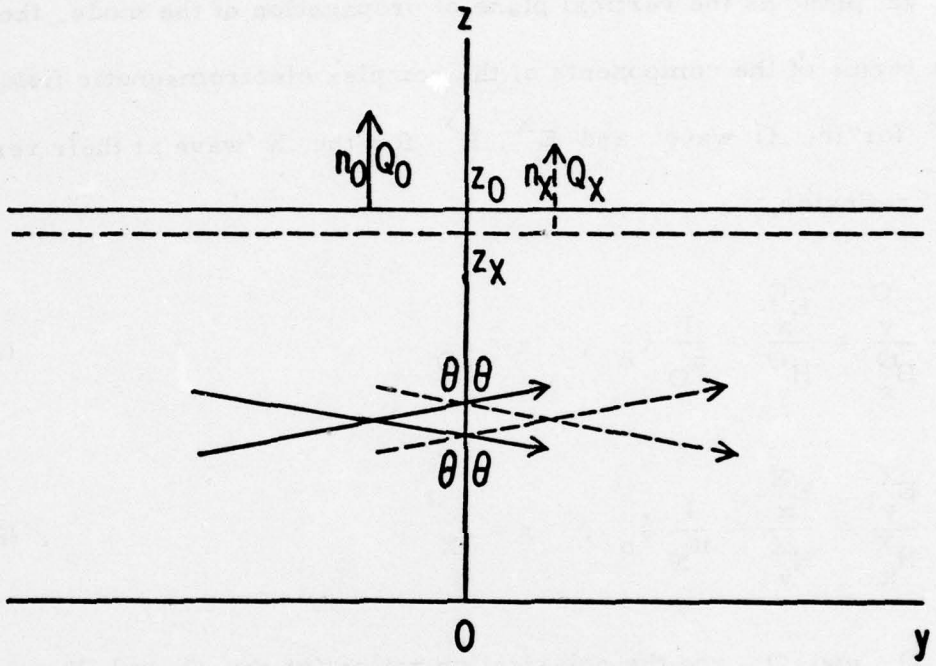

Figure 2. Illustrating the four crossing plane waves involved in a mode in the earth-ionosphere wave-guide.

Equation (28) combined with a pair of crossing plane waves at the same angle θ having an elliptic polarization whose horizontal projection corresponds to Equation (29). From the vertical standing-wave pattern formed by these waves we may write down, by standard matrix methods for one-dimensional transmission systems (see, for example, Booker, 1948), the complex electromagnetic field $(\underset{\sim}{E}, \underset{\sim}{H})$ at the ground in terms of the electromagnetic fields at the levels of reflexion. We obtain:

$$E_y = \cos \frac{2\pi z_o C}{\lambda_o} E_y^o - j \zeta_o C \sin \frac{2\pi z_o C}{\lambda_o} H_x^o$$

$$+ \cos \frac{2\pi z_x C}{\lambda_o} E_y^x - j \zeta_o C \sin \frac{2\pi z_x C}{\lambda_o} H_x^x \qquad (30)$$

$$H_x = -j \frac{1}{\zeta_o C} \sin \frac{2\pi z_o C}{\lambda_o} E_y^o + \cos \frac{2\pi z_o C}{\lambda_o} H_x^o$$

$$-j \frac{1}{\zeta_o C} \sin \frac{2\pi z_x C}{\lambda_o} E_y^x + \cos \frac{2\pi z_x C}{\lambda_o} H_x^x \qquad (31)$$

$$E_x = \cos \frac{2\pi z_o C}{\lambda_o} E_x^o + j \frac{\zeta_o}{C} \sin \frac{2\pi z_o C}{\lambda_o} H_y^o$$

$$+ \cos \frac{2\pi z_x C}{\lambda_o} E_x^x + j \frac{\zeta_o}{C} \sin \frac{2\pi z_x C}{\lambda_o} H_y^x \qquad (32)$$

$$H_y = j \frac{C}{\zeta_o} \sin \frac{2\pi z_O C}{\lambda_o} E_x^O + \cos \frac{2\pi z_O C}{\lambda_o} H_y^O$$

$$+ j \frac{C}{\zeta_o} \sin \frac{2\pi z_X C}{\lambda_o} E_x^X + \cos \frac{2\pi z_X C}{\lambda_o} H_y^X \qquad (33)$$

To satisfy the mode condition these values of E_x, E_y, H_x and H_y must obey the boundary conditions at the surface of the earth.

By employing the ratios (26), (27), (28) and (29) one can express all the electromagnetic field components on the right hand sides of Equations (30), (31), (32) and (33) in terms of H_x^O and H_x^X, which are the components of the magnetic field for the O and X waves at their levels of reflection, taken in the direction transverse to that of propagation in the earth-ionosphere wave-guide. We obtain:

$$E_y = - \left\{ \frac{1}{n_O} \cos \frac{2\pi z_O C}{\lambda_o} + jC \sin \frac{2\pi z_O C}{\lambda_o} \right\} \zeta_o H_x^O$$

$$- \left\{ \frac{1}{n_X} \cos \frac{2\pi z_X C}{\lambda_o} + jC \sin \frac{2\pi z_X C}{\lambda_o} \right\} \zeta_o H_x^X \qquad (34)$$

$$H_x = \left\{ j \frac{1}{n_O C} \sin \frac{2\pi z_O C}{\lambda_o} + \cos \frac{2\pi z_X C}{\lambda_o} \right\} H_x^O$$

$$+ \left\{ j \frac{1}{n_X C} \sin \frac{2\pi z_X C}{\lambda_o} + \cos \frac{2\pi z_X C}{\lambda_o} \right\} H_x^X \qquad (35)$$

$$E_x = \left\{ \frac{1}{n_O} \cos \frac{2\pi z_O C}{\lambda_o} + j \frac{1}{C} \sin \frac{2\pi z_O C}{\lambda_o} \right\} Q_O \zeta_o H_x^O$$

$$+ \left\{ \frac{1}{n_X} \cos \frac{2\pi z_X C}{\lambda_o} + j \frac{1}{C} \sin \frac{2\pi z_X C}{\lambda_o} \right\} Q_X \zeta_o H_x^X \qquad (36)$$

$$H_y = \left\{ j \frac{C}{n_O} \sin \frac{2\pi z_O C}{\lambda_o} + \cos \frac{2\pi z_O C}{\lambda_o} \right\} Q_O H_x^O$$

$$+ \left\{ j \frac{C}{n_X} \sin \frac{2\pi z_X C}{\lambda_o} + \cos \frac{2\pi z_X C}{\lambda_o} \right\} Q_X H_x^X \qquad (37)$$

We will now restrict ourselves to the transmission-line mode, for which the angles

$$\frac{2\pi z_O C}{\lambda_o} \quad \text{and} \quad \frac{2\pi z_X C}{\lambda_o}$$

are sufficiently small that their sines may be replaced by the angles and their cosines by unity. Equations (34) - (37) may then be written

$$E_y = -\left(\frac{1}{n_O} + j \frac{2\pi z_O}{\lambda_o} C^2 \right) \zeta_o H_x^O - \left(\frac{1}{n_X} + j \frac{2\pi z_X}{\lambda_o} C^2 \right) \zeta_o H_x^X \qquad (38)$$

$$H_x = \left(j \frac{1}{n_O} \frac{2\pi z_O}{\lambda_o} + 1 \right) H_x^O + \left(j \frac{1}{n_X} \frac{2\pi z_X}{\lambda_o} + 1 \right) H_x^X \qquad (39)$$

$$E_x = \left(\frac{1}{n_O} + j \frac{2\pi z_O}{\lambda_o} \right) Q_O \zeta_o H_x^O + \left(\frac{1}{n_X} + j \frac{2\pi z_X}{\lambda_o} \right) Q_X \zeta_o H_x^X \qquad (40)$$

$$H_y = \left(j \frac{1}{n_O} \frac{2\pi z_O}{\lambda_o} C^2 + 1 \right) Q_O H_x^O + \left(j \frac{1}{n_X} \frac{2\pi z_O}{\lambda_o} C^2 + 1 \right) Q_X H_x^X \qquad (41)$$

In these equations the quantities

$$\frac{1}{n_O}, \frac{1}{n_X}, \frac{2\pi z_O}{\lambda_o}, \frac{2\pi z_X}{\lambda_o} \text{ and } C^2 \tag{42}$$

are all small in practice. Care is therefore necessary in making further approximations in Equations (38) and (40). However, Equations (39) and (41) can safely be simplified to

$$H_x = H_x^O + H_x^X \tag{43}$$

$$H_y = Q_O H_x^O + Q_X H_x^X \tag{44}$$

These equations relate the two Cartesian components (H_x, H_y) of the horizontal magnetic field of the wave at the earth's surface to the quantities H_x^O and H_x^X that measure the strengths of the O and X waves at their respective levels of reflexion.

We now have to satisfy the boundary conditions at the earth's surface. There is, of course, some leakage of energy into the earth from the earth-ionosphere transmission line. We know how to calculate the corresponding contribution to attenuation in the transmission line (Wait 1962) and we know that it is additive to the ionospheric contribution. Since we are at present interested in calculating the ionospheric contribution, we can take the earth as a perfect conductor and write the boundary condition at the earth's surface as

$$E_x = E_y = 0, \quad z = 0 \tag{45}$$

It follows from Equations (38) and (40) that

$$\left(\frac{1}{n_O} + j\,\frac{2\pi z_O}{\lambda_o}\right)C^2\; H_x^O + \left(\frac{1}{n_X} + j\,\frac{2\pi z_X}{\lambda_o}C^2\right)H_x^X = 0 \tag{46}$$

$$\left(\frac{1}{n_O} + j\,\frac{2\pi z_O}{\lambda_o}\right)Q_O H_x^O + \left(\frac{1}{n_X} + j\,\frac{2\pi z_X}{\lambda_o}\right)Q_X H_x^X = 0 \tag{47}$$

Elimination of the ratio H_x^O/H_x^X between this pair of equations gives the equation for the value of C appropriate to the transmission-line mode:

$$\left(\frac{1}{n_O} + j\,\frac{2\pi z_O}{\lambda_o}C^2\right)\left(\frac{1}{n_X} + j\,\frac{2\pi z_X}{\lambda_o}\right)Q_X = \left(\frac{1}{n_O} + j\,\frac{2\pi z_O}{\lambda_o}\right)\left(\frac{1}{n_X} + j\,\frac{2\pi z_X}{\lambda_o}C^2\right)Q_O \tag{48}$$

The solution of this equation is

$$C^2 = j\,\frac{Q_O\left(\frac{2\pi z_O}{\lambda_o} - j\,\frac{1}{n_O}\right)\frac{1}{n_X} - Q_X\left(\frac{2\pi z_X}{\lambda_o} - j\,\frac{1}{n_X}\right)\frac{1}{n_O}}{Q_O\left(\frac{2\pi z_O}{\lambda_o} - j\,\frac{1}{n_O}\right)\frac{2\pi z_X}{\lambda_o} - Q_X\left(\frac{2\pi z_X}{\lambda_o} - j\,\frac{1}{n_X}\right)\frac{2\pi z_O}{\lambda_o}} \tag{49}$$

The complex propagation constant along the earth-ionosphere transmission line is then

$$\frac{2\pi S}{\lambda_o} \tag{50}$$

where

$$S = (1 - C^2)^{1/2} \tag{51}$$

and C^2 is given by Equation (49). The real part of S is the ratio of velocity of light to the velocity of phase propagation in the earth-ionosphere transmission line, while the imaginary part of expression (50) with the sign reversed is the rate of attenuation in nepers per unit distance.

If one is interested in the relative degree of excitation of the O and X waves, this is given by Equation (47) in the form

$$\frac{H_x^O}{H_x^X} = -\frac{Q_X}{Q_O}\,\frac{\frac{2\pi z_X}{\lambda_o} - j\frac{1}{n_X}}{\frac{2\pi z_O}{\lambda_o} - j\frac{1}{n_O}} \tag{52}$$

If one is interested in the slight degree of horizontal elliptic polarization existing at ground level, one divides Equation (44) by Equation (43) and uses Equation (52) to obtain

$$\frac{H_y}{H_x} = \frac{\left(\frac{2\pi z_O}{\lambda_o} - j\frac{1}{n_O}\right) - \left(\frac{2\pi z_X}{\lambda_o} - j\frac{1}{n_X}\right)}{\frac{1}{Q_X}\left(\frac{2\pi z_O}{\lambda_o} - j\frac{1}{n_O}\right) - \frac{1}{Q_O}\left(\frac{2\pi z_X}{\lambda_o} - j\frac{1}{n_X}\right)} \tag{53}$$

4. Useful Analytical Approximations

While for numerical purposes there is no problem about making mode calculations using Equations (49) - (53), it should be noted that, for analytical purposes, some further approximations can usefully be made. Although all the quantities (42) are small, they are not of the same order of smallness. In practice we have

$$\frac{1}{n_O} << \frac{2\pi z_O}{\lambda_o}, \quad \frac{1}{n_X} << \frac{2\pi z_X}{\lambda_o} \tag{54}$$

but we also have

$$\frac{1}{n_O} \not< \frac{2\pi z_O}{\lambda_o} C^2, \quad \frac{1}{n_X} \not< \frac{2\pi z_X}{\lambda_o} C^2 \tag{55}$$

In consequence the brackets in Equation (40) simplify, whereas those in Equation (38) do not, and a corresponding statement applies for Equations (46) and (47). Hence Equation (49) simplifies to

$$C^2 = j \frac{\lambda_o}{2\pi} \frac{\frac{1}{z_O n_O Q_O} - \frac{1}{z_X n_X Q_X}}{\frac{1}{Q_O} - \frac{1}{Q_X}} \tag{56}$$

Moreover Equation (51) may usually be written approximately as

$$S = 1 - \frac{1}{2} C^2 \tag{57}$$

with the result that the value of S to be used in the propagation constant (50) is given by

$$S = 1 - j \frac{\lambda_o}{4\pi} \frac{\frac{1}{z_O n_O Q_O} - \frac{1}{z_X n_X Q_X}}{\frac{1}{Q_O} - \frac{1}{Q_X}} \tag{58}$$

Likewise Equation (52) for the relative excitation of the O and X waves becomes

$$\frac{H_x^O}{H_x^X} = - \frac{Q_X}{Q_O} \frac{z_X}{z_O} \tag{59}$$

while Equation (52) for the horizontal elliptic polarization at ground level becomes

$$\frac{H_y}{H_x} = \frac{z_O - z_X}{\frac{z_O}{Q_X} - \frac{z_X}{Q_O}} \tag{60}$$

The slight ellipticity in the horizontal field at ground level depends primarily on the small difference in the heights of reflexion for the O and X waves.

5. Cold Magneto-plasma Relations

To apply the methods developed above, it is necessary to use expressions for the complex refractive indices and polarization ratios of the O and X waves. At ELF, it is desirable to take into account ions, positive and negative, atomic and molecular. Five species of charge carriers are therefore involved: electrons (e), positive atomic ions (a+), negative atomic ions (a-), positive molecular ions (m+), and negative molecular ions (m-). For each of these species we can define angular magnetic gyro frequencies $-\omega_{Me}$, $+\omega_{Ma+}$, $-\omega_{Ma-}$, $+\omega_{Mm+}$ and $-\omega_{Mm-}$; notice that the definitions of ω_{Me}, ω_{Ma-} and ω_{Mm-} are such that they are numerically negative. For each of the species we can define angular plasma frequencies ω_{Ne}, ω_{Na+}, ω_{Na-}, ω_{Nm+} and ω_{Nm-}. Moreover we may employ a collisional frequency ν_e for the electrons and a collision frequency ν_i for the ions. In terms of these quantities we may define, for an angular wave frequency ω, complex angular gyro and plasma frequencies as follows (Booker, 1975):

$$\Omega_{Me} = \frac{\omega_{Me}}{1 - j\frac{\nu_e}{\omega}} \qquad \Omega_{Ne}^2 = \frac{\omega_{Ne}^2}{1 - j\frac{\nu_e}{\omega}}$$

$$\Omega_{Ma+} = \frac{\omega_{Ma+}}{1 - j\frac{\nu_i}{\omega}} \qquad \Omega_{Na+}^2 = \frac{\omega_{Na+}^2}{1 - j\frac{\nu_i}{\omega}}$$

$$\Omega_{Ma-} = \frac{\omega_{Ma-}}{1 - j\frac{\nu_i}{\omega}} \qquad \Omega^2_{Na-} = \frac{\omega^2_{Na-}}{1 - j\frac{\nu_i}{\omega}}$$

$$\Omega_{Mm+} = \frac{\omega_{Mm+}}{1 - j\frac{\nu_i}{\omega}} \qquad \Omega^2_{Nm+} = \frac{\omega^2_{Nm+}}{1 - j\frac{\nu_i}{\omega}}$$

$$\Omega_{Mm-} = \frac{\omega_{Mm-}}{1 - j\frac{\nu_i}{\omega}} \qquad \Omega^2_{Nm-} = \frac{\omega^2_{Nm-}}{1 - j\frac{\nu_i}{\omega}}$$

Using these quantities, the longitudinal, transverse and Hall susceptibilities of a plasma at angular frequency ω are respectively

$$\varkappa_L = -\frac{1}{\omega^2}\ \Sigma\Omega^2_N\,,\quad \varkappa_T = \Sigma\ \frac{\Omega^2_N}{\Omega^2_M - \omega^2}\ ,\quad \varkappa_H = \frac{1}{j\omega}\ \Sigma\ \frac{\Omega^2_N\,\Omega_M}{\Omega^2_M - \omega^2} \tag{61}$$

For vertical propagation in the ionosphere at a latitude where the inclination of the earth's magnetic field to the horizontal is I, the complex refractive indices of the O and X waves are given by

$$\left.\begin{matrix} n^2_O \\ n^2_X \end{matrix}\right\} = (1 + \varkappa_L)\ \frac{1 + \varkappa_T - \varkappa_H\left\{\frac{1}{2}\tau\cos^2 I \mp \left(\frac{1}{4}\tau^2\cos^4 I - \sin^2 I\right)^{1/2}\right\}}{(1 + \varkappa_L) - (\varkappa_L - \varkappa_T)\cos^2 I} \tag{62}$$

where

$$\tau = \frac{(1 + \varkappa_T)(\varkappa_L - \varkappa_T) - \varkappa_H^2}{\varkappa_H(1 + \varkappa_L)} \tag{63}$$

The transition between quasi-longitudinal and quasi-transverse propagation occurs where

$$|\tau| = \frac{2 \sin |I|}{\cos^2 I} \tag{64}$$

At a magnetic pole of the earth the O and X waves are the waves for which the electromagnetic vectors rotate respectively in the left and right handed senses round the positive direction of the earth's magnetic field. Except at the magnetic equator the O and X waves may also be referred to as the L and R waves respectively.

Care is necessary in evaluating the polarization ratios Q used in earlier sections because the axes of coordinates that it has been convenient to use in this paper differ from those often used in the cold plasma wave theory. The relation between the sets of axes involved is shown in Figure 3. The axes (x, y, z) are those used in this paper, with z vertically upwards and y in the horizontal direction of transmission in the earth-ionosphere transmission line. Let us assume that this direction points at an angle Δ east of magnetic north. The axes (N, W, V) in Figure 3 have the respective directions of magnetic north, magnetic west and the upward vertical. These are the axes often used by ionospherists in the cold plasma wave theory for vertical propagation. The V axis coincides with the z axis but the (E, N) axes are rotated through an

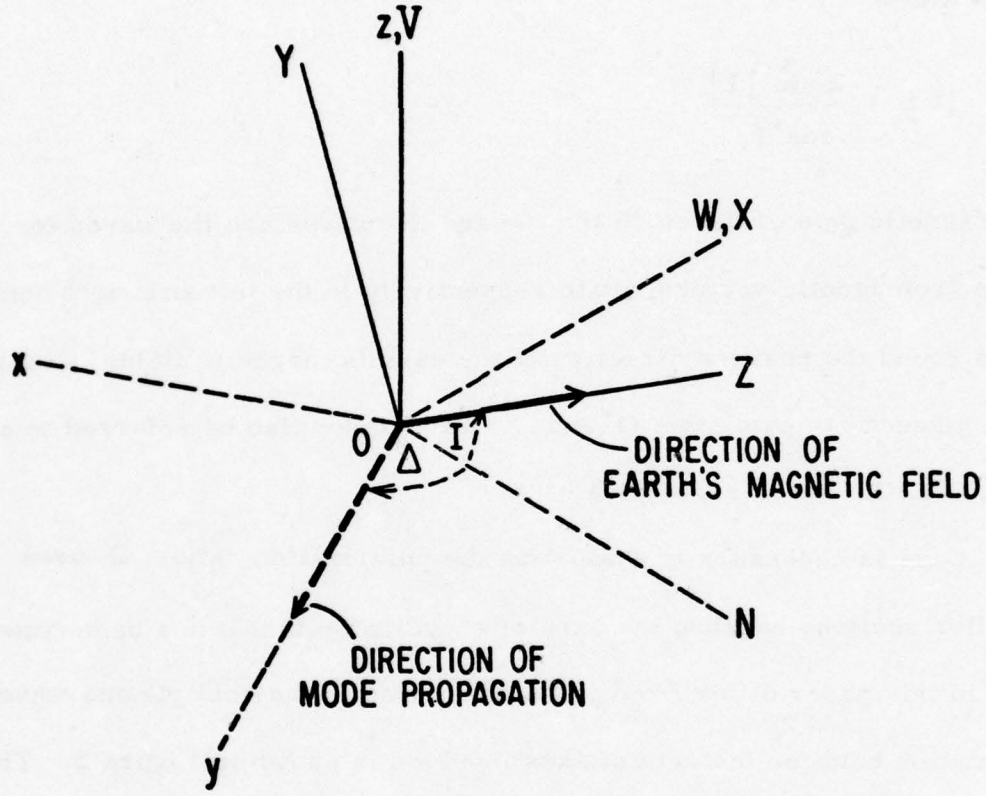

Figure 3. Illustrating the relation between the axes (x, y, z), (X, Y, Z) and (E, N, V).

angle Δ relative to the (x, y) axes. The polarization ratio commonly used in association with the (E, N, V) axes is

$$P = \frac{E_W}{E_N} \tag{65}$$

where E_W and E_N are the westerly and northerly components of the complex electric field of the wave. The polarization ratio that it has been convenient to use in this paper is (Equations (28) and (29))

$$Q = - \frac{E_x}{E_y} \ . \tag{66}$$

It is easily shown that the relation between the two is

$$Q = \frac{\sin \Delta + P \cos \Delta}{\cos \Delta - P \sin \Delta} \tag{67}$$

However, it must further be noticed that, if one is to make use of the coefficients of susceptivity listed in Equations (61) in a susceptivity tensor of the form

$$\begin{pmatrix} \varkappa_T & \varkappa_H & 0 \\ -\varkappa_H & \varkappa_T & 0 \\ 0 & 0 & \varkappa_L \end{pmatrix} \tag{68}$$

the axes involved are those marked (X, Y, Z) in Figure 3, in which the X axis is easterly and the Z axis is in the direction of the earth's magnetic

field. If one performs the cold plasma wave calculations with these axes, one uses the polarization ratios (Booker, 1975)

$$\frac{E_X}{E_Y} = Q_1 = \frac{\varkappa_H}{n^2 - 1 - \varkappa_T} \tag{69}$$

$$\frac{E_Z}{E_Y} = Q_2 = \frac{n^2 \cos I \sin I}{n^2 \cos^2 I - 1 - \varkappa_L} \tag{70}$$

and in terms of these expressions the polarization ratio (65) is, from Figure 3,

$$P = \frac{Q_1}{Q_2 \cos I - \sin I} \tag{71}$$

Substitution from this equation into Equation (67) then gives

$$Q = \frac{\sin I \sin \Delta - Q_1 \cos \Delta - Q_2 \cos I \sin \Delta}{\sin I \cos \Delta + Q_1 \sin \Delta - Q_2 \cos I \cos \Delta} \tag{72}$$

To obtain Q_O and Q_X for use in previous sections of this paper, we use for n^2 in Equations (69) and (70) the values n_O^2 and n_X^2 from Equations (62) and then substitute into Equation (72).

It should be noted that the limiting values of Q_2 in Equation (70) at the equator (I = 0) are

$$Q_2 = \begin{cases} \infty & O \text{ wave} \\ 0 & X \text{ wave} \end{cases}$$

This is because, for the O wave, the denominator of Q_2 also tends to zero.

6. Quasi-transverse and Quasi-longitudinal Approximations

(a) Equatorial behavior

At the magnetic equator vertical propagation of the O wave involves no westerly component of the electric vector, and that of the X wave involves no northerly component. Hence

$$P_O = 0 , \quad P_X = \infty \tag{73}$$

and it follows from Equation (67) that

$$Q_O = \tan \Delta , \quad Q_X = - \cot \Delta \tag{74}$$

Substitution into Equations (58), (59) and (60) then gives

$$S = 1 - j \frac{\lambda_o}{4\pi} \left(\frac{1}{z_O n_O} \cos^2 \Delta + \frac{1}{z_X n_X} \sin^2 \Delta \right) \tag{75}$$

$$\frac{H_x^O}{H_y^X} = \frac{z_X}{z_O} \cot^2 \Delta \tag{76}$$

$$\frac{H_y}{H_x} = - \frac{(z_O - z_X) \sin \Delta \cos \Delta}{z_O \sin^2 \Delta + z_X \cos^2 \Delta} \tag{77}$$

For equatorial propagation in the north-south direction ($\Delta = 0$) we deduce from Equation (76) that only the O wave is excited, and we verify from Equation (75) that the propagation properties in the earth-ionosphere transmission-line depend only on the ionospheric behavior of the O wave;

we also deduce from Equation (77) that the horizontal elliptic polarization at ground-level is linear (perpendicular to the direction of propagation). Similar statements are true for the X wave for equatorial propagation in the east-west direction ($\Delta = \frac{1}{2}\pi$).

We may note that, if the earth's magnetic field were completely neglected, we would have

$$\left.\begin{aligned} n_O &= n_X = n_R \\ z_O &= z_X = z_R \end{aligned}\right\} \tag{78}$$

and Equation (75) would becomes

$$S = 1 - j \frac{\lambda_o}{4\pi} \frac{1}{z_R n_R} \tag{79}$$

in accordance with Wait (1962, p. 290).

(b) Quasi-longitudinal behavior

Vertical propagation of the O and X waves is quasi-longitudinal at the level of reflection in the ELF band over a large part of the world. Under these circumstances

$$P_O = -j, \quad P_X = j \tag{80}$$

from which it follows that

$$Q_O = -j, \quad Q_X = j \tag{81}$$

and consequently that

$$S = 1 - j \frac{\lambda_o}{8\pi} \left(\frac{1}{z_O n_O} + \frac{1}{n_X n_X} \right) \tag{82}$$

$$\frac{H_x^O}{H_x^X} = \frac{z_X}{z_O} \tag{83}$$

and

$$\frac{H_y}{H_x} = j \frac{z_O - z_X}{z_O + z_X} \tag{84}$$

Since z_O and z_X are normally not very different numerically, we deduce from Equation (84) that the transmission-line mode, under quasi-longitudinal conditions in the ionosphere, is nearly but not quite linearly polarized perpendicular to the direction of propagation, and from Equation (83) that the degree of excitation of the O and X waves at their respective levels of reflection is nearly but not quite the same.

We can also see from Equation (82) that, so far as S is concerned, the effects of the O and X waves are mathematically additive. However, the corresponding physical significance requires a rather different statement. At the level of ELF reflection under quasi-longitudinal conditions the O wave behaves largely evanescently and n_O in Equation (82) is close to a pure imaginary, whereas the X wave is the whistler mode and n_X in Equation (82) is close to a real quantity. This meant that the O wave term in Equation (82) contributes mainly to the real part of S and therefore to the departure of the velocity of propagation in the earth-ionosphere transmission-line from c. On the other hand, the X wave term in Equation (82) contributes mainly to the imaginary part of S and therefore to the rate of

attenuation. In other words, the modification in the velocity of transmission of ELF waves is associated mainly with storage of energy by the O wave immediately above the level of reflexion, whereas attenuation of ELF waves in the earth-ionosphere transmission line due to leakage of energy into the region above the level of reflexion is associated mainly with the X wave (the whistler wave).

(c) Relative importance of the quasi-longitudinal and quasi-transverse approximations

In the ELF band there is a drastic difference between the practical importance of the quasi-longitudinal approximation and that of the quasi-transverse approximation. Application of Equation (64) shows that, for vertical transmission in the ionosphere in this band, propagation is quasi-longitudinal at practically all latitudes. The change from quasi-longitudinal to quasi-transverse propagation occurs extremely close to the magnetic equator. Even at a magnetic latitude of 1^{o}, vertical propagation is quasi-longitudinal at all heights and all frequencies less than 300 hz. At these frequencies, therefore, the equatorial zone where there can be any significant departure from quasi-longitudinal propagation is less than $\lambda_{o}/(2\pi)$ in width, and consequently has little influence on world-wide propagation of ELF waves in the earth-ionosphere transmission line.

The almost complete dominance of the quasi-longitudinal approximation for calculation of ELF propagation in the earth-ionosphere transmission line has a practical consequence of the greatest importance. Under quasi-longitudinal or quasi-transverse conditions coupling between the O and X waves is unimportant. It is only in the transition between quasi-longitudinal and

quasi-transverse propagation that coupling is liable to be important, and even then not at all heights. The almost complete dominance of the quasi-longitudinal approximation implies, therefore, that coupling between the O and X waves is unlikely to be of practical importance for ELF communications. This constitutes a major simplification in the theory of ELF propagation in the earth-ionosphere transmission line.

7. The Frequency Dependence of the Height of Reflexion

The general character of the frequency dependence of the height of reflexion given by Equation (22) may be illustrated in the following way. Except very close to the equator, vertical propagation in the ionosphere at ELF is quasi-longitudinal. Moreover, as we move above the level where

$$\nu_e = |\omega_{Me} \sin I| \tag{85}$$

electronic collisions contribute a relative minor correction to the magnitude of the complex refractive index. Since the level (85) is about 70 km except near the equator and since the level (22) is frequently above the level (85), electronic collisions often have only a limited influence in determining the level of reflexion.

On the other hand, for ions of angular gyro frequency ω_{Mi}, the level

$$\nu_i = |\omega_{Mi} \sin I| \tag{86}$$

occurs at about 120 km or higher and is appreciably above the level of ELF reflexion. Below the level (86) the ions are prevented by collisions from developing much motion and consequently from contributing in a major way to the magnitude of the complex refractive index. Even at frequencies below the ionic gyro frequency, it is only above the level (86) that the O and X waves develop Alfven behavior. Between the levels (85) and (86), whistler-band behavior extends downwards in frequency below the ionic gyro-frequency because the ions are largely held at rest by collisions. Consequently, over the entire ELF band and over most of the world, useful approximations to the refractive indices of the O and X waves are often provided by the whistler-band formulae

$$\left.\begin{matrix} n_O^2 \\ n_X^2 \end{matrix}\right\} = 1 \mp \frac{\omega_{Ne}^2}{\omega \left| \omega_{Me} \sin I \right|} \tag{87}$$

For an exponential increase of electron density with height (scale height h), Equation (87) has the form of Equation (1) with

$$\psi = \begin{cases} 0 & \text{O wave} \quad (88) \\ \pi & \text{X wave} \quad . \quad (89) \end{cases}$$

The corresponding values of γ in Figure 1 are

$$\begin{cases} \gamma(0) = 2.00 & \text{O wave} \quad (90) \\ \gamma(\pi) = 2.57 & \text{X wave} \quad . \quad (91) \end{cases}$$

If the quantity

$$\frac{\omega_{Ne}^2}{|\omega_{Me} \sin I|} \tag{92}$$

evaluated at the reference height $z = a$ is written ω_o, and if the unity in Equation (87) is dropped, the height variations of the refractive indices of the O and X waves become

$$\left.\begin{matrix} n_O^2 \\ n_X^2 \end{matrix}\right\} = \mp \frac{\omega_o}{\omega} \exp \frac{z - a}{h} \tag{93}$$

So that

$$|n_O| = |n_X| = \left(\frac{\omega_o}{\omega}\right)^{1/2} \exp \frac{z-a}{2h} \tag{94}$$

Equation (22) for the heights of reflexion z_O and z_X of the O and X waves therefore gives

$$\left(\frac{\omega_o}{\omega}\right)^{1/2} \exp \frac{z_O - a}{2h} = \frac{1}{\gamma(0)} \frac{\lambda_o}{2\pi h} \tag{95}$$

$$\left(\frac{\omega_o}{\omega}\right)^{1/2} \exp \frac{z_X - a}{2h} = \frac{1}{\gamma(\pi)} \frac{\lambda_o}{2\pi h} \tag{96}$$

From these equations we deduce the following approximate expressions for the ELF reflexion heights:

$$z_O = a + 2h \ln [c / \{\gamma(0) (\omega\omega_o)^{1/2} h\}] \quad (97)$$

$$z_X = a + 2h \ln [c / \{\gamma(\pi) (\omega\omega_o)^{1/2} h\}] \quad (98)$$

Equations (97) and (98) illustrate the fact that heights of reflexion in the ELF band increase as the frequency decreases. This behavior continues below the ionic gyro-frequency until tunnel-effect through to the Alfven region above the level (86) results in penetration of the ionosphere at micropulsation frequencies. The rise in the level of reflection as we go down in frequency through the ELF band, culminating in penetration of the ionosphere in the micropulsation band, is to be compared and contrasted with the rise in the level of reflexion as we go up in frequency through the LF, MF and HF bands, culminating in penetration of the ionosphere in the VHF band.

Because $\gamma(0) < \gamma(\pi)$ in accordance with Equations (90) and (91), it follows from Equations (97) and (98) that $z_O > z_X$. This illustrates the fact that the level of reflexion for the O wave in the ELF band is normally a little greater than that for the X wave.

Finally, let us deduce, for refractive index profiles based on Equations (87), the propagation properties of the transmission-line mode in the earth-ionosphere wave-guide. From Equations (93)-(96), the complex refractive

indices for the O and X waves at their respective levels of reflexion may be written

$$n_O = -j \frac{1}{\gamma(0)} \frac{\lambda_o}{2\pi h} \tag{99}$$

$$n_X = \frac{1}{\gamma(\pi)} \frac{\lambda_o}{2\pi h} \tag{100}$$

Substitution into Equation (82) then gives

$$S = 1 + \frac{\gamma(0)}{4} \frac{h}{z_O} - j \frac{\gamma(\pi)}{4} \frac{h}{z_X} \tag{101}$$

For a profile that is not precisely exponential we would deduce the scale height from Equation (23) and obtain slightly different values h_O and h_X at the levels z_O and z_X respectively. Equation (101) would then become

$$S = 1 + \frac{\gamma(0)}{4} \frac{h_O}{z_O} - j \frac{\gamma(\pi)}{4} \frac{h_X}{z_X} \tag{102}$$

or, using Equations (90) and (91),

$$S = 1 + 0.50 \frac{h_O}{z_O} - j\, 0.64 \frac{h_X}{z_X} \tag{103}$$

It follows that, over a large part of the world under commonly encountered ionospheric conditions, the phase velocity in the earth-ionosphere transmission line is decreased below the velocity of light by approximately the fraction

$$0.50 \frac{h_O}{z_O} \tag{104}$$

while the attention rate due to leakage into the upper ionosphere in nepers per $\lambda_o/(2\pi)$ is approximately

$$0.64 \frac{h_X}{z_X} \tag{105}$$

In decibels per megameter at a frequency f measured in hertz, the attenuation rate is approximately

$$0.117 \; f \frac{h_X}{z_X} \tag{106}$$

8. Absorption below the level of reflexion

The method that we have devised for calculating attenuation in the earth-ionosphere transmission line at ELF takes account of the leakage of energy into the ionosphere above the level of reflexion, but it does not take account of collisional absorption of energy below the level of reflexion. For an engineering transmission line the leakage-loss would be called "metal-loss" or "series-loss," while absorption between the conductors would be called "dielectric-loss" or "shunt-loss." For the earth-ionosphere transmission line we have taken account of the series-loss but we have not yet discussed the shunt-loss.

Calculations to be reported in a later paper show that shunt-loss is small compared with series-loss in the ELF band under a wide variety of circumstances. Nevertheless, it is clearly possible to devise an ionospheric profile for which the shunt-loss is comparable with or larger than the series-loss. It is desirable, therefore, to have a method for estimating attenuation in the earth-ionosphere transmission line due to collisional absorption below the level of reflexion. The method described below is similar to that used for taking into account conductivity of the insulating material between the conductors of an engineering transmission line.

Between the earth's surface and the level of reflexion in the ELF band the electric field of a wave in the earth-ionosphere transmission line is practically vertical. Because some plasma is present, the medium possesses conductivity. It is the loss due to this conductivity that we have to calculate, taking into account the effect of the earth's magnetic field. Using the axes (X, Y, Z) in Figure 3, the conductivity is described by means of the conductivity tensor

$$\begin{pmatrix} \sigma_T & \sigma_H & 0 \\ -\sigma_H & \sigma_T & 0 \\ 0 & 0 & \sigma_L \end{pmatrix} \qquad (107)$$

This tensor is $j\omega\varepsilon_o$ times the susceptivity tensor (68) so that, from Equations (61),

$$\sigma_L = \frac{\varepsilon_o}{j\omega} \Sigma \Omega_N^2 \, , \quad \sigma_T = j\omega\varepsilon_o \Sigma \frac{\Omega_N^2}{\Omega_M^2 - \omega^2} \, , \quad \sigma_H = \varepsilon_o \Sigma \frac{\Omega_N^2 \Omega_M}{\Omega_M^2 - \omega^2} \tag{108}$$

At a location where the vertical electric field in the transmission line is E and the inclination of the earth's magnetic field to the horizontal is I, the cartesian components of the electric field for the axes (X, Y, Z) in Figure 3 are given by

$$\underset{\sim}{E} = (0, \cos I, \sin I)\, E \tag{109}$$

and those of the current density are given by

$$\underset{\sim}{J} = (\sigma_H \cos I, \sigma_T \cos I, \sigma_L \sin I)\, E \tag{110}$$

Hence

$$\underset{\sim}{E} \cdot \underset{\sim}{J} = (\sigma_T \cos^2 I + \sigma_L \sin^2 I)\, E^2 \tag{111}$$

and the energy absorbed per unit volume is

$$\{R(\sigma_T) \cos^2 I + R(\sigma_L) \sin^2 I\}\, E^2 \tag{112}$$

where R denotes real part, and E is the rms field. The rate of horizontal flow of energy per unit area at the same location is

$$R(n)\, \zeta_o^{-1}\, E^2 \tag{113}$$

where n is the refractive index at this location and ζ_o is the impedance of free space (377 ohms). By dividing expression (112) by expression (113) we see that the fraction of energy removed from the horizontal flow per unit horizontal distance is

$$\zeta_o \{R(n)\}^{-1} \{R(\sigma_T) \cos^2 I + R(\sigma_L) \sin^2 I\} \quad . \tag{114}$$

If we assume that the horizontal flow of energy in the earth-ionosphere transmission line is approximately uniform between the surface of the earth and the level of reflexion z_R, it follows that the rate of attenuation in decibels per unit distance due to collisional absorption below the level of reflexion z_R is approximately

$$4 \cdot 343 \, \zeta_o \, z_R^{-1} \int_o^{z_R} \{R(n)\}^{-1} \{R(\sigma_T) \cos^2 I + R(\sigma_L) \sin^2 I\} \, dz \tag{115}$$

The question arises as to whether the refractive index n and the level of reflexion z_R in Equation (115) are those appropriate to the O wave, those appropriate to the X wave, or some average of the two. At the lower ionospheric levels, n_O and n_X are not substantially different and it makes little difference which is used. However, above the level corresponding to Equation (85), n_O and n_X are substantially different as illustrated in Equations (87). Moreover it is then the X wave that sustains the flow of energy, the O wave being largely evanescent. We therefore take n in

expression (115) to be n_X, and z_R to be z_X. It follows that a reasonable estimate of the rate of attenuation in decibels per unit distance due to collisional absorption below the level of reflexion is

$$4 \cdot 343 \, \zeta_o \, z_X^{-1} \int_0^{z_X} \{R(n_X)\}^{-1} \{R(\sigma_T) \cos^2 I + R(\sigma_L) \sin^2 I\} \, dz \quad . \qquad (116)$$

In the course of calculating n_O and n_X in Equations (62), the quantities $\varkappa_L$, $\varkappa_T$ and $\varkappa_H$ in Equations (61) are calculated; consequently the values of the quantities σ_L, σ_T and σ_H in Equations (108) are available as functions of height z. All the quantities in expression (116) are therefore immediately available, and the integral can easily be calculated numerically without further approximation. It may be noted however that, at the levels involved, the angular frequency ω in the ELF band is small compared with both the electronic and ionic collisional frequencies ν_e and ν_i. Consequently the conductivities σ_T and σ_L in expression (116) have substantially their d.c. values and the quantity $R(\sigma_T)\cos^2 I + R(\sigma_L)\sin^2 I$ in the integrand is approximately equal to

$$\varepsilon_o \left\{ \frac{\omega_{Ne}^2}{\nu_e} \, \frac{\omega_{Me}^2 \sin^2 I + \nu_e^2}{\omega_{Me}^2 + \nu_e^2} + \frac{\omega_{Ni}^2}{\nu_i} \, \frac{\omega_{Mi}^2 \sin^2 I + \nu_i^2}{\omega_{Mi}^2 + \nu_i^2} \right\} \qquad (117)$$

where ω_{Ni} is the angular plasma frequency for the ions (positive and negative).

9. Application of the theory

For given ionospheric profiles of electron density, ion density, electronic collisional frequency and ionic collisional frequency, we have devised an approximate method of calculating, for the earth-ionosphere transmission line at ELF, (i) the velocity of phase propagation, (ii) the rate of attenuation due to leakage of energy into the ionosphere above the level of reflexion, and (iii) the rate of attenuation due to collisional absorption below the level of reflexion. The calculations are affected in a major way by the presence of the earth's magnetic field. Even though propagation is quasi-longitudinal except almost exactly at the magnetic equator, the inclination of the earth's magnetic field to the horizontal enters as a parameter and causes substantial variation with latitude in the velocity and attenuation rate in the earth-ionosphere transmission line.

Additional dependence of the velocity and attenuation rate on latitude arises from the variation, between the equator and the poles, of the ionospheric profiles of ionization density. In principle, it is possible to allow for all of these features, and to study the variations of the velocity and attenuation rate with time of day, latitude, season of the year, and epoch in the sunspot cycle. In addition, it is possible to perform the calculations for profiles representative of sudden ionospheric disturbances and polar cap absorption events.

Because application of the theory developed in this paper is inexpensive, it is not only possible but easy to use it to explore the way in which ELF propagation depends on all of these phenomena. The results of such an attempt at a comprehensive approximate theoretical treatment of the various features of ELF communications will be presented in a forthcoming paper.

Bibliography

Barr, R. 1972 Some new features of ELF attenuation, Journal of Atmospheric and Terrestrial Physics 34, 411-420.

Booker, H. G. 1948 The elements of wave propagation using the impedance concept, Journal of the IEE 94, 171-204.

Booker, H. G. 1975 Electromagnetic and hydromagnetic waves in a cold magnetoplasma, Philosophical Transactions of the Royal Society of London A280, 57-93.

Budden, K. G. 1961a Radio waves in the ionosphere, Cambridge University Press, Cambridge.

Budden, K. G. 1961b The wave-guide mode theory of wave *propagation, Logos Press,* London.

Chapman, F. W. and Jones, D. L. 1964 Observations of earth-ionospheric cavity resonances and their interpretation in terms of a two-layer ionospheric model, Radio Science Journal of Research of the National Bureau of Standards 68D, 1177-1185.

Cole, R. K. 1965 The Schumann resonances, Radio Science Journal of Research of the National Bureau of Standards 69D, 1345-1349.

Galejs, J. 1972 Terrestrial propagation of long electromagnetic waves, Pergamon Press, New York.

Hughes, H. G. and Theisen, J. F. 1970 Diurnal variations in the apparent attenuations of ELF atmospherics over two different propagation paths, Journal of Geophysical Research 75, 2795-2801.

Jones, D. L.	1967	Schumann resonances and ELF propagation for inhomogeneous isotropic ionospheric profiles, Journal of Atmospheric and Terrestrial Physics 29, 1037-1044.
Konrad, A. and Poverlein, H.	1972	Schnelle und langsame Wellenmodes bei extrem niedrigen Frequenzen, Kleinheubacher Berichte 15, 197-207.
Large, D. B. and Wait, J. R.	1968	Theory of electromagnetic coupling phenomena in the earth-ionosphere cavity, Journal of Geophysical Research 73, 4335-4362.
Madden, T. and Thompson, W.	1965	Low frequency electromagnetic oscillations of the earth-ionosphere cavity, Reviews of Geophysics 3, 211-253.
Pappert, R. A. and Moler, W. F.	1974	Propagation theory and calculations at lower ELF, IEEE Transactions on Communications 22, 438-451.
Wait, J. R.	1958	An extension of the mode theory of VLF ionospheric propagation, Journal of Geophysical Research 63, 125-135.
Wait, J. R.	1962	Electromagnetic waves in stratified media, Macmillan, New York.
Wait, J. R.	1974	Special issue on extremely low frequency communications, IEEE Transactions on Communications 22, 353-587.
Watson, G. N.	1919	The transmission of electric waves round the earth, Proceedings of the Royal Society A95, 546-563.

Appendix B

Calculations

30 November 1976

The relation between ionospheric profiles and ELF propagation in the earth-ionosphere transmission line (2) calculations

by

Henry G. Booker and Michael D. Shuster*

University of California, San Diego

La Jolla, California 92093

and

F. Lefeuvre

Centre de Recherches en Physique de l'Environnement

Avenue de la Recherche Scientifique

Orléans, France

---

*These authors were supported by the U.S. Office of Naval Research under Contract No. N00014-75-C-0959.

Abstract

An approximate method, based on a wave-solution, is used to sketch the dependence of ELF propagation in the earth-ionosphere transmission line on time of day, latitude, season of the year, epoch in the sunspot cycle, and occurrence of sudden ionospheric disturbances and polar cap absorption events. As the frequency descends through the ELF band, penetration of the D region occurs in succession for the O and X waves, leading to reflexion from the E region at the Schumann resonant frequency. Under quiet day-time ionospheric conditions the penetration frequency-band is around 20-60 hz in middle and high latitudes, but around 75-150 hz near the equator. At a frequency low enough to be reflected primarily from the E region under quiet ionospheric conditions, an increase in D region ionization that is just sufficient to transfer primary reflexion from the E region to the D region results in an increase in the rate of attenuation. On the other hand, when once reflexion is firmly established at the lower level, further increase of ionization in the D region causes a reduction in the rate of attenuation. Similar effects are expected to occur at night in association with a sub-E region ledge of ionization. Small variations in the ionization profile of such a ledge are the likely cause of night-time fluctuations of transmission at 45 and 75 hz.

1. Introduction

In a recent paper (Booker and Lefeuvre, 1977), to be referred to as paper 1, a relatively inexpensive approximate method is developed for calculating propagation at ELF in the earth-ionosphere transmission line taking account of simple profiles of electron density and of other ionospheric parameters. In the present paper an attempt is made to apply this theory on a world-wide scale. We investigate the types of changes that can be expected in ELF communications with time of day, latitude, season of the year, and epoch in the sunspot cycle. We also investigate the likely effects on ELF communications of sudden ionospheric disturbances and polar cap absorption events.

The theory developed in paper 1 is based on a wave-solution, but nevertheless substantial approximations are involved. The basic wave-solution is that for an exponentially increasing electron-density given by Budden (1961) and by Wait (1962). At ELF, $1/(2\pi)$ times the wavelength λ_o in free space is large compared with the scale-height. Approximations on this basis are feasible, and they greatly simplify the handling of propagation at ELF. There is a reflecting stratum the thickness of which is about one scale-height h, defined in terms of the profile of the square of refractive index. The center of the reflecting stratum occurs where $1/(2\pi)$ times the local wavelength λ is equal to γ times the local scale-height h, where γ is a factor that lies between 2 and 3. Above the reflecting stratum the medium can be assumed to be slowly varying, and here the direction of phase

propagation can nearly always be assumed to be approximately vertical regardless of the directions of propagation of the incident and reflected waves below the ionosphere. It is shown in paper 1 that almost the same complex reflexion coefficient is obtained if the ionosphere below the center of the reflecting stratum is abolished and the ionosphere above the center of the reflecting stratum is treated as a slowly varying medium.

In this way the concept that the ionosphere can be regarded as having a discontinuous lower boundary at ELF is analytically justified in paper 1. Moreover a method is deduced for deriving from an ionospheric profile the level at which the discontinuity should be placed and the characteristics that should be assumed for the ionosphere above this level. It is shown in paper 1 that the level of reflexion at ELF is independent of the angle of incidence upon the ionosphere. The level does, however, depend on frequency. A wave penetrates further into the ionosphere as the frequency descends through the ELF band.

Over the entire radio spectrum, the frequency where the height of reflexion from the ionosphere has its lowest value occurs in the VLF band. As the frequency is shifted either upwards or downwards from the VLF band, a radio wave penetrates further into the ionosphere, and it ultimately pierces the ionosphere at VHF on the high frequency side and at micropulsation frequencies on the low frequency side. It is in the VLF band where the theory of ionospheric propagation is most difficult to handle. Simplifications can be introduced both as the frequency is raised above VLF and as

it is lowered below VLF. It was the objective of paper 1 to develop these simplifications in a form convenient to apply in the frequency range 7.5-300 hz. It is the objective of this paper to explore the consequences of applying these ideas numerically in as comprehensive a manner as seems possible at the present time.

The results obtained in this paper differ substantially from those of previous authors (Wait, 1958; Chapman and Jones, 1964; Madden and Thompson, 1965; Jones, 1967; Large and Wait, 1968; Galejs, 1972; Pappert and Moler, 1974). Part of the reason for this may be that we have taken into account the effect of the earth's magnetic field more completely than have many previous authors. In one case, however (Pappert and Moler, 1974), a reason for the difference could be that we have not taken the effect of the earth's magnetic field into account sufficiently completely. The approximations developed in paper 1 are rather different from those used by previous authors. The method of approximation has been designed to take ionospheric profiles into account inexpensively but nevertheless with reasonable accuracy, and to do so in such a way as to be able to pinpoint the causes of the various phenomena encountered. However, we doubt that the substantial differences between our results and those of previous authors are primarily associated either with the method of calculation or with the degree to which the effect of the earth's magnetic field has been taken into account.

During the past decade, major progress has been made in the extent in which the day-time profile of ionospheric electron density below 100 km is understood. This has arisen largely through the application of in situ

rocket techniques (Mechtly and Smith, 1968; Mechtly, Rao, Skaperdas and Smith, 1969; Mechtly and Smith, 1970; Mechtly, Bowhill and Smith, 1972; Mechtly and Bilitza , 1974). These and other investigations have culminated in the day-time profiles currently being proposed for the International Reference Ionosphere (Rawer, Ramakrishnan and Bilitza, 1975). In this paper we use day-time profiles of electron density based on this work. These profiles differ substantially from those used by previous authors in studies of day-time ELF propagation in the earth-ionosphere transmission line. We believe that the use of up-to-date profiles of electron density is the principal reason for the substantial differences existing between our results and those of previous authors.

While the day-time profile of electron density below 100 km has been the subject of intensive studies during the past decade, it is difficult to say the same for the night-time profile. Under normal ionospheric conditions there is virtually no D layer to be studied at night in the 60-80 km region, and the details of the profile of electron density below 100 km have little influence on HF communications. This is not true, however, at VLF (Berry and Davis, 1976; Morfitt, 1976), nor is it true at ELF.

Based on the work of Soboleva (19), profiles of electron density for the night-time ionosphere have been proposed for the International Reference Ionosphere by Rawer, Ramakrishnan and Bilitza (1975), and in the present paper we attempt to use night-time profiles of this type. The attempt leads, however, to the unacceptable conclusion that the Schumann resonance

(Schumann, 1952a, 1952b, 1952c, 1954, 1957) in the earth-ionosphere cavity would not be observable. We have therefore devised a modified night-time profile of electron density more acceptable for describing ELF phenomena. This profile is, however, substantially different from the profiles used by previous authors for study of ELF propagation in the earth-ionosphere transmission line and leads to substantially different results.

2. Effect of the earth's magnetic field

In this investigation, the earth's magnetic field is taken to be that of a central dipole: differences between magnetic, geomagnetic and geographic latitude are ignored. Allowance for the effect of the earth's magnetic field at ELF is greatly simplified by the fact that phase propagation in the ionosphere is approximately vertical regardless of the directions of the incident and reflected waves below the ionosphere. It is also greatly simplified by the fact that vertical propagation in the ionosphere at ELF is quasi-longitudinal except almost exactly at the equator. As one approaches the equator it is only within the last degree of latitude that vertical propagation switches from quasi-longitudinal to quasi-transverse behavior. At frequencies less than 300 hz, the equatorial zone in which vertical propagation departs from quasi-longitudinal behavior is less than $\lambda_o/(2\pi)$ in width, and consequently a wave in the earth-ionosphere transmission line scarcely responds to the existence of the zone. Nevertheless, in the calculations reported in this paper no algebraic approximations based on the quasi-longitudinal approximation have been introduced.

The fact that propagation in the ionosphere at ELF is predominantly quasi-longitudinal is important in this investigation for the following reason. We have assumed no coupling between propagation of the ordinary and extraordinary waves. In the coupled wave-equations for the O and X waves we have calculated, at all heights in all cases, the ratio of the coupling terms to the other terms, in order to monitor the degree of coupling likely to exist. The coupling terms were always found to be small, although they rose in significance at latitudes a fraction of a degree on either side of the equator where the transition from quasi-longitudinal to quasi-transverse propagation takes place. The assumption of independence of propagation of the O and X waves is therefore justified. The reason for near independence of propagation of the O and X waves under a wide range of conditions at ELF is the dominance of the quasi-longitudinal type of propagation.

When propagation in the ionosphere is practically vertical and its character is quasi-longitudinal, ELF propagation in the earth-ionosphere transmission line is not very dependent on the azimuthal angle Δ between the magnetic meridian and the vertical plane of propagation. The locations where a major dependence on Δ might be expected are in the neighborhood of the equator where departure from quasi-longitudinal propagation takes place. Even here, however, the dependence on Δ turned out to be numerically small in our calculations in spite of the fact that, at the equator, the wave transmitted into the ionosphere is the O wave for $\Delta = 0°$ and the X wave for $\Delta = 90°$. In consequence, the angle between the magnetic meridian and the vertical plane of propagation in the earth-ionosphere transmission

line does not appear as a parameter in the diagrams and tables of this paper, even though Δ does appear in the formulae of paper 1. Calculations have been carried out both for $\Delta = 0°$ and $\Delta = 90°$, but only the curves for $\Delta = 90°$ are presented.

It should be noted that Pappert and Moler (1974) also obtained no appreciable variation with Δ for ELF propagation in the earth-ionosphere transmission line at high latitudes. At lower latitudes, however, their variation with Δ is considerably greater than ours. Their results imply that substantial reflexion occurs near the bottom of the ionosphere where the refractive index is not radically different from unity and the transmitted wave is consequently not approximately vertical. We would not expect such low-level reflexion even for their model of the ionosphere unless it were caused inadvertently by a step-by-step computer integration process.

3. Calculation of propagation velocity and attenuation rate

The method devised in paper 1 for approximately calculating the velocity v of phase propagation in the earth-ionosphere transmission line, and the attenuation rate α due to leakage of energy into the region above the level of reflexion may be summarized as follows.

We consider a given location on the earth's surface (for example, a pole). We select appropriate profiles of ionization density versus height (for example, those shown in Figure 1). We select an angular frequency ω (for example, that corresponding to 45 hz) and, using the cold plasma theory for vertical propagation, we calculate as functions of height the complex

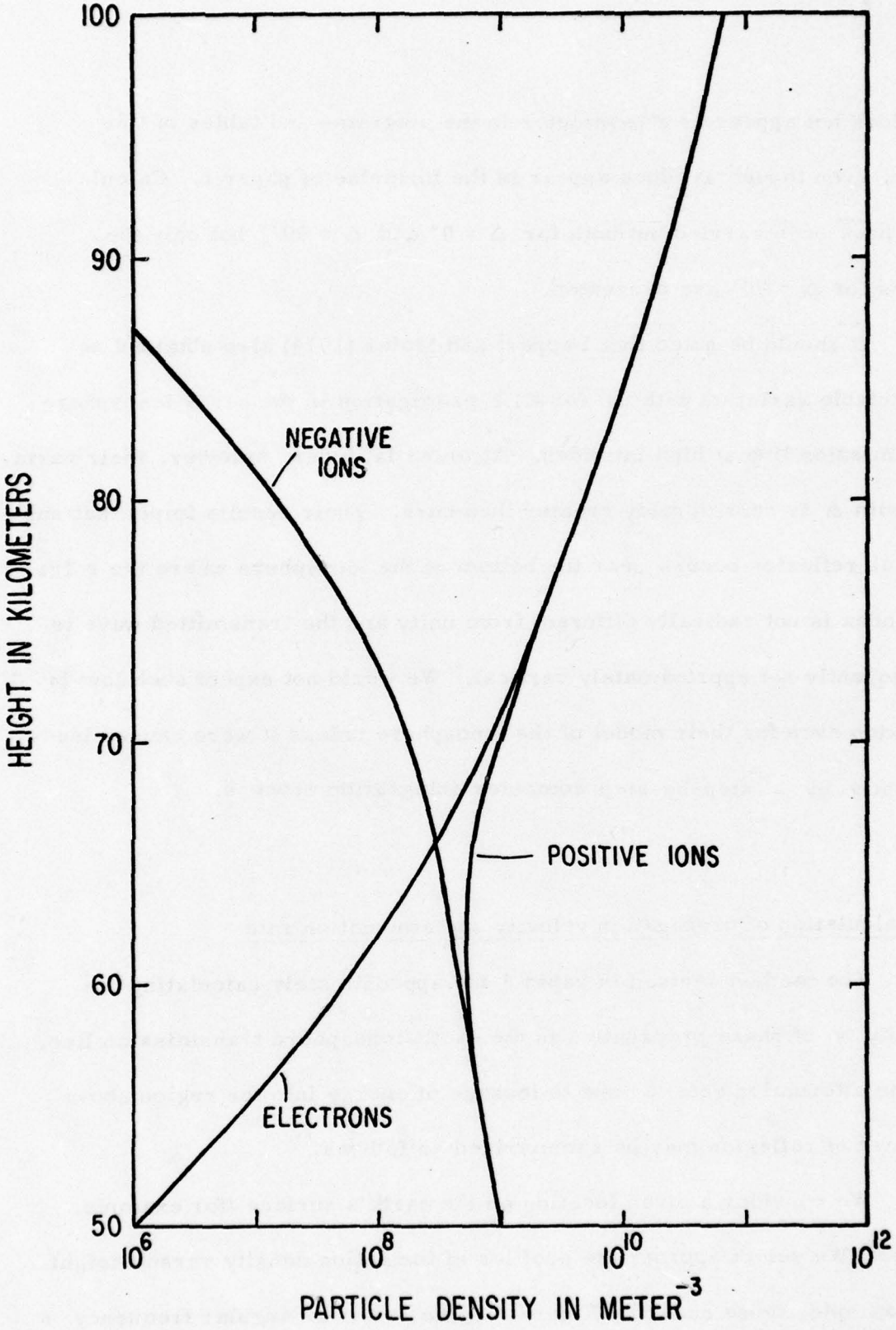

Figure 1. A simple ionospheric profile used for illustrating the method of calculation.

refractive indices n_O and n_X for the O and X waves as shown in Figure 2. We also calculate the corresponding polarization ratios Q_O and Q_X defined in paper 1 but not shown in Figure 2.

From the values of n_O and n_X we calculate the local wavelengths

$$\lambda_O = \frac{2\pi c}{\omega} \frac{1}{|n_O|}, \quad \lambda_X = \frac{2\pi c}{\omega} \frac{1}{|n_X|} \tag{1}$$

and the local scale-heights

$$h_O = \frac{1}{n_O^2 - 1} \frac{d}{dz} (n_O^2 - 1), \; h_X = \frac{1}{n_X^2 - 1} \frac{d}{dz} (n_X^2 - 1) \tag{2}$$

We then take the centers of the reflecting strata for the O and X waves to be at the heights given by

$$\frac{\lambda_O}{2\pi h_O} = \gamma_O, \quad \frac{\lambda_X}{2\pi h_X} = \gamma_X \tag{3}$$

where the first approximations to γ_O and γ_X are

$$\gamma_O = 2.0, \quad \gamma_X = 2.57 \tag{4}$$

In paper 1 a method of successive approximation to the values of γ_O and γ_X is described. This has been systematically applied in this paper, although experience showed that the first approximation was nearly always adequate.

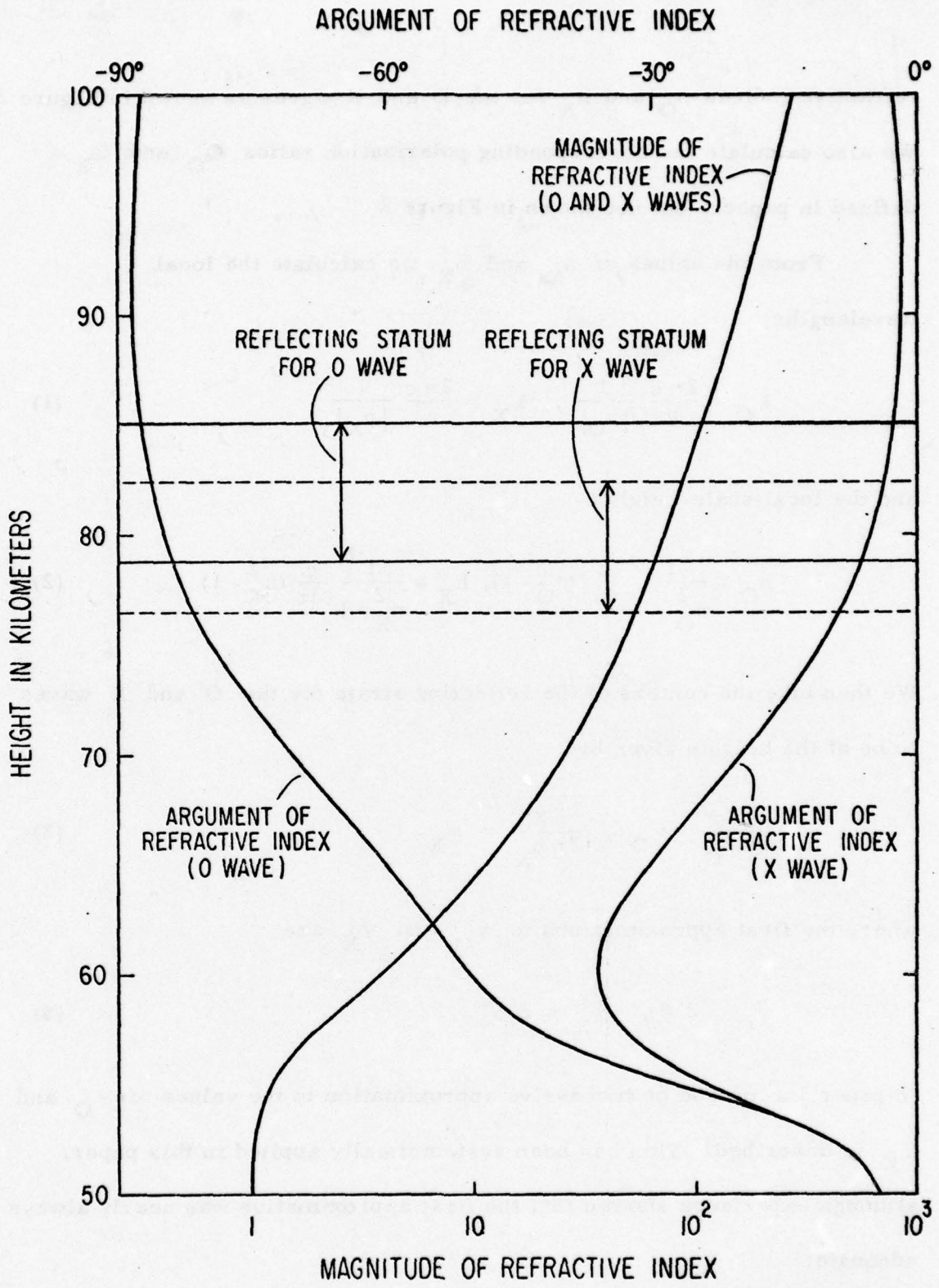

Figure 2. Height variations of the complex reflective indices for the O and X waves at a magnetic pole for a frequency of 45 hz using the profile illustrated in Figure 1.

A convenient way of locating the height z_O of the center of the reflecting stratum for the O wave is to draw $\lambda_O/(2\pi h_O)$ as a function of height as shown in Figure 3. The value of z_O is then the height where this curve crosses the ordinate γ_O. A similar procedure applies for the X wave, using the ordinate γ_X. The two curves for $\lambda_O/(2\pi h_O)$ and $\lambda_X/(2\pi h_X)$ are no nearly identical that they cannot be separately drawn in Figure 3. In this diagram the intersections determining the levels z_O and z_X are marked by an O and an X. Using these values of z_O and z_X, together with the values of the scale heights h_O and h_X at these levels, we may mark the locations of the reflecting strata for the O and X waves on Figure 2 as shown.

From Figure 2 may be read the values of n_O and n_X corresponding to the levels of reflexion z_O and z_X for the O and X waves, respectively, and from curves for the polarization ratios we may also read the corresponding values of Q_O and Q_X. For the velocity and attenuation rate in the earth-ionosphere transmission line, the values of c/v and of α (in decibels per unit distance) are then given by (see paper 1, section 3)

$$c/v = R(S), \quad \alpha = -8.686\,(\omega/c)\,I(S) \tag{5}$$

where R and I denote real and imaginary parts, and

$$S^2 = 1 - j\,\frac{Q_O\left(\frac{2\pi z_O}{\lambda_O} - j\frac{1}{n_O}\right)\frac{1}{n_X} - Q_X\left(\frac{2\pi z_X}{\lambda_O} - j\frac{1}{n_X}\right)\frac{1}{n_O}}{Q_O\left(\frac{2\pi z_O}{\lambda_O} - j\frac{1}{n_O}\right)\frac{2\pi z_X}{\lambda_O} - Q_X\left(\frac{2\pi z_X}{\lambda_O} - j\frac{1}{n_X}\right)\frac{2\pi z_O}{\lambda_O}} \tag{6}$$

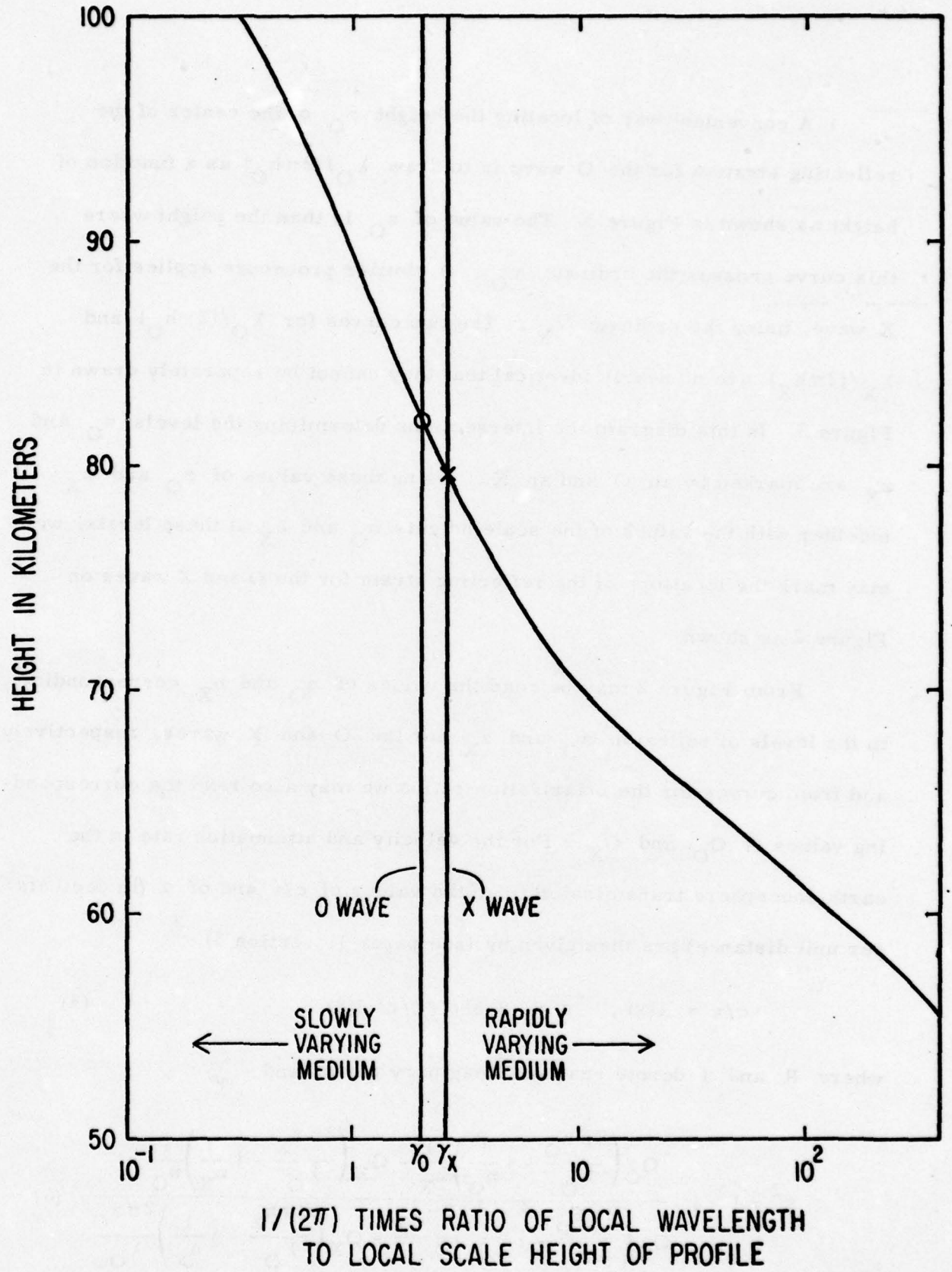

Figure 3. Illustrating the method for estimating the heights of the centers of the reflecting strata for the O and X waves (frequency 45 hz, magnetic pole, profile illustrated in Figure 1).

While most of the attenuation in the earth-ionosphere transmission line is normally due to leakage of energy into the part of the ionosphere above the level of reflexion, some attenuation is also caused by collisional absorption below the level of reflexion. An integral for estimating the latter attenuation rate α' is given by expression (116) in paper 1. The total ionospheric attenuation rate is then $\alpha + \alpha'$. It is the values for $\alpha + \alpha'$ that are quoted in this paper except where otherwise indicated.

To the ionospheric attenuation rate it is also necessary to add the attenuation rate due to leakage into the earth, calculated as described by Wait (1962) and Galejs (1972). Likewise to the value of $(c/v) - 1$ calculated for the ionosphere in accordance with the first of Equations (5) must be added the value of $(c/v) - 1$ associated with skin-effect at the earth's surface in order to obtain the overall value of $(c/v) - 1$.

4. Ionospheric profiles

In constructing a set of ionospheric profiles to describe world-wide propagation at ELF in the earth-ionospheric transmission line we have attempted to follow the profiles proposed by Rawer, Ramakrishnan and Bilitza (1975) for the International Reference Ionosphere. These profiles are at present only available for two latitudes, for two times of day, for a few months of the year, and for sunspot numbers of 10 and 100. Considerable interpolation and extrapolation is therefore necessary to obtain a comprehensive set of profiles for world-wide application under all circumstances.

In view of the necessity for this interpolation and extrapolation, some simplifications are made in the RRB profiles. Their midday profiles have roughly the same shape. We have used precisely the same shape at all latitudes. However we have varied the electron densities in the D and E regions proportionally to square root of the sun's zenith angle χ. In this way we arrive at the set of day-time profiles of electron density indicated in Figure 4; only the profiles for $\chi = 0°$ and $\chi = 75°$ are shown. For the variation with the sunspot number R we have assumed that electron densities in the day-time D and E regions are proportional to $(1 + 0.01\ R)^{1/2}$.

The profiles were represented as analytic functions of height using the method of Booker (1977). In this model, electron density N is expressed as a function of height z by means of the equation

$$\log_{10} N = \log_{10} N_o + A_{01}(z - z_o)$$

$$= \sum_{n=1}^{m} (A_{n,n+1} - A_{n-1,n}) \{ f(z - z_n, B_n) - f(z_o - z_n, B_n) \} \quad (7)$$

where

$$f(z, B) = B^{-1} \ln \{ 1 + \exp(Bz) \} \quad (8)$$

For the day-time profiles adopted (Figure 4), the parameters m, N_o, z_n, $A_{n-1,n}$ and B_n in Equation (7) have the values listed in Table 1.

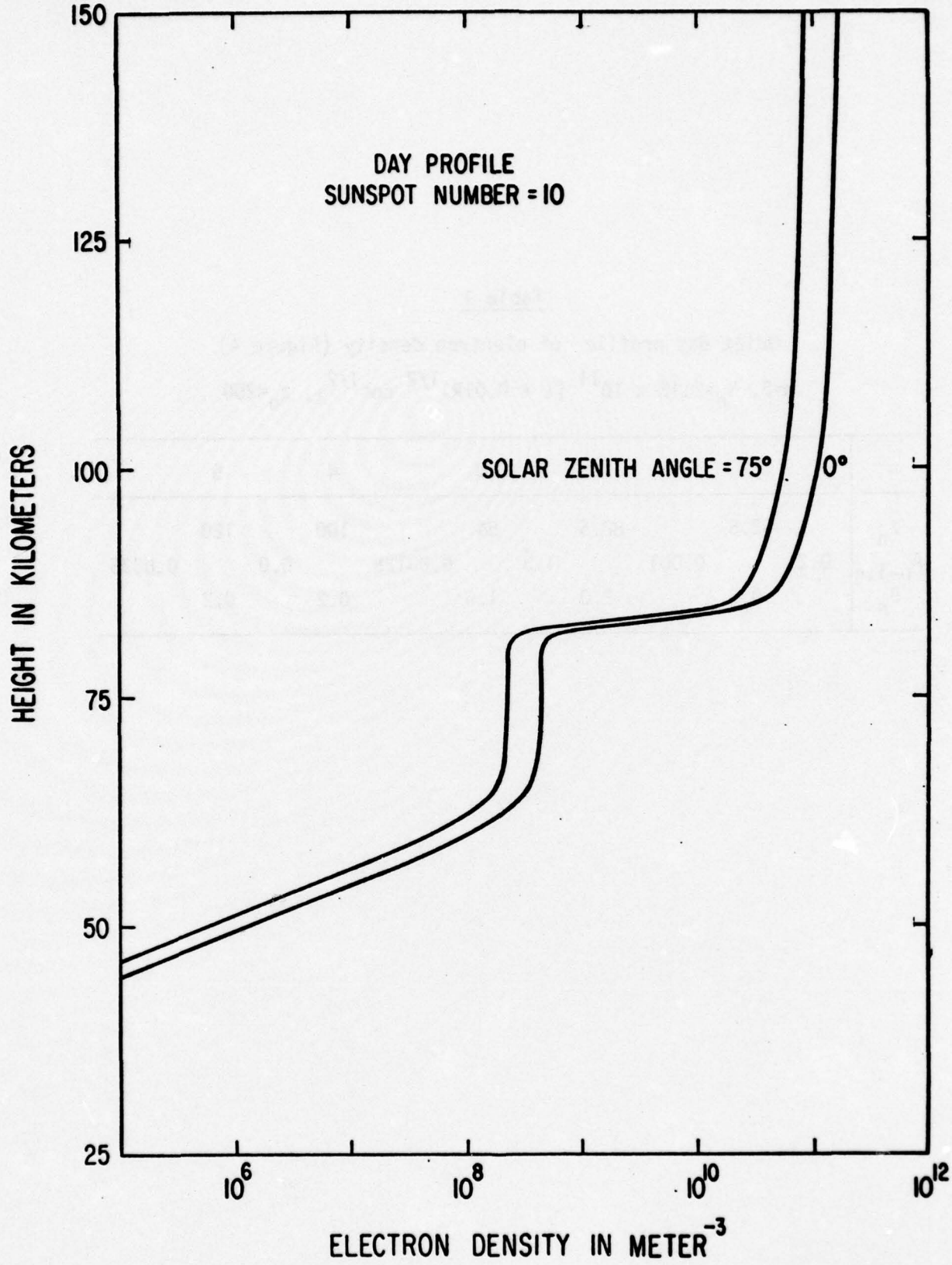

Figure 4. Adopted day-time profiles of electron density.

Table 1

Quiet day profile of electron density (Figure 4)

$m=5$, $N_o=2.12 \times 10^{11} (1 + 0.01R)^{1/2} \cos^{1/2}\chi$, $z_o=200$

n	1		2		3		4		5	
z_n		62.5		82.5		84		100		120
$A_{n-1,n}$	0.2		0.001		$1.\dot{3}$		0.03125		0.0	0.0025
B_n		0.5		2.0		1.5		0.2	0.2	

The night-time RRB profiles were idealized to those shown in Figure 5. These are represented analytically by means of Equation (7) with the parameters listed in Table 2, where Λ denotes latitude. It was assumed that no variation of maximum electron density in the E region takes place during the night hours but that the maximum electron density increases by a factor of 4 in going from the equator to a pole. The dependence upon sunspot number at night was assumed to involve proportionality of electron density to $(1 + 0.02\ R)^{1/2}$.

While the day-time profiles shown in Figure 4 were found to work satisfactorily, the night-time profiles shown in Figure 5 lead to the conclusion that the Schumann resonance would be unobservable (see next section). We were therefore forced to reject the night profiles shown in Figure 5. By trial and error we arrived at new night profiles shown in Figure 6. These are represented analytically by means of Equation (7) with the parameters listed in Table 3. In arriving at these new night profiles note was taken of the profiles that have been found necessary for the explanation of VLF propagation at night (Morfitt, 1976). However, the profiles in Figure 6 were primarily adjusted to obtain results at 7.5 hz that permit the Schumann resonance to exist, and to obtain propagation velocities at 75 hz that are of the order of magnitude observed by Hughes and Gallenberger (1974).

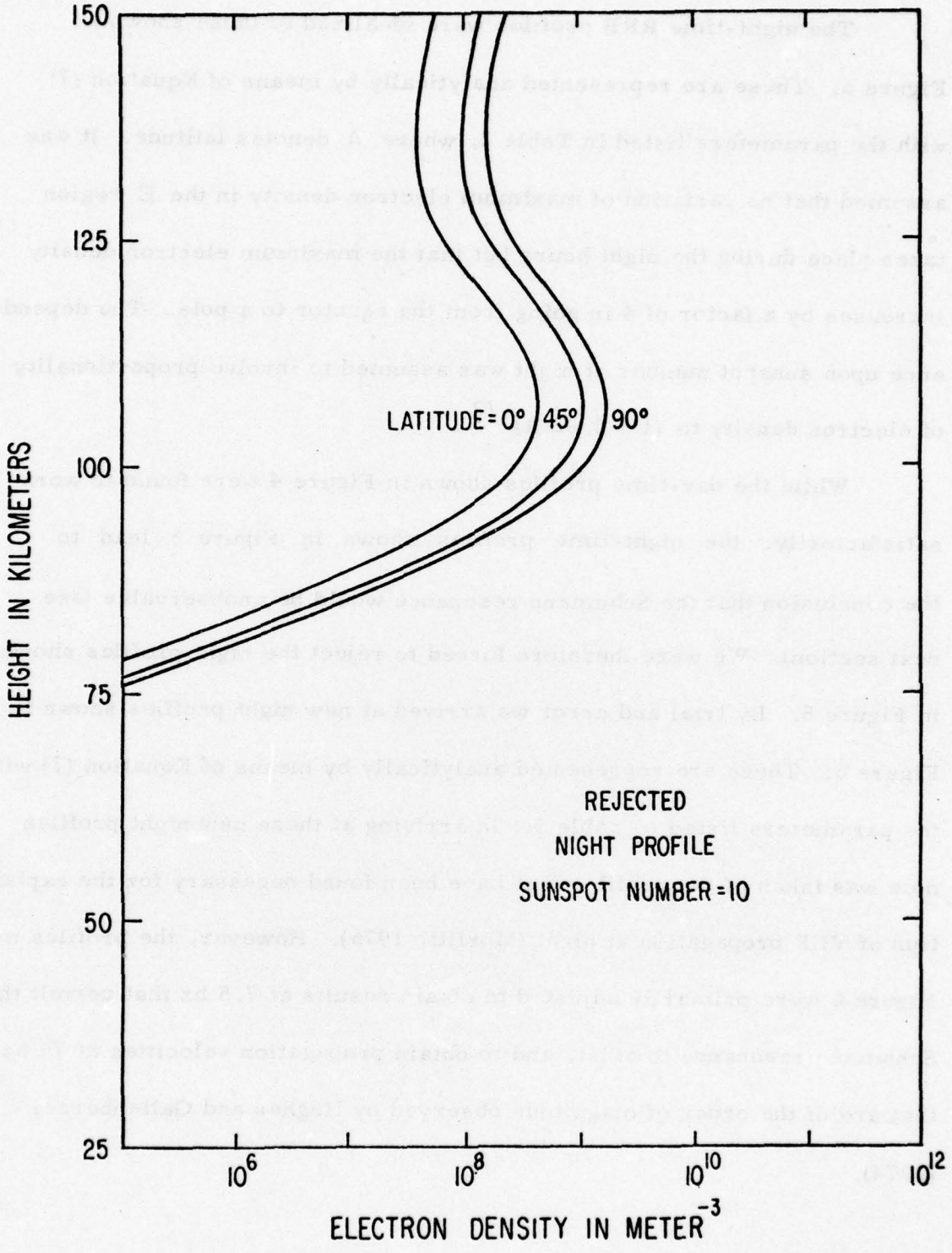

Figure 5. Rejected night-time profiles of electron density.

Table 2

Rejected quiet night profile of electron density (Figure 5)

$m=3$, $N_o=1.83 \times 10^9 (1 + 0.02R)^{1/2} (1 - 0.6 \cos 2\Lambda)$, $z_o=220$

n		1		2		3	
z_n		96		112		127	
$A_{n-1,n}$	0.225		0.0		$-0.10\dot{3}$		$0.01\dot{6}$
B_n		0.2		0.2		0.2	

Table 3

Accepted quiet night profile of electron density (Figure 6)

$m=5$, $N_o=1.83 \times 10^9 (1 + 0.02R)^{1/2} (1 - 0.6 \cos 2\Lambda)$, $z_o=220$

n	1		2		3		4		5	
z_n	80		89		90		112		127	
$A_{n-1,n}$	0.75	0.0		0.75		0.0022727		$-0.10\dot{3}$		$0.01\dot{6}$
B_n	0.65		2.0		2.0		$0.\dot{3}$		0.2	

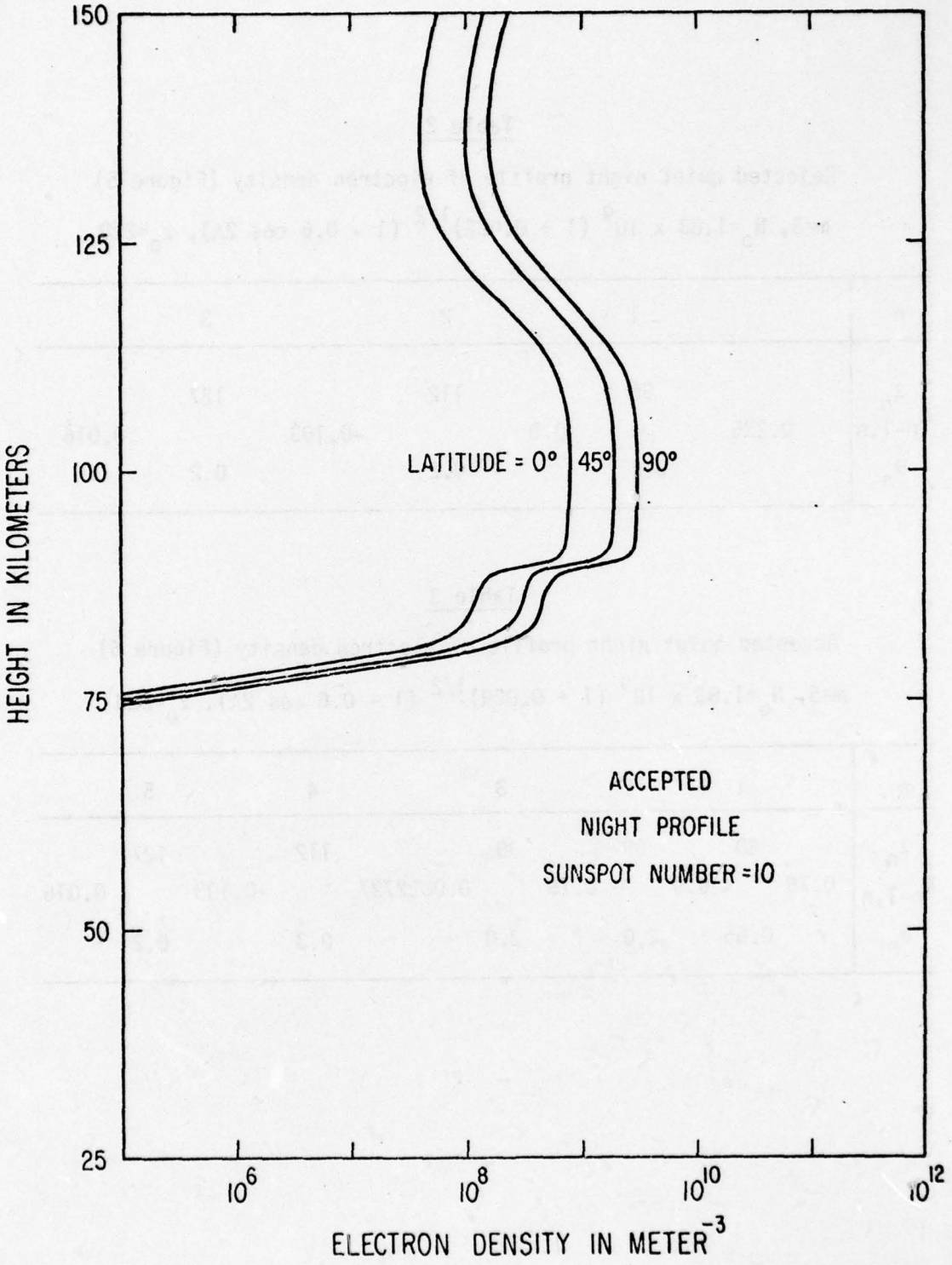

Figure 6. Accepted night-time profiles of electron density.

When the calculations reported in this paper had been carried out it was possible to identify respects in which the profiles shown in Figures 4 and 6 could be improved. In particular, although the night-time profiles in Figure 6 have been used for quiet ionospheric conditions, in fact they probably correspond to a slightly disturbed ionosphere. Under quiet night-time ionospheric conditions the electron densities in the sub-E region ledge shown in Figure 6 should probably be somewhat smaller.

In order to study the effects on ELF communications of enhanced ionization below the E region, calculations were performed for the series of profiles of electron density shown in Figure 7. The profile marked 0 is the profile already adopted for latitude 75° at midday under quiet conditions. For the profiles marked 1, 2 and 3 in Figure 7, the D region electron-density has been increased by 1, 2 and 3 powers of ten, respectively. A similar series of profiles for night conditions is shown in Figure 8. Profile 3 might be appropriate to a polar cap absorption event and profiles 1 and 2 to solar particle events of lesser intensity. A sudden ionospheric disturbance associated with a solar flare might correspond to profile 1 in Figure 7 extrapolated to the rest of the day-time ionosphere on the assumption that the electron density is proportional to $\cos^{1/2}\chi$.

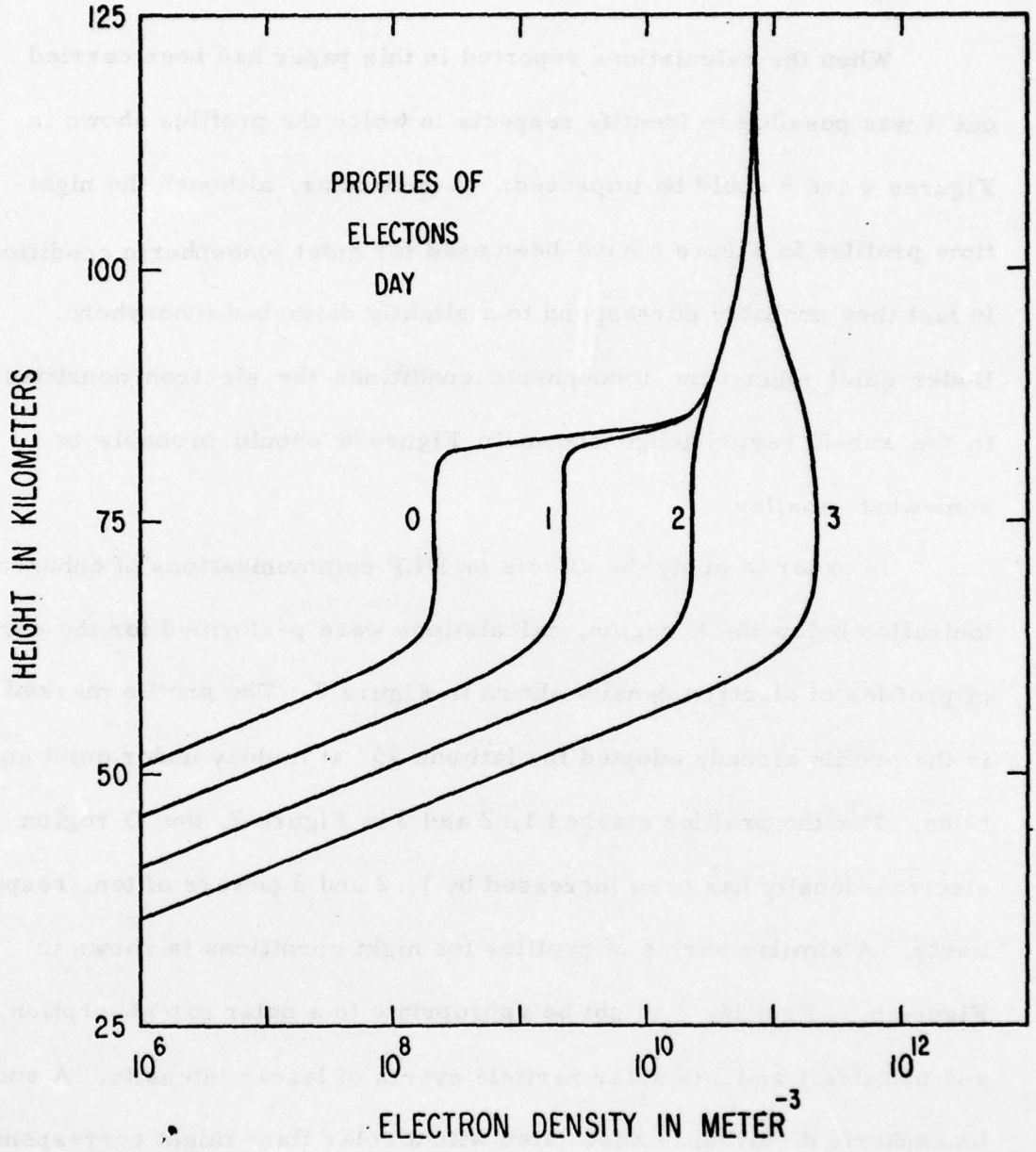

Figure 7. Illustrating three degrees of disturbance in the midday profile of electron density at latitude 75°.

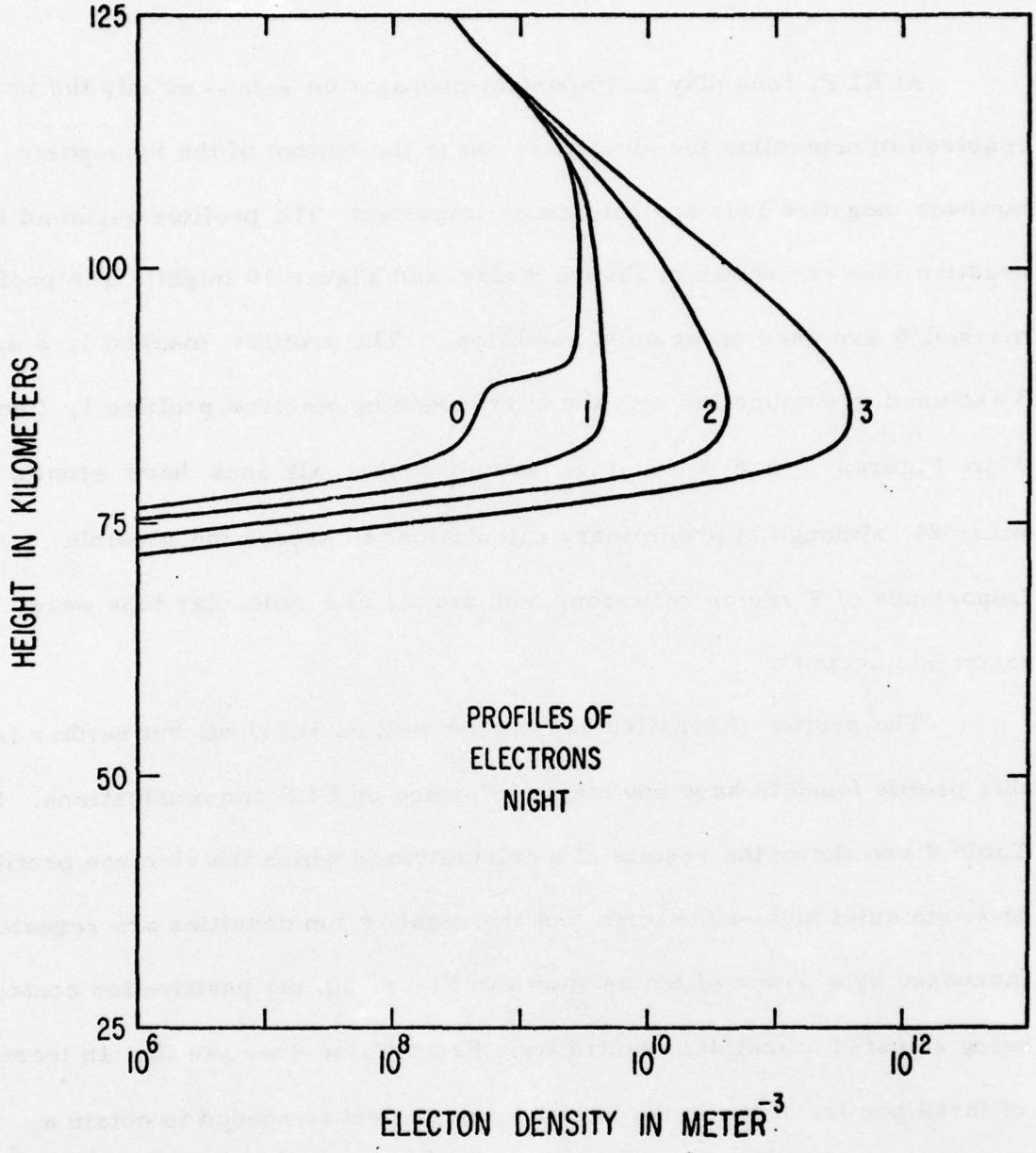

Figure 8. Illustrating three degrees of disturbance in the night-time profile of electron density at latitude 75°.

At ELF, ions play an important propagation role -- mainly the ions required to neutralize the electrons. Near the bottom of the ionosphere, however, negative ions are potentially important. The profiles assumed for negative ions are shown in Figure 9 (day) and Figure 10 (night). The profiles marked 0 are used under quiet conditions. The profiles marked 1, 2 and 3 are used in conjunction with the corresponding electron profiles 1, 2 and 3 in Figures 7 and 8. It is assumed that all ions have atomic mass 29, although in preliminary calculations to assess the possible importance of F region reflexion, both atomic and molecular ions were taken into account.

The profile of negative ions is not well established, but neither is this profile found to have any major influence on ELF communications. In Table 4 are shown the results of a calculation in which the electron profile is given its quiet night-time form, but the negative ion densities are repeatedly increased by a power of ten as shown in Figure 10, the positive ion content being adjusted to maintain neutrality. From Table 4 we see that an increase of three powers of ten in the negative ion content is needed to obtain a modification in c/v (upper number) or attenuation in db Mm^{-1} (lower number).

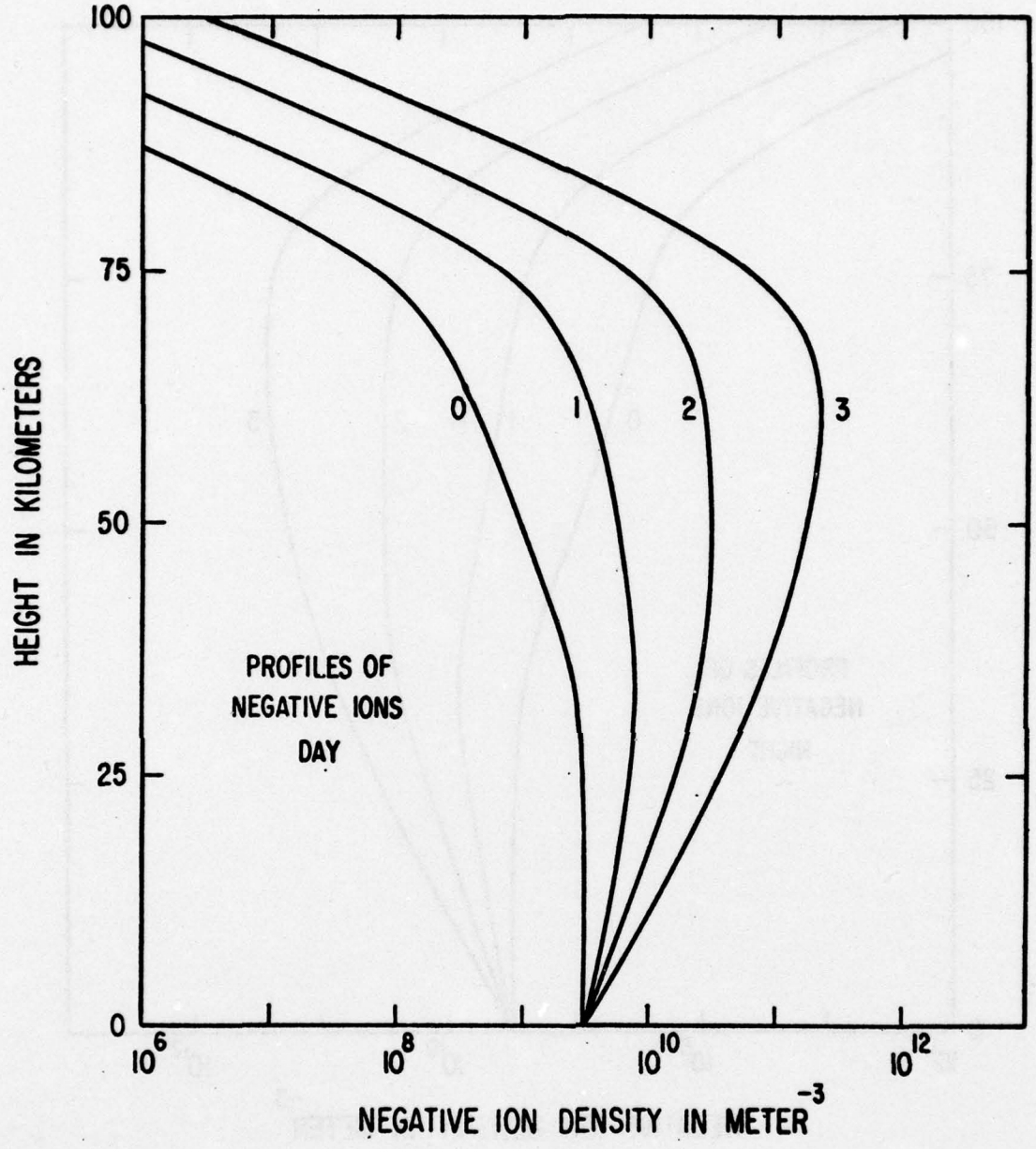

Figure 9. Illustrating four day-time profiles of negative ion density.

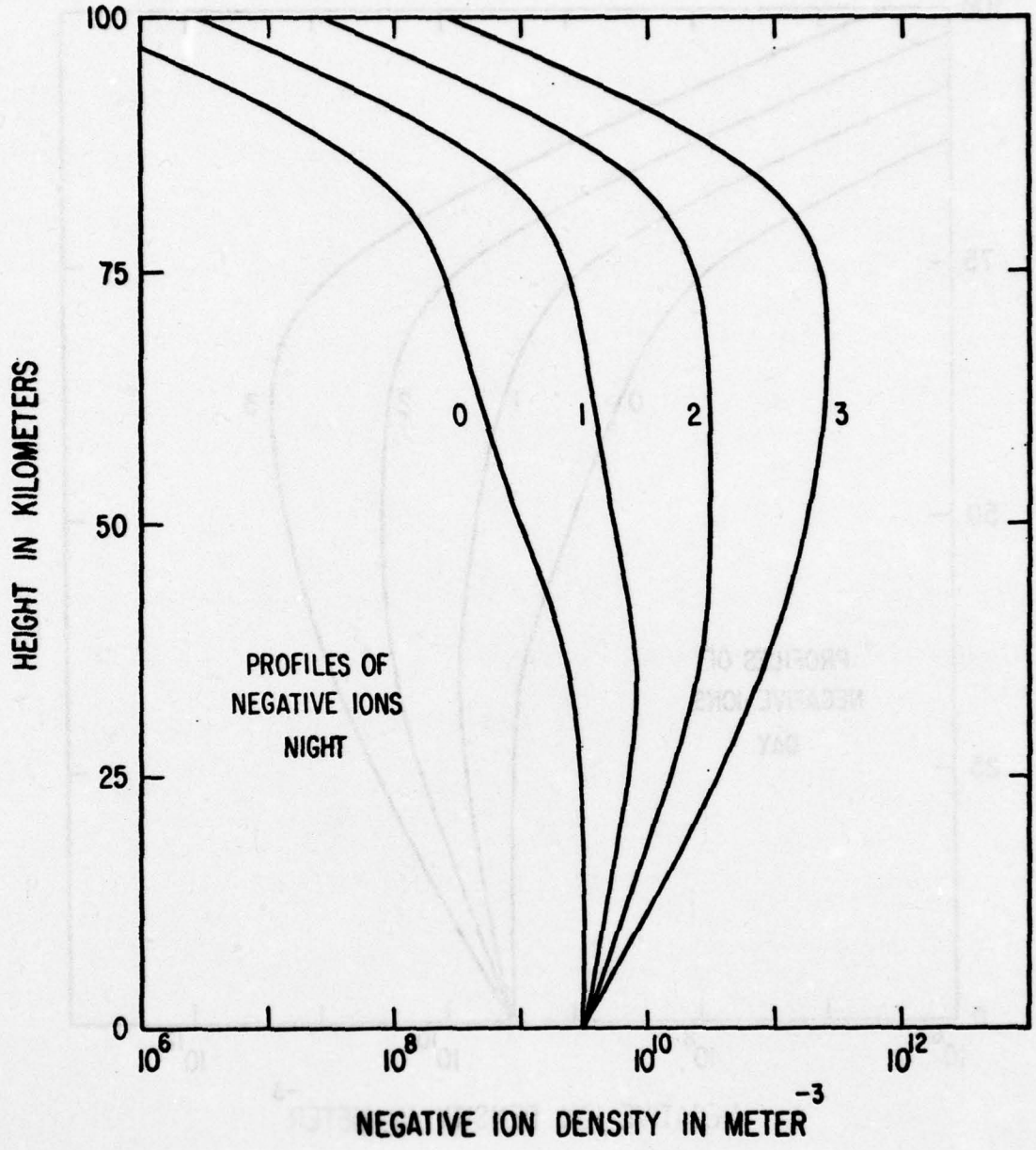

Figure 10. Illustrating four night-time profiles of negative ion density.

Table 4

Effect on c/v and attenuation (db Mm^{-1}) of
enhanced negative ion content
(night, latitude = 45^{o}, sunspot number = 10)

Frequency (hertz)	Negative ion profile number (Figure 10)			
	0	1	2	3
7.5	1.15	1.15	1.15	1.16
	0.32	0.32	0.32	0.33
75	1.13	1.13	1.13	1.10
	1.94	1.94	1.95	1.29

In addition to the profiles of electron density and ion density, knowledge is required of the profiles of collisional frequency. The collisional frequencies involved are ν_e and ν_i, of which the first is that for electrons with neutral molecules and the second is that for ions with neutral molecules. Their values in sec^{-1} as functions of height z in km are assumed to be given by:

$$\left.\begin{aligned} \log_{10} \nu_e &= 5.4 - 0.077\,(z - 90) \\ \log_{10} \nu_i &= 4.6 - 0.077\,(z - 90) \end{aligned}\right\} \qquad (9)$$

At the levels of greatest importance for ELF propagation in the earth-ionosphere transmission line Equations (9) are in reasonable agreement with values given by Banks and Kockarts (1973).

5. The Schumann resonance at 7.5 hz

Using the method outlined in Section 3, calculations of ELF propagation in the earth-ionosphere transmission line, based on the quiet ionospheric profiles described in the previous section, were first undertaken at a frequency of 7.5 hz in order to verify that results at this frequency are approximately in accord with the facts concerning the existence of the Schumann resonance (Balser and Wagner, 1962a, b; Madden and Thompson, 1965; Galejs, 1972; Jones, 1974). Detailed calculations of the quality factor Q of the earth-ionosphere cavity resonance were not undertaken. It was

merely desired to verify that the Q is of roughly the right order of magnitude. This means that the total attenuation for an average circuit of the earth at 7.5 hz must be appreciably less than one neper, say of the order of a few decibels.

Let us consider an equinoctial situation at a time when the sunspot number is 10, and let us calculate the total attenuation at 7.5 hz for one circuit of the earth along the midday and midnight meridians. On the midday meridian at latitude 45° using the profiles described in the previous section, Figure 2 takes the form shown in Figure 11. We see that reflexion takes place at about 86 km. Application of Equations (5) and (6) then leads to a value of c/v of 1.05 and an attenuation rate of 0.10 db Mm^{-1} due to leakage of energy into the region above 86 km. After adding attenuation due to collisional absorption below 86 km, the total ionospheric attenuation rate in the earth-ionosphere transmission line at 7.5 hz amounts to 0.15 db Mm^{-1}. Repetition of the calculation at other latitudes along the midday meridian gives attenuation rates varying from 0.03 db Mm^{-1} at the equator to 0.21 db Mm^{-1} at latitude 75°. Consequently, the total ionospheric attenuation at 7.5 hz along the midday meridian from pole to pole is between 2 and 3 db, while the total ionospheric attenuation along the equator from sunrise to sunset via midday is less than 1 db. It follows that

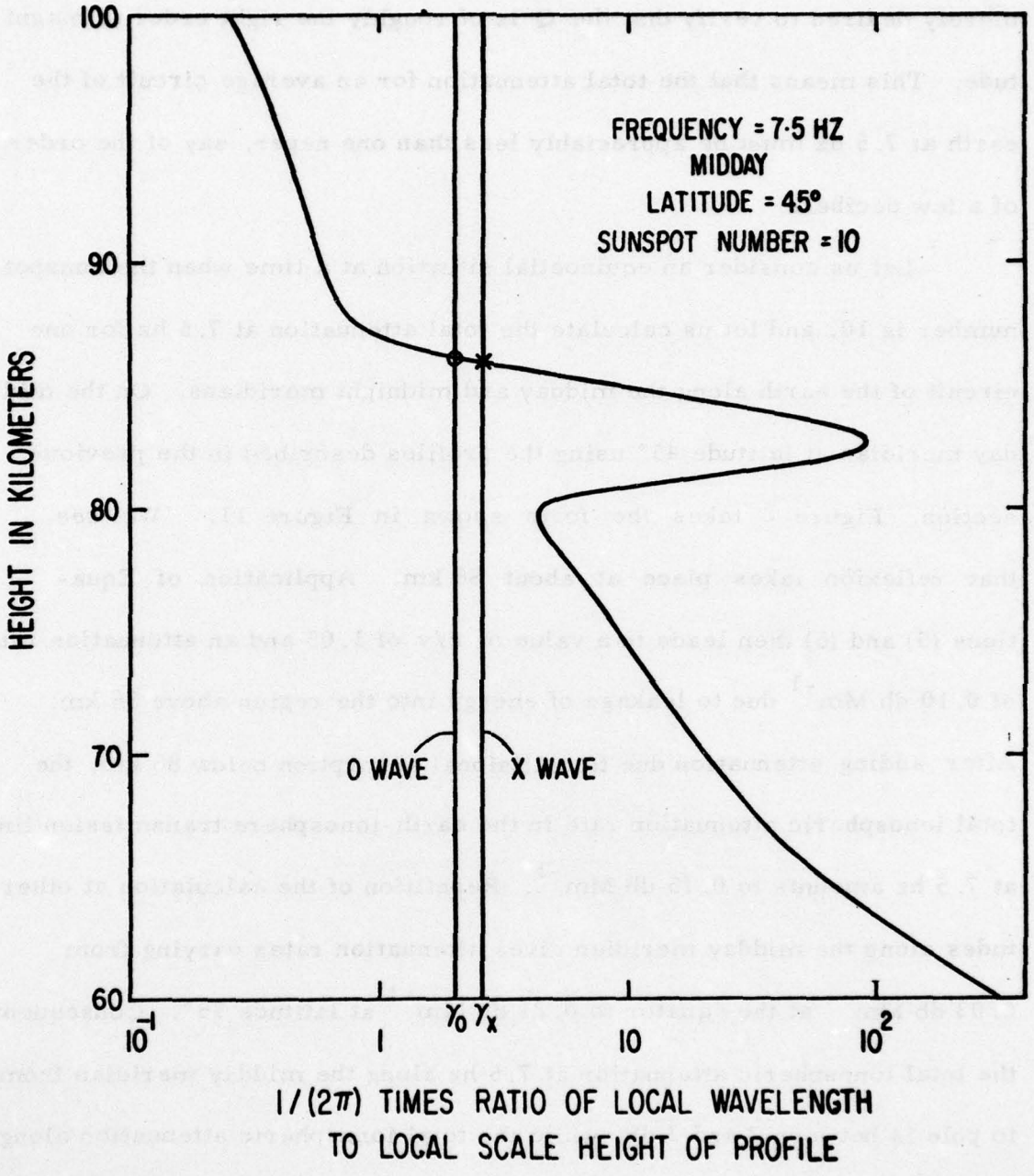

Figure 11. Illustrating determination of the day-time height of reflexion at the Schumann resonant frequency.

the day-time profiles shown in Figure 4 are entirely consistent with the Q of the earth-ionosphere cavity being high enough for the Schumann resonance to be easily observable.

It may be mentioned that the calculation just described was carried out not merely for the profiles of electron density shown in Figure 4 but also for a number of other potential day-time profiles. In particular, an investigation was made of the importance of the steep gradient of electron density shown in Figure 4 just above the 80 km level. The more this gradient was reduced the higher were the losses at 7.5 hz. Progressive reduction of the gradient quickly produced a situation in which the losses become so high that the Schumann resonance would be difficult to observe. Thus, not only are the day-time profiles presented in Figure 4 on the basis of the work of Rawer, Ramakrishnan and Bilitza (1975) acceptable for explaining the existence of the Schumann resonance, but the steep gradient of electron density just above the 80 km level is an essential feature of this acceptability.

Let us now make similar calculations at 7.5 hz for the midnight meridian. Using the night profiles presented in Figure 5, one obtains the results shown in Figure 12. The attenuation rate varies from 0.07 db Mm^{-1} at the equator to 1.76 db Mm^{-1} at a pole. The total ionospheric attenuation at 7.5 hz along the midnight meridian from pole to pole is about 20 decibels. This is much too high; if this value were realistic there would be no phenomenon of Schumann resonance. One is forced to conclude that the night profiles presented in Figure 5 are in error. An analysis was therefore

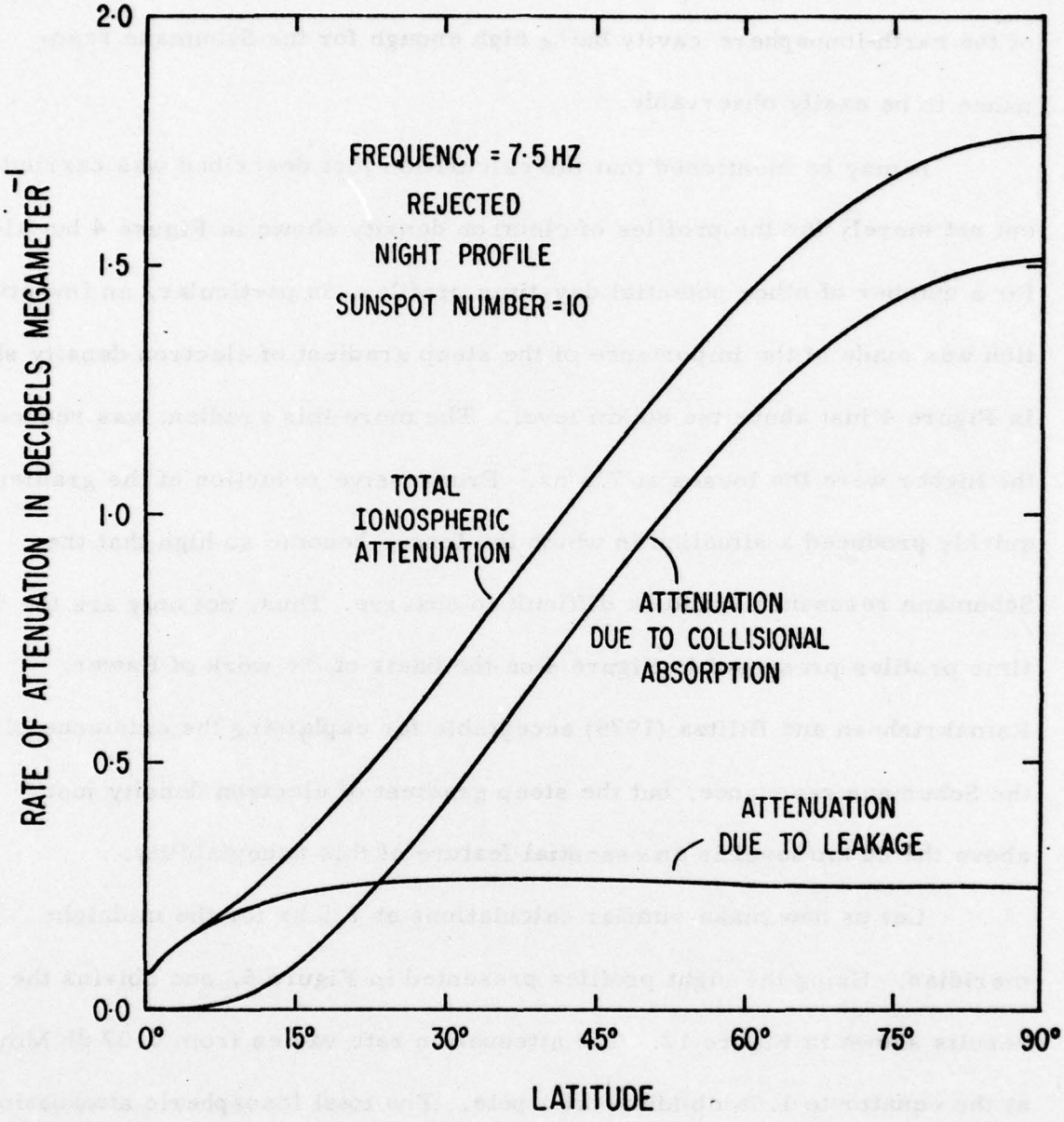

Figure 12. Illustrating the attenuation rates at the Schumann resonant frequency for the rejected night profile.

made to ascertain the cause of this unexpectedly high night-time loss at 7.5 hz.

Figure 12 shows that, due solely to leakage of energy from the earth-ionosphere transmission line into the region above the level of reflexion, the attenuation from pole to pole along the midnight meridian at 7.5 hz is somewhat greater than the total ionospheric attenuation from pole to pole along the mid-day meridian. The prime cause of the substantial leakage from the night hemisphere is the low maximum electron density in the nocturnal E region. The value of this maximum electron density is not available for major adjustment, although the values used in Figure 5 are probably too low. Calculations showed that variation of the night-time profile of electron density, keeping the maximum electron density fixed, had little influence on the loss due to leakage of energy into the region above the level of reflexion. For the same maximum electron density in the E region, the leakage loss is greater in polar regions than in equatorial regions due to the effect of the earth's magnetic field. However, this is largely off-set in our calculations by the fact that, in Figure 5, higher nocutrnal maximum electron densities have been assumed for the E region in polar regions than in equatorial regions. There is little that can be done to reduce significantly the leakage loss through the E region at 7.5 hz at night.

It might be wondered whether reflexion from the F region at night might be significant at 7.5 hz (Galejs, 1972). But ionic attenuation is

important, especially at levels where ν_i is of the order of the angular ionic gyro-frequency, that is, in the vicinity of 120 km. Consequently, the wave reflected from the F region at 7.5 hz is weakened to the point of unimportance.

Even though leakage of energy at 7.5 hz through the nocturnal E region is higher than might have been anticipated, nevertheless this loss is merely such that, when combined with the losses in the day hemisphere, the Q for the earth-ionosphere cavity is of the order of magnitude that is observed. Figure 12 shows that it is collisional absorption below the level of reflexion that is the cause of the difficulty at 7.5 hz with the profiles presented in Figure 5.

Part of the reason why the nocturnal attenuation rate due to collisional absorption is so high at 7.5 hz arises from ionic absorption already mentioned. The level of reflexion at 7.5 hz for the profiles shown in Figure 5 is about 100 km, and at this level ionic attenuation is more important than electronic attenuation. Moreover, on the under side of the E region, absorption due to ionic collisions does not decrease with increase of height as the ionic collisional frequency decreases. On the contrary the absorption due to ionic collisions increases with height as the ionic collisional frequency decreases. To prevent ionic attenuation from being important at night at 7.5 hz a significantly lower height of reflexion is needed.

However, even the electronic contribution to the nocturnal absorption at 7.5 hz is serious for the profiles exhibited in Figure 5 because the gradient of

AD-A034 129 CALIFORNIA UNIV SAN DIEGO LA JOLLA F/G 4/1
THE RELATION BETWEEN IONOSPHERIC PROFILES AND ELF PROPAGATION I--ETC(U)
NOV 76 H G BOOKER N00014-75-C-0959
UNCLASSIFIED NL

2 OF 2
ADA034129

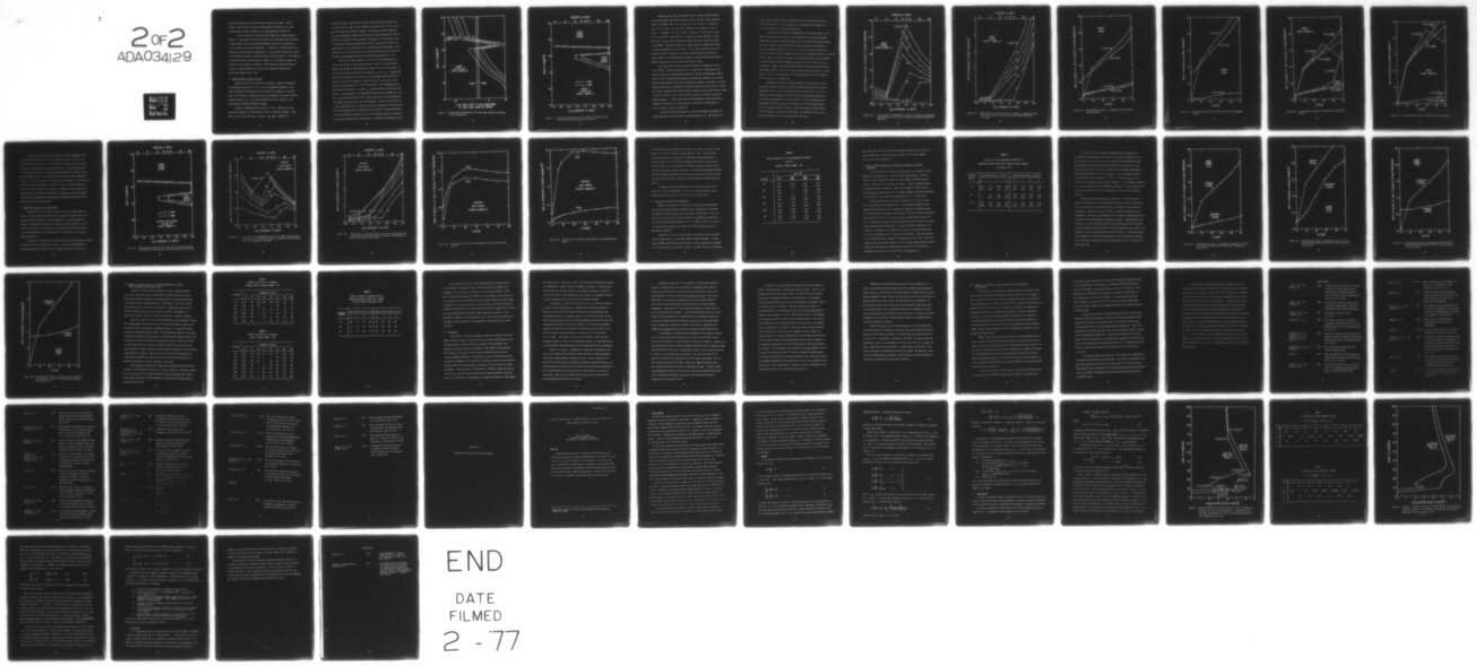

END

DATE
FILMED
2 - 77

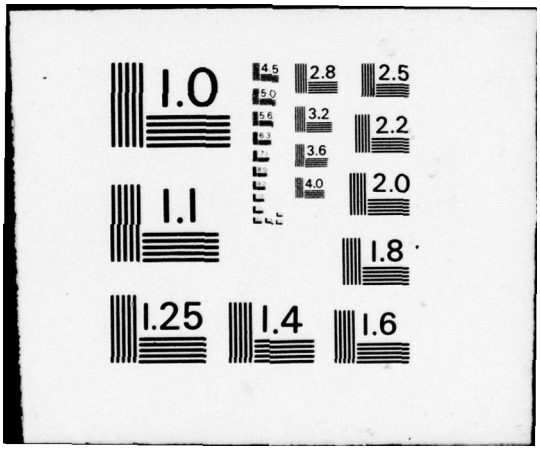
1.0
1.1
1.25
1.4
1.6
1.8
2.0
2.2
2.5
2.8
3.2
3.6
4.0
4.5
5.0
5.6

electron density on the underside of the E region is not high. Consequently, both electronic and ionic attenuation are operative over a substantial range of height, leading to the result depicted in Figure 12.

It is now clear what is wrong with the night-time profiles shown in Figure 5. The gradient of electron density on the underside of the nocturnal E region needs to be increased substantially and the level of reflexion at 7.5 hz needs to be lowered substantially. In addition, a modest increase in maximum electron density is appropriate. It was in this way that we arrived at the night-time profiles of electron density shown in Figure 6. The ledge of ionization below the main E region in Figure 6 is not needed to explain the existence of the Schumann resonance. This ledge was added subsequently in order to acquire flexibility in the results obtained at frequencies a power of ten higher than 7.5 hz.

6. Midday behavior in the ELF band

Having arrived at a model of the ionosphere capable of explaining the Schumann resonance at 7.5 hz, let us investigate propagation in the earth-ionosphere transmission line as a function of frequency in the ELF band. We continue to consider an equinoctial situation at an epoch when the sunspot number is 10. Let us first examine day-time conditions, and especially the situation existing at midday.

Figure 11 illustrates the fact that, at 7.5 hz, reflexion from the day-time ionosphere is at about 86 km, that is, from the E region. At the upper end of the ELF band, however, day-time reflexion is

from the D region. The level of reflexion must therefore drop from the E region to the D region as the frequency increases from 7.5 hz. This is part of the process, deduced in paper 1, whereby the level of reflexion rises as the frequency falls in the ELF band, leading ultimately to penetration of the ionosphere at micropulsation frequencies. In particular, there is a frequency-band where penetration of the D region sets in and the E region takes over as the location of the primary reflecting stratum. What we have seen in the previous section is that penetration of the D region is already an accomplished fact when the frequency has fallen to 7.5 hz.

The curve shown in Figure 11 for 7.5 hz (strictly speaking, two curves, one for the O wave and one for the X wave, too close to draw separately) changes as the frequency is varied. As the curve changes, so also do the intersections with the ordinates at γ_O and γ_X. Consequently the levels of reflexion for the O and X waves change with the frequency. The way in which this happens is shown in Figure 13, where curves are drawn for frequencies of 7.5, 30, 75 and 300 hz. The resulting intersections with the ordinates at γ_O and γ_X therefore behave as shown in Figure 14. In this diagram, the calculated intersections are marked as O for the O wave and X for the X wave. The intersections were calculated for the frequencies shown at the top of the diagram. The intersections for the O wave and those for the X wave each lie on a continuous curve possessing an S bend insufficiently well delineated by the number of points calculated. In this and subsequent diagrams the actual calculated points are connected by rectilinear segments as an alternative to sketching in continuous curves.

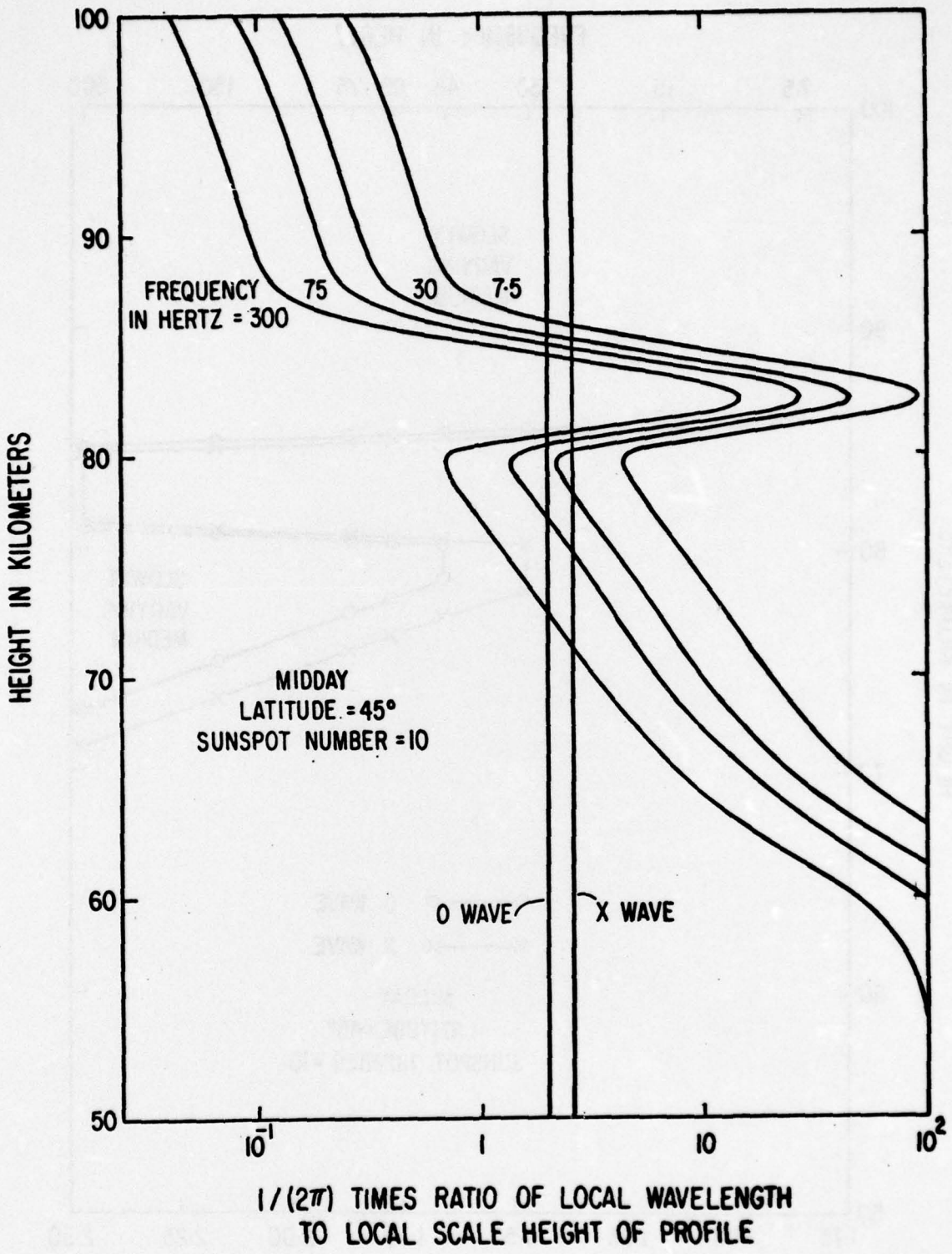

Figure 13. Illustrating determination of the day-time heights of reflexion at four frequencies.

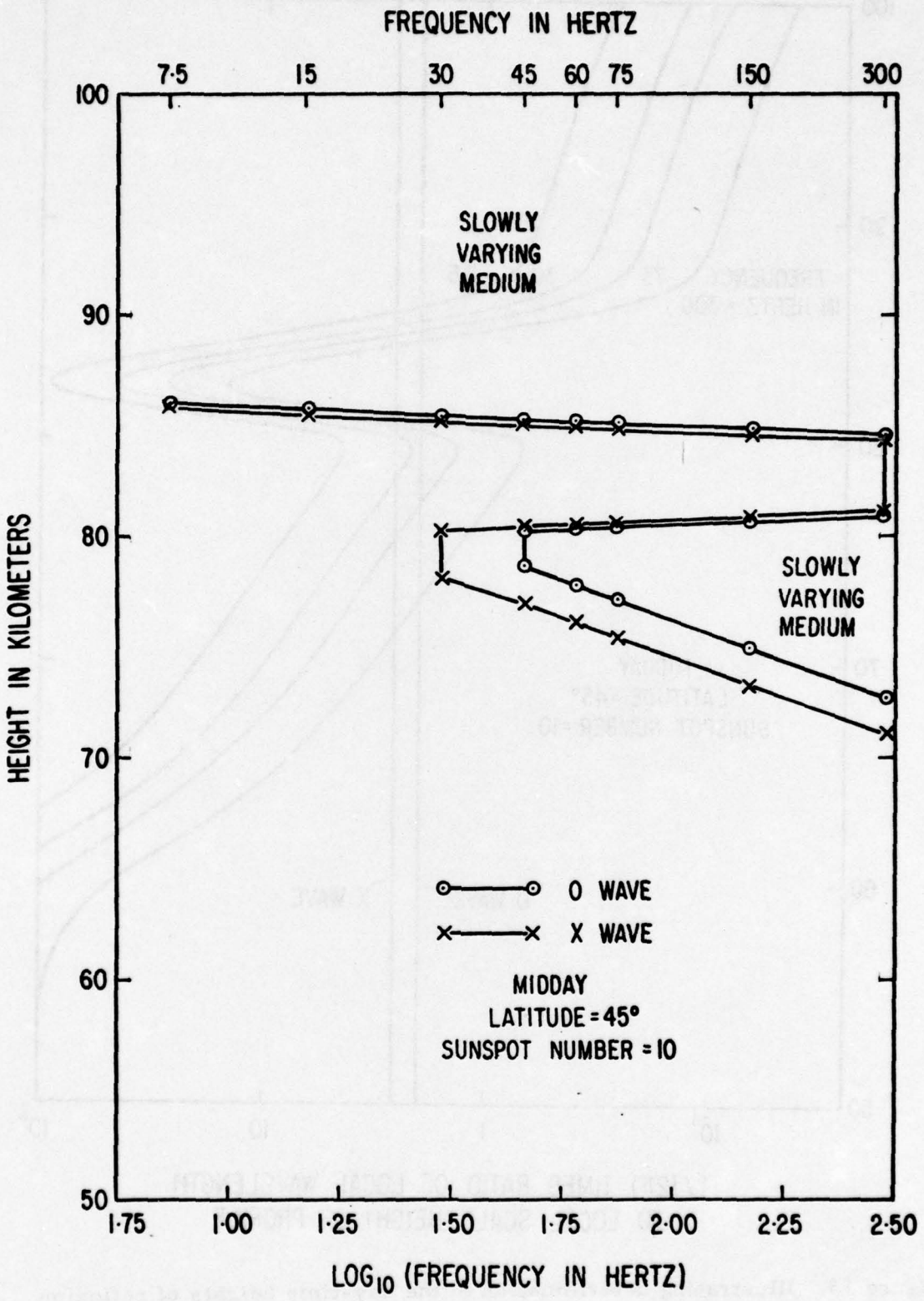

Figure 14. Illustrating penetration of the day-time D region as the frequency descends through the ELF band.

Reflexion takes place principally from the vicinity of the boundary of the region where the medium becomes slowly varying. Taken literally, Figure 14 implies that, at 7.5 and 15 hz, the X wave is reflected from the E region, but at 30 hz reflexion has dropped to the D region. Likewise, for the O wave, reflexion is from the E region at 7.5, 15 and 30 hz, but from the D region from 45 hz upwards. In fact, of course, transfer of the reflecting stratum from one region to the other is not sudden. Reflexion from the E region weakens as reflexion from the D region strengthens, and vice-versa. The O wave and the X wave each possess a band of frequencies over which reflecting strata in both the D and E regions are simultaneously important, and this band is at somewhat higher frequencies for the O wave than for the X wave.

It is clear that a theory is required capable of dealing with a situation in which a reflecting stratum in the D region and a reflecting stratum in the E region are simultaneously important. The theory presented in paper 1 has not yet been adequately developed for handling this situation. In the meantime, we shall apply the theory in the form given in paper 1 on either side of the frequency-band where simultaneous reflexion from the D and E regions is dominant. When a diagram such as that shown in Figure 14 shows that primary reflexion of the O and X waves is from different regions, we shall not apply the theory of paper 1. On the other hand, when the diagram shows that primary reflexion of both waves is from the same region then we shall apply the theory of paper 1 without modification.

It should be noted that Figure 14 is drawn for midday in latitude 45° at the equinox for an epoch when the sunspot number is 10. The location of

the frequency-band involved in penetration of the D region varies with time of day, latitude, season of the year, and epoch in the sunspot cycle. It is also shifted by ionospheric disturbance.

For equinoctial conditions at midday when the sunspot number is 10, Figure 15a shows the variation of c/v with frequency at various latitudes. The broken sections of the plots indicate where transfer from predominantly E region reflexion to predominantly D region reflexion is taking place. Note the associated major increase in c/v. Note also that the broken sections of the plots should be replaced not merely by a single S bend but by a double S bend. This is because the transfer from predominantly E region reflexion to predominantly D region reflexion takes place for the X and O waves in succession. Figure 15a shows that the frequency-band where the transition takes place is of the order of 75-150 hz near the equator whereas it is of the order of 15-45 hz near the poles. Corresponding plots for the attenuation rate are shown in Figure 15b.

The difference between a sunspot number of 10 and one of a 100 is indicated in Figures 16a and b, where the latitude variations of c/v and of attenuation rate are shown for frequencies of 7.5 and 75 hz. At 7.5 hz reflexion is predominantly from the E region at all latitudes and there is no significant dependence on sunspot number. At 75 hz reflexion is predominantly from the D region at all latitudes for a high sunspot number. For a low sunspot number, however, reflexion transfers to the E region near the equator. Except near the equator, the attenuation rate at 75 hz decreases somewhat as the sunspot number increases.

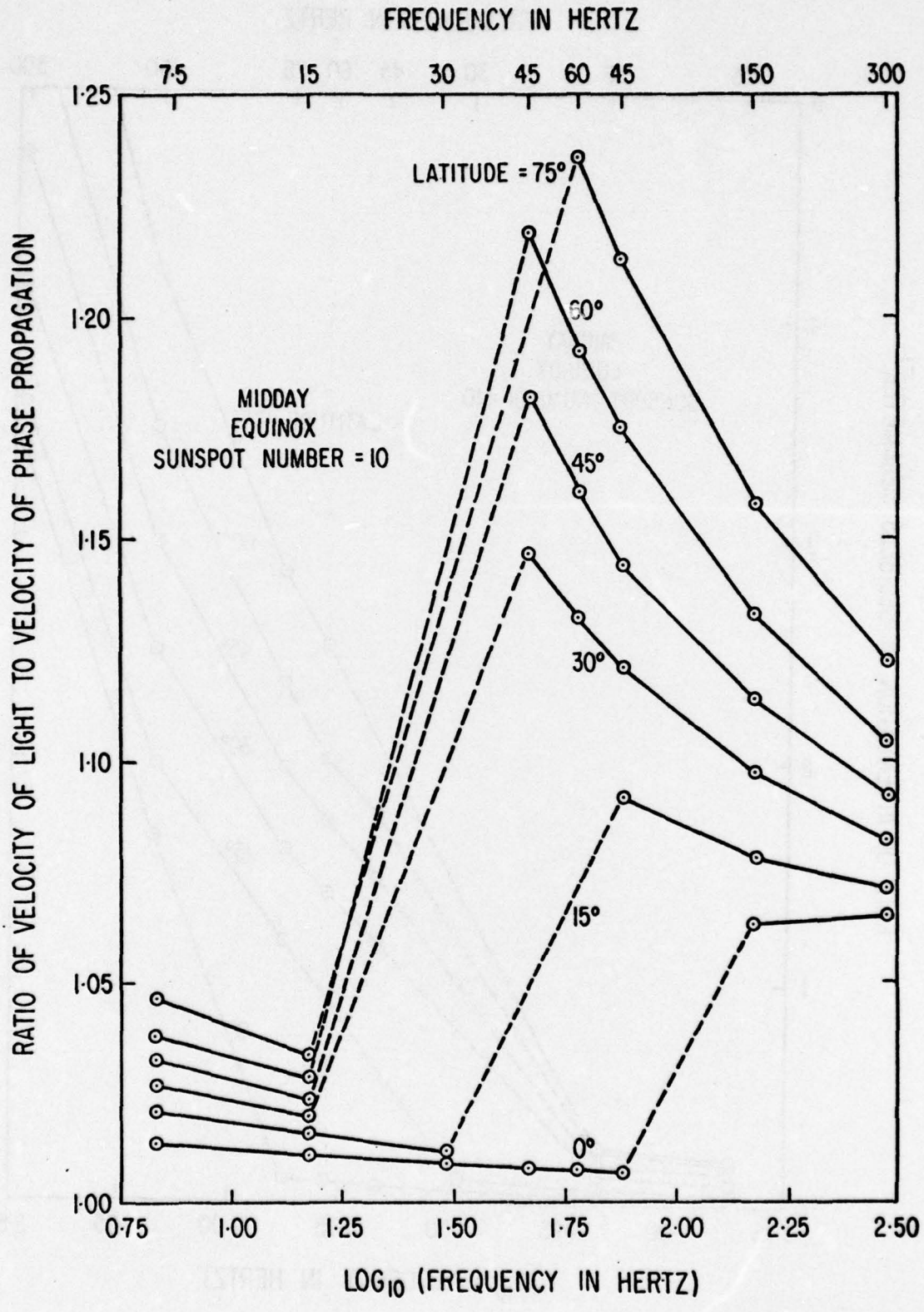

Figure 15a. Illustrating, for propagation velocity, the effect of penetrating the day-time D region as the frequency descends through the ELF band.

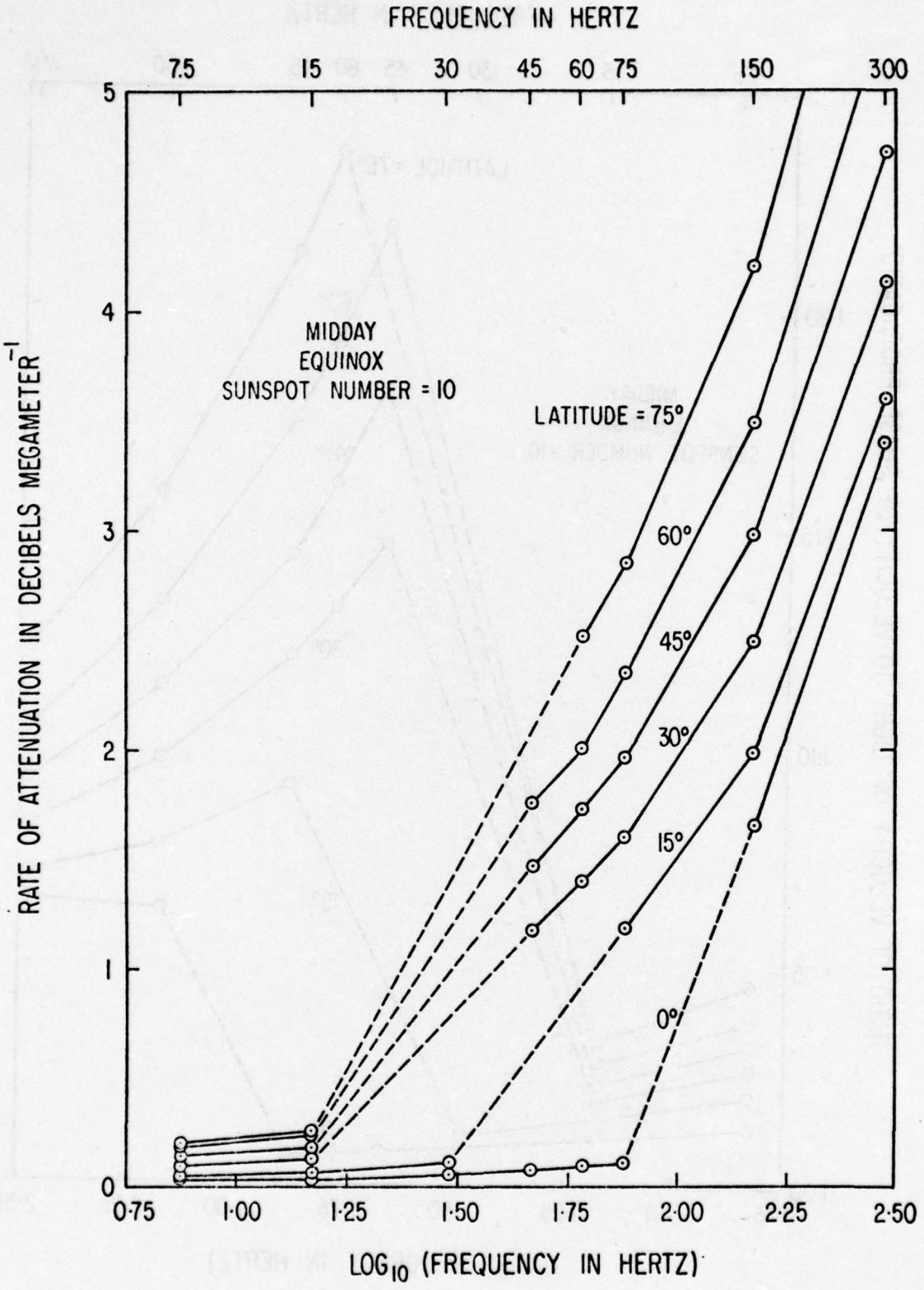

Figure 15b. Illustrating, for attenuation rate, the effect of penetrating the day-time D region as the frequency descends through the ELF band.

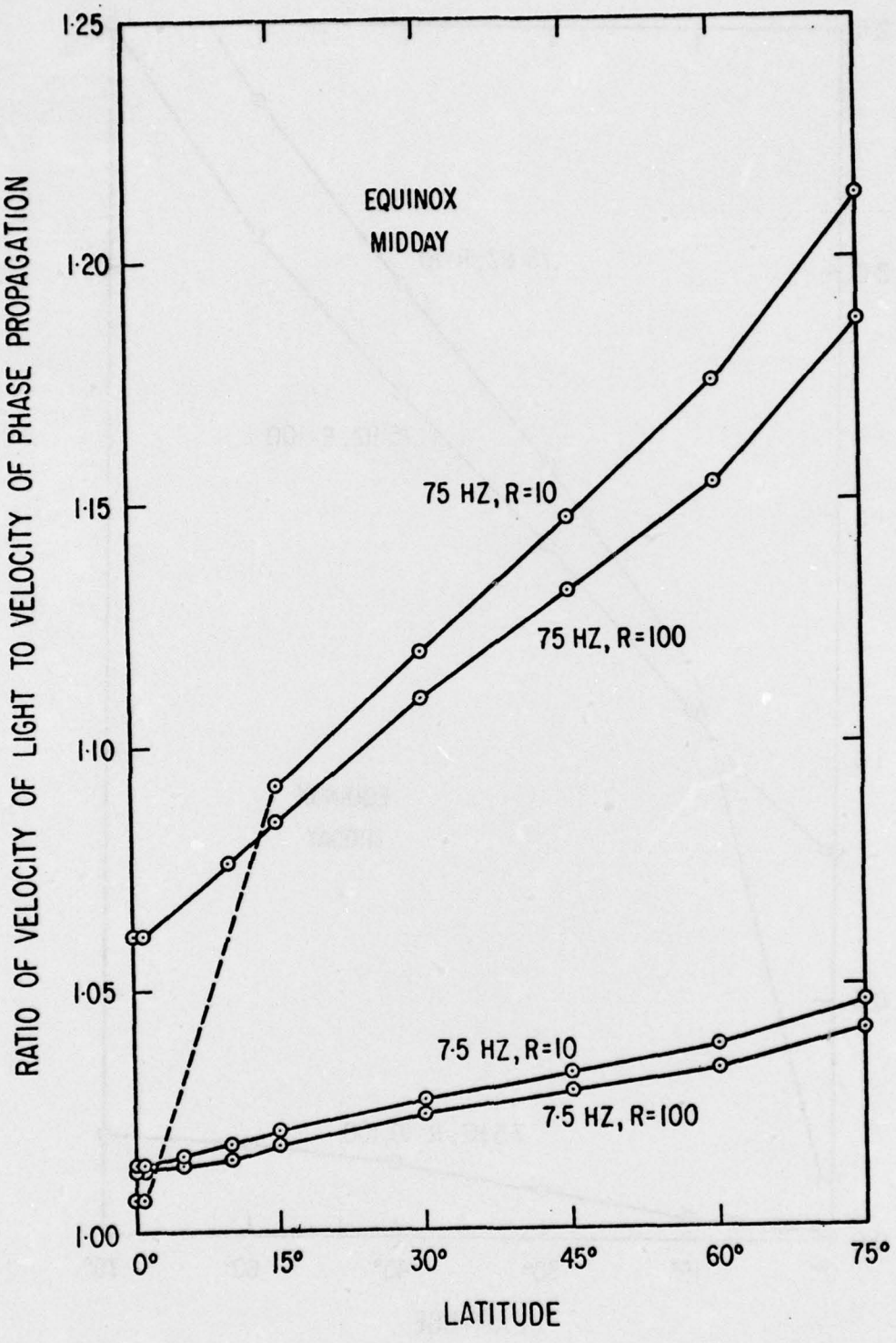

Figure 16a. Illustrating the change in propagation velocity with sunspot number.

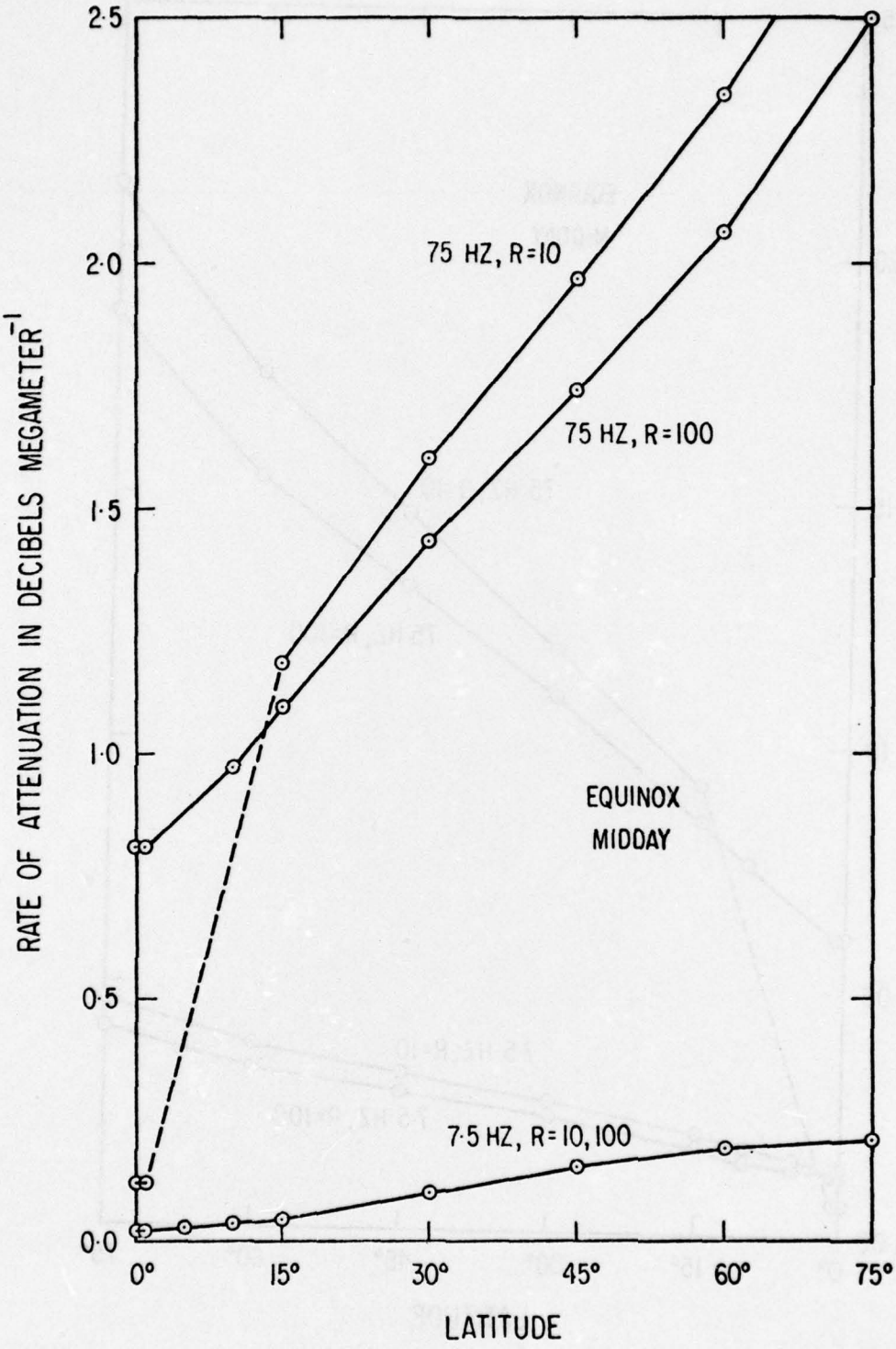

Figure 16b. Illustrating the change in attenuation rate with sunspot number.

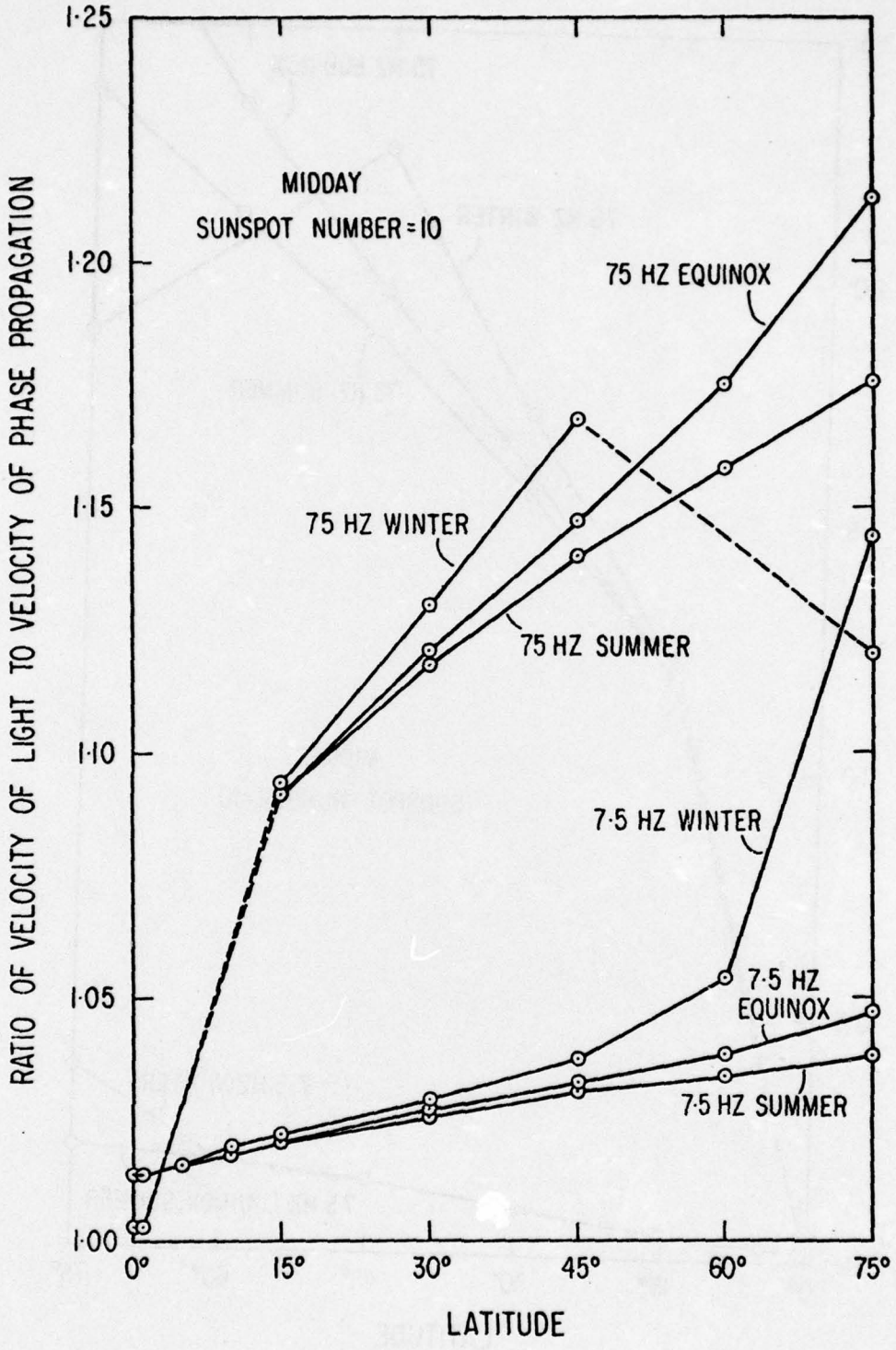

Figure 17a. Illustrating the change in propagation velocity with season.

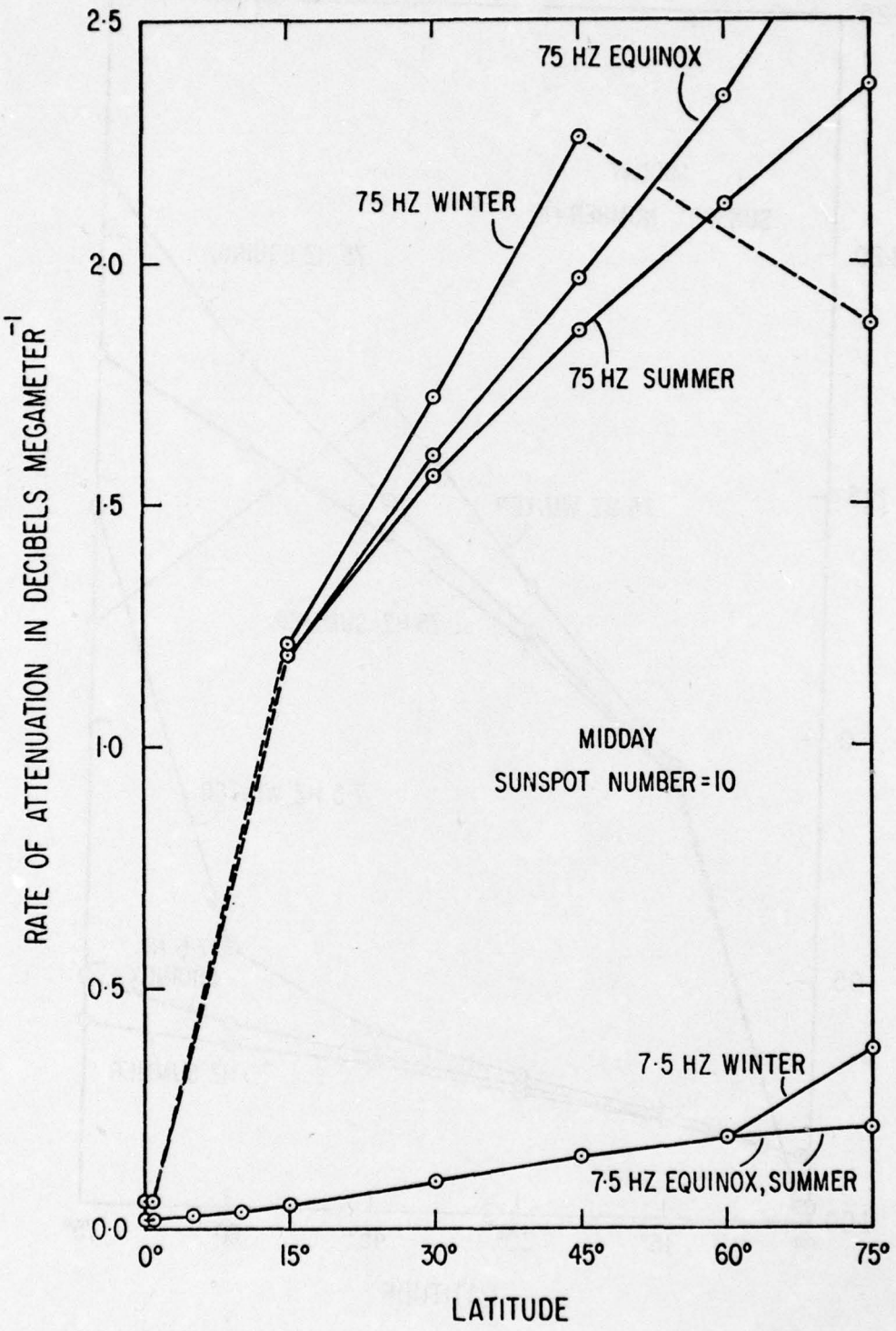

Figure 17b. Illustrating the change in attenuation rate with season.

An indication of the seasonal variation in ELF propagation in the earth-ionosphere transmission line is given in Figures 17a and b for a sunspot number of 10. For 7.5 hz and 75 hz the variations of c/v and of attenuation rate with latitude are shown for winter, equinox and summer. In winter the terminator is crossed between latitudes 60° and 75° so that the calculations for 75° are made using the night-time profile indicated in Figure 6. At 7.5 hz reflexion is from the E region under all circumstances. At 75 hz reflexion is primarily from the D region in middle latitudes but transfers to the E region at low latitudes. Reflexion at 75 hz is also primarily from the D region at high latitudes in summer and at an equinox, but in winter at high latitudes simultaneous reflexion from strata in the D and E regions becomes important.

7. Night-time behavior in the ELF band

Replacement of the day-time profiles of electron density shown in Figure 4 by the night-time profiles shown in Figure 6 (together with corresponding action for negative ions using profiles 0 in Figures 9 and 10) results in replacement of Figure 14 by Figure 18 and of Figures 15a and b by Figures 19a and b, respectively. The resulting nocturnal variations of c/v and of attenuation rate with latitude at 7.5 hz and 75 hz are shown in Figures 20a and b.

In Figure 19a reflexion at the lower end of the frequency-range is from the main part of the E region above 90 km. At this end of the frequency-band the progressive decrease of c/v to values less than 1.1 has to be

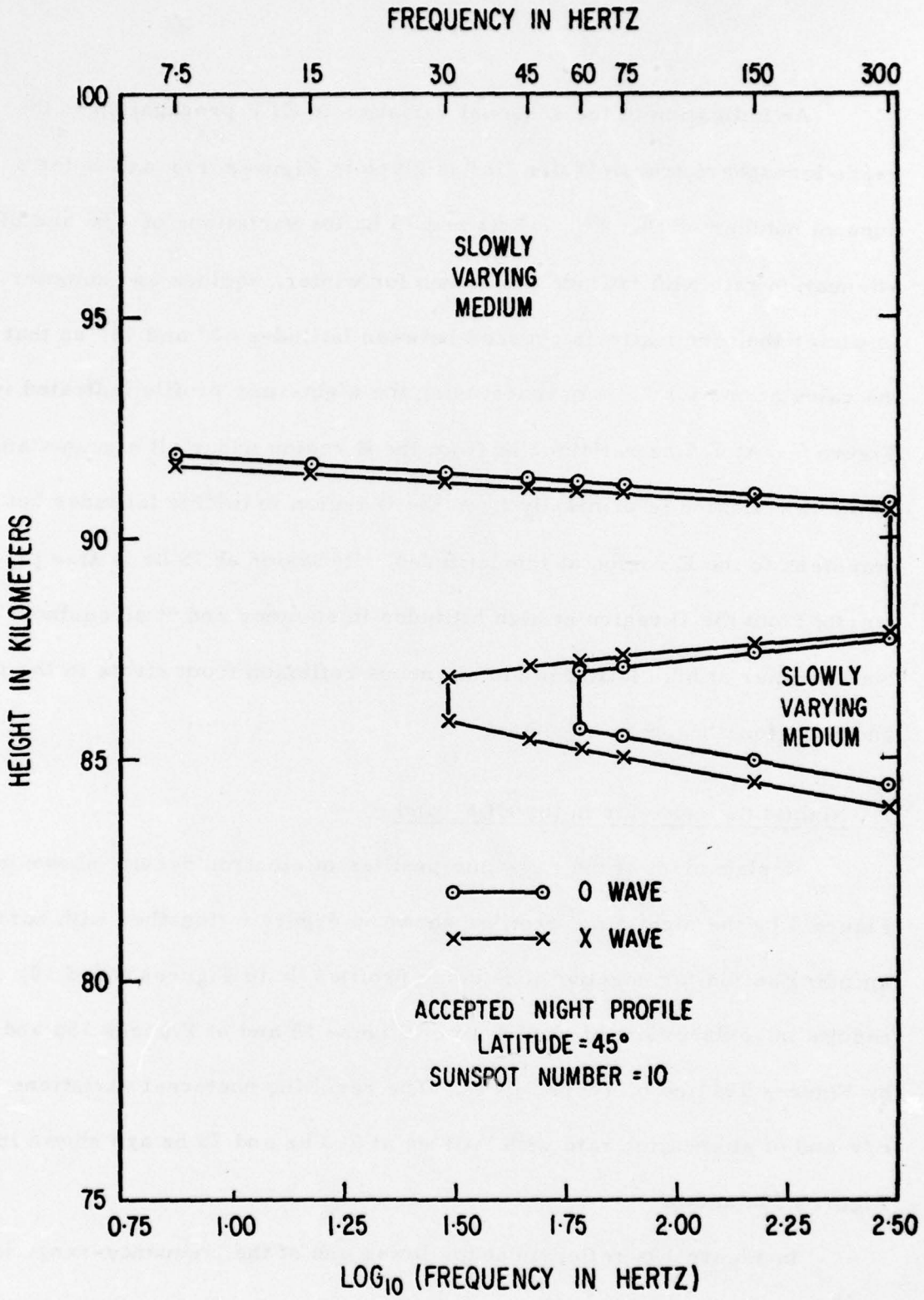

Figure 18. Illustrating penetration of the night-time sub-E region ledge of ionization as the frequency descends through the ELF band.

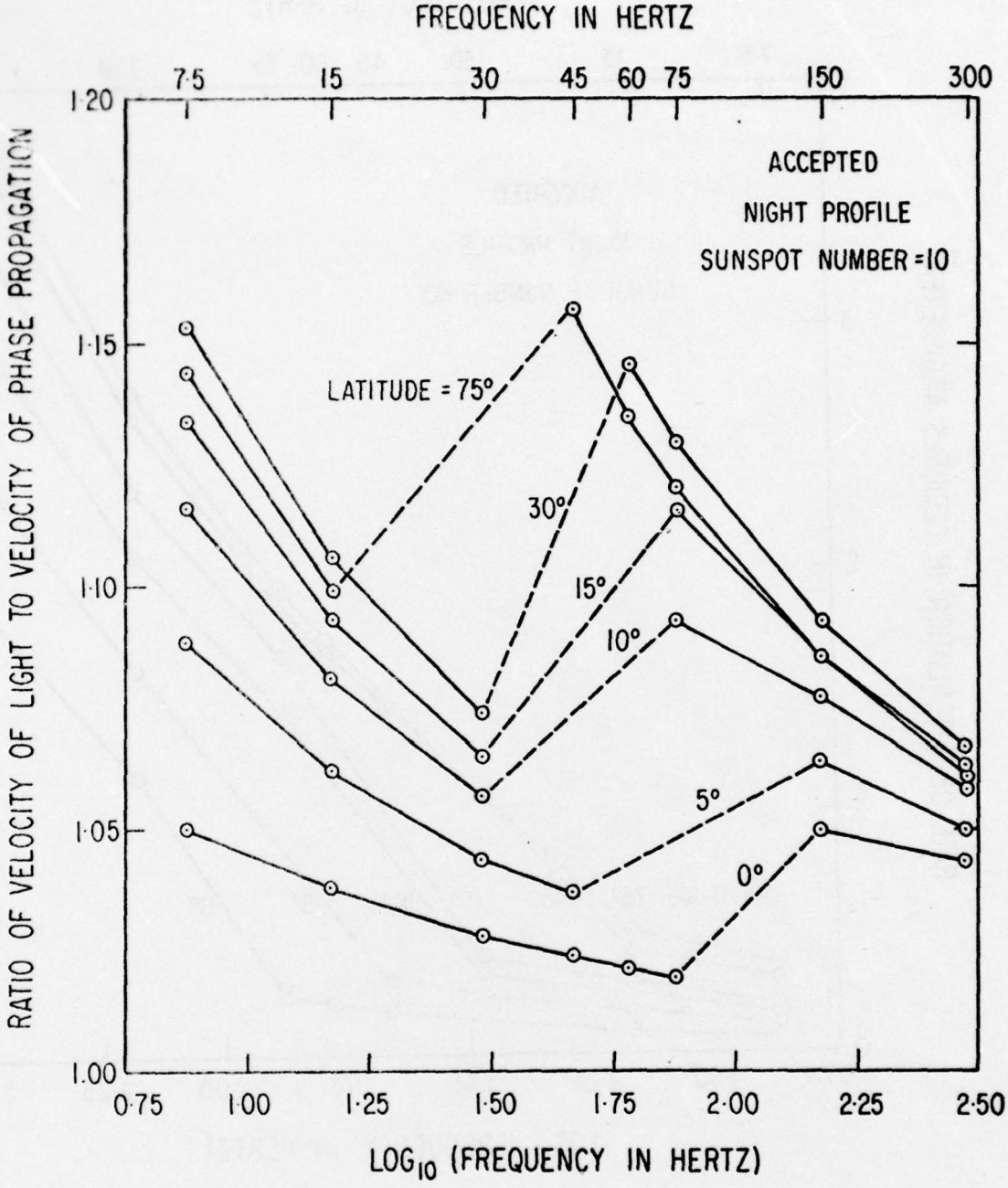

Figure 19a. Illustrating, for propagation velocity, the effect of penetrating the night-time sub-E region ledge of ionization as the frequency descends through the ELF band.

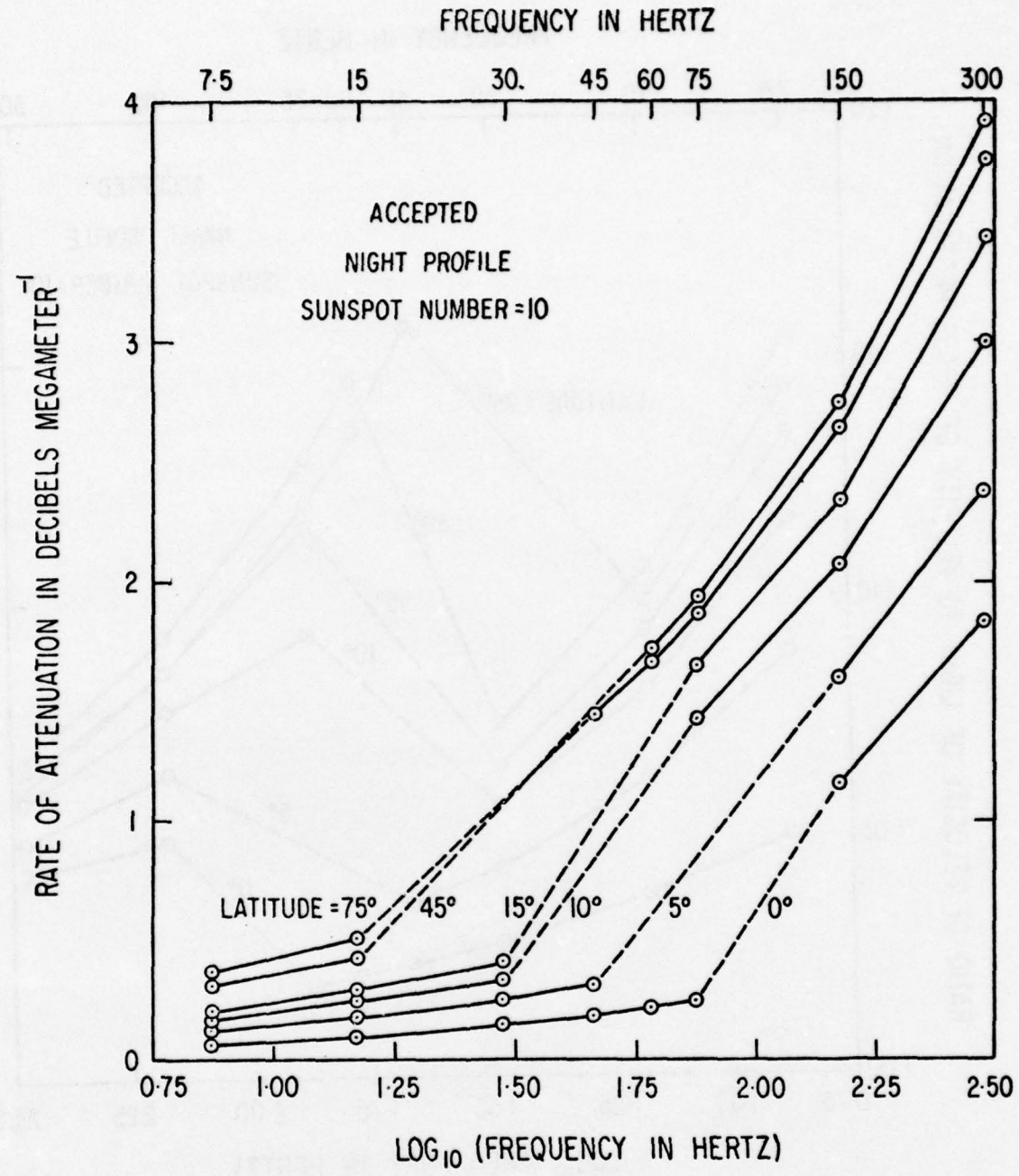

Figure 19b. Illustrating, for attenuation rate, the effect of penetrating the night-time sub-E region ledge of ionization as the frequency descends through the ELF band.

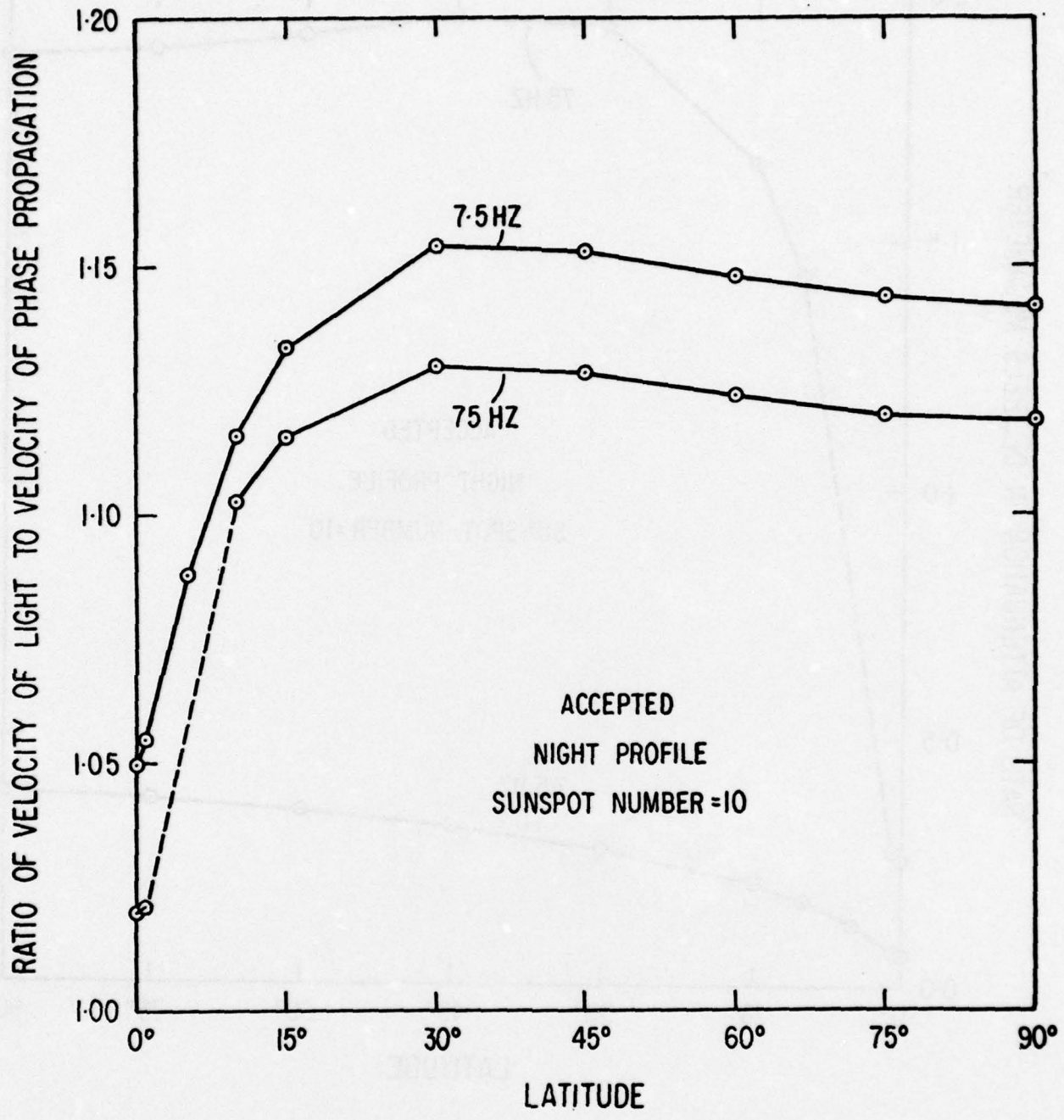

Figure 20a. Illustrating the variation of propagation velocity with latitude at night.

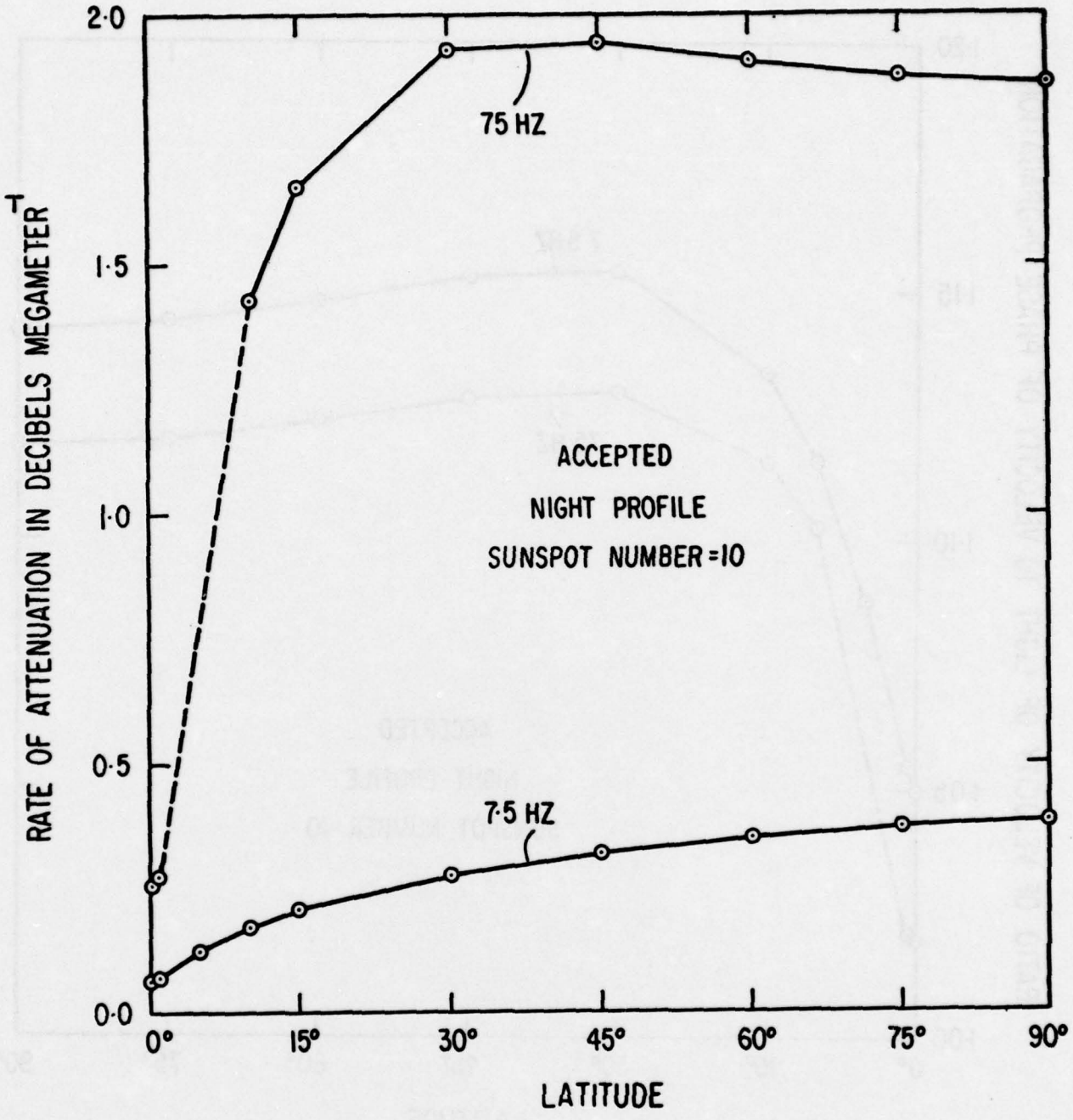

Figure 20b. Illustrating the variation of attenuation rate with latitude at night.

reconciled with the fact that, observationally, the values of c/v are of the order of 1.1 at 75 hz (Hughes and Gallenberger, 1974). It was for this reason that the ledge of ionization was added to the underside of the E region in Figure 6. The reflecting stratum then transfers from the main E region above 90 km to the ledge below 90 km as indicated by the broken sections of the plots in Figures 19a and b. These broken sections should be replaced by double S bends (one for the X wave and one for the O wave) that can only be delineated with a theory more elaborate than that developed in paper 1.

In Figures 20a and b reflexion is from the main E region above 90 km at 7.5 hz for all latitudes. At 75 hz, however, reflexion is predominantly from the ledge below 90 km except at low latitudes.

8. Diurnal variation of ELF propagation

Based on calculations of the type described in the two preceding sections the complete diurnal variation of ELF propagation in the earth-ionosphere transmission line can, in principle, be described. For a frequency of 75 hz results are shown in Table 5 for equinoctial conditions at an epoch when the sunspot number is 10. The upper numbers are values of c/v and the lower numbers are values of the total ionospheric rate of attenuation in db Mm^{-1}.

Reflexion is from the main E region at the equator but it transfers to the D region (day) or to the ledge (night) at higher latitudes. At local times of 0800 and 1600 hours this transfer is still in progress at a latitude of 15° and no numbers have been recorded. In Table 5 there is no variation

Table 5

Diurnal variation of c/v and attenuation (db Mm^{-1})

at 75 hz

(equinox, sunspot number = 10)

Latitude	Local time			
	Night	0800 1600	1000 1400	1200 noon
0^{o}	1.02	1.01	1.01	1.01
	0.26	0.13	0.12	0.12
15^{o}	1.12	--	1.09	1.09
	1.66	--	1.21	1.19
30^{o}	1.13	1.14	1.12	1.12
	1.93	1.83	1.64	1.60
45^{o}	1.13	1.17	1.15	1.15
	1.94	2.27	2.02	1.97
60^{o}	1.12	1.20	1.18	1.18
	1.90	2.72	2.41	2.34
75^{o}	1.12	1.25	1.22	1.21
	1.87	3.31	2.94	2.85

during the night-time by virtue of the ionospheric model in use (Figure 6). Some variation does occur during the day-time, but the main changes occur near sunrise and sunset.

9. Effect on ELF propagation of enhanced ionization in the lower ionsophere

Let us consider first a polar cap absorption event, and let us focus attention on a latitude of 75°. Let us assume that profiles 1, 2 and 3 in Figures 7 and 9 (day) and in Figures 8 and 10 (night) constitute various degrees of disturbance in the lower ionosphere, with the profiles marked 0 representing quiet conditions. Table 6 then shows the effect of these various degrees of disturbance on c/v (upper number) and on the attenuation rate in db Mm^{-1} (lower number) at frequencies of 7.5, 45 and 75 hz.

Under quiet day-time conditions, reflexion is from the E region at 7.5 hz and from the D region at 75 hz, while reflecting strata in both regions are important at 45 hz. Under quiet night-time conditions reflexion is from the main E region above 90 km at 7.5 hz but from the ledge below 90 km at 45 hz and 75 hz. For all the degrees of disturbance shown, however, reflexion is from the D region during the day-time and from the sub-E region ledge during the night-time. In going from quiet conditions to disturbance 1 conditions it is possible for an increase in the attenuation rate to occur, for example, for 7.5 hz during the day-time. When this happens it is in association with a transfer of reflexion to a lower level. When once reflexion from the D region (day) or the sub-E region ledge (night) has been established, the bigger the disturbance becomes the less is the rate of attenuation and the nearer is the velocity of propagation to c.

Table 6

Effect on c/v and attenuation (db Mm^{-1}) of enhanced ionization below the E region in polar regions (latitude = 75^{o})

Frequency (hertz)	Day profiles (Figs. 7 and 9)				Night profiles (Figs. 8 and 10)			
	0	1	2	3	0	1	2	3
7.5	1.05	1.21	1.09	1.05	1.14	1.12	1.04	1.02
	0.21	0.31	0.14	0.11	0.37	0.25	0.17	0.17
45	--	1.11	1.06	1.03	1.16	1.05	1.02	1.01
	--	0.84	0.47	0.32	1.45	0.56	0.32	0.26
75	1.21	1.09	1.05	1.03	1.12	1.04	1.02	1.01
	2.85	1.19	0.68	0.46	1.87	0.72	0.40	0.31

Let us now consider a sudden ionospheric disturbance that occurs at mid-day at the equinox and that causes an increase of a power of ten in the ionization of the day-time D region. We take the disturbed and undisturbed profiles of electron density for a solar zenith angle of 75° to be those marked 1 and 0 in Figure 7, and from them we deduce the profiles of electron density for other zenith angles χ on the assumption that the electron density is proportional to $\cos^{1/2}\chi$. For the negative ions we use the corresponding profiles 1 and 0 in Figure 9. The resulting variations of c/v and attenuation rate with latitude at midday are shown in Figures 21a and b for a frequency of 7.5 hz and in Figures 22a and b for a frequency of 75 hz.

With the unenhanced D region, reflexion at 7.5 hz *is from the* E region at all latitudes. With the enhanced D region, however, reflexion at 7.5 hz is from the D region except close to the equator. Except close to the equator, reflexion at 75 hz is from the D region when this region is unenhanced. The effect of enhancement is to establish reflexion from the D region for 75 hz at all latitudes including the equator. Examination of Figures 21a, 21b, 22a and 22b shows that, when enhancement of the D region results in reflexion being transferred from the E region to the D region, the values of c/v and of the attenuation rate are increased. On the other hand, when reflexion is already predominantly from the D region before enhancement, the effect of enhancement is to reduce the values of c/v and of the attenuation rate.

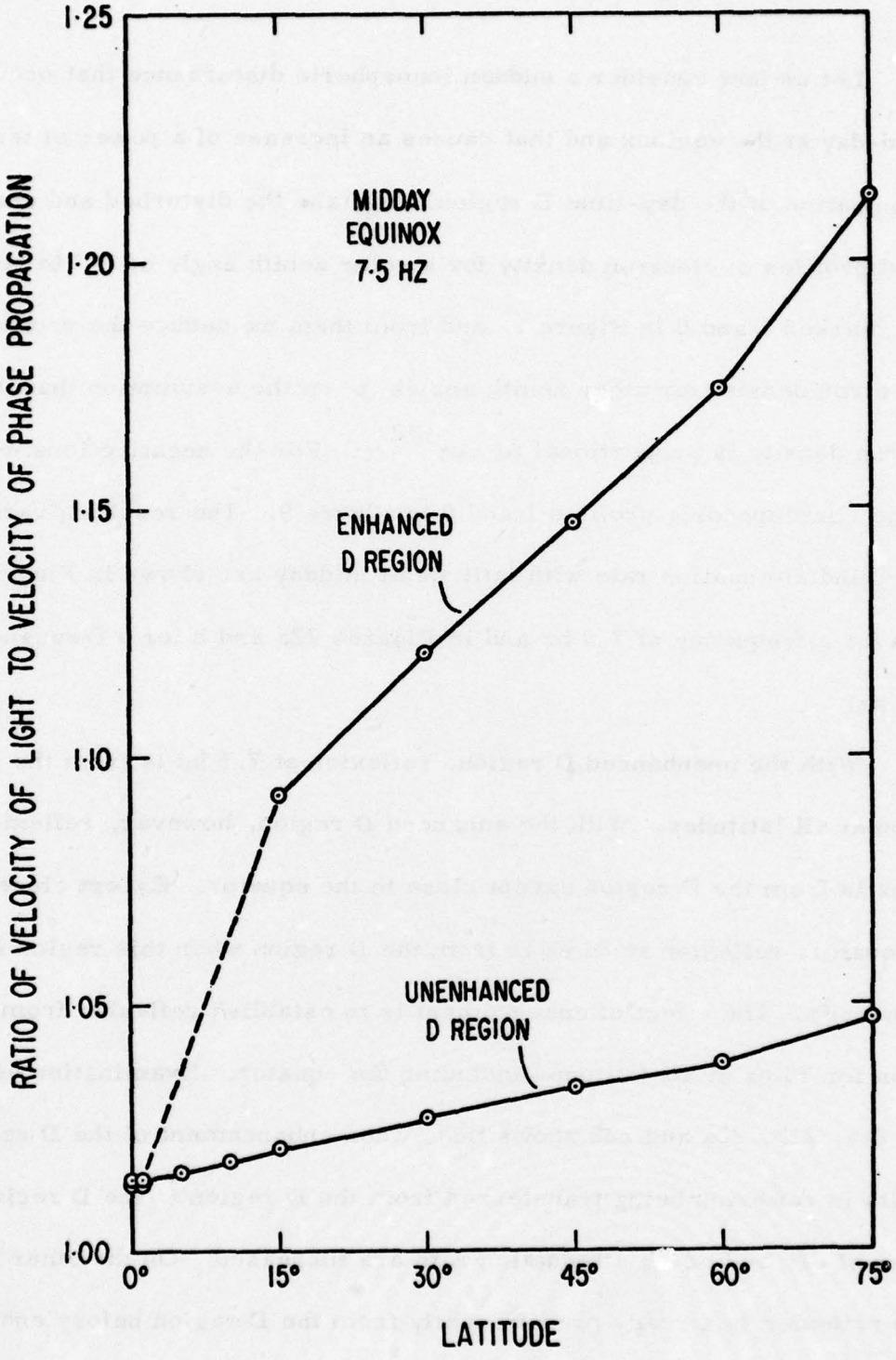

Figure 21a. Illustrating the effect on propagation velocity at 7.5 hz of increasing the ionization in the day-time D region by a factor of ten.

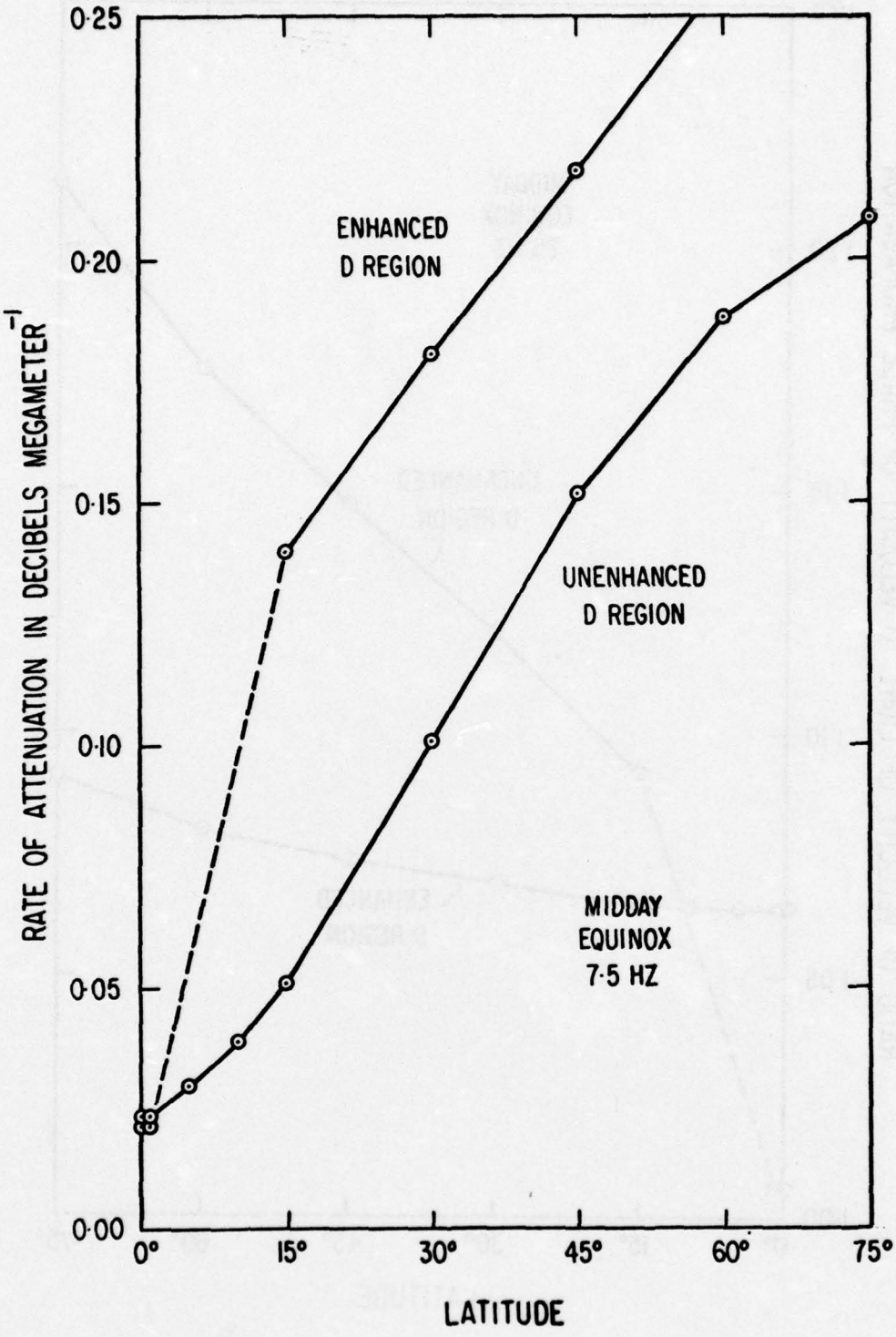

Figure 21b. Illustrating the effect on attenuation rate at 7.5 hz of increasing the ionization in the day-time D region by a factor of ten.

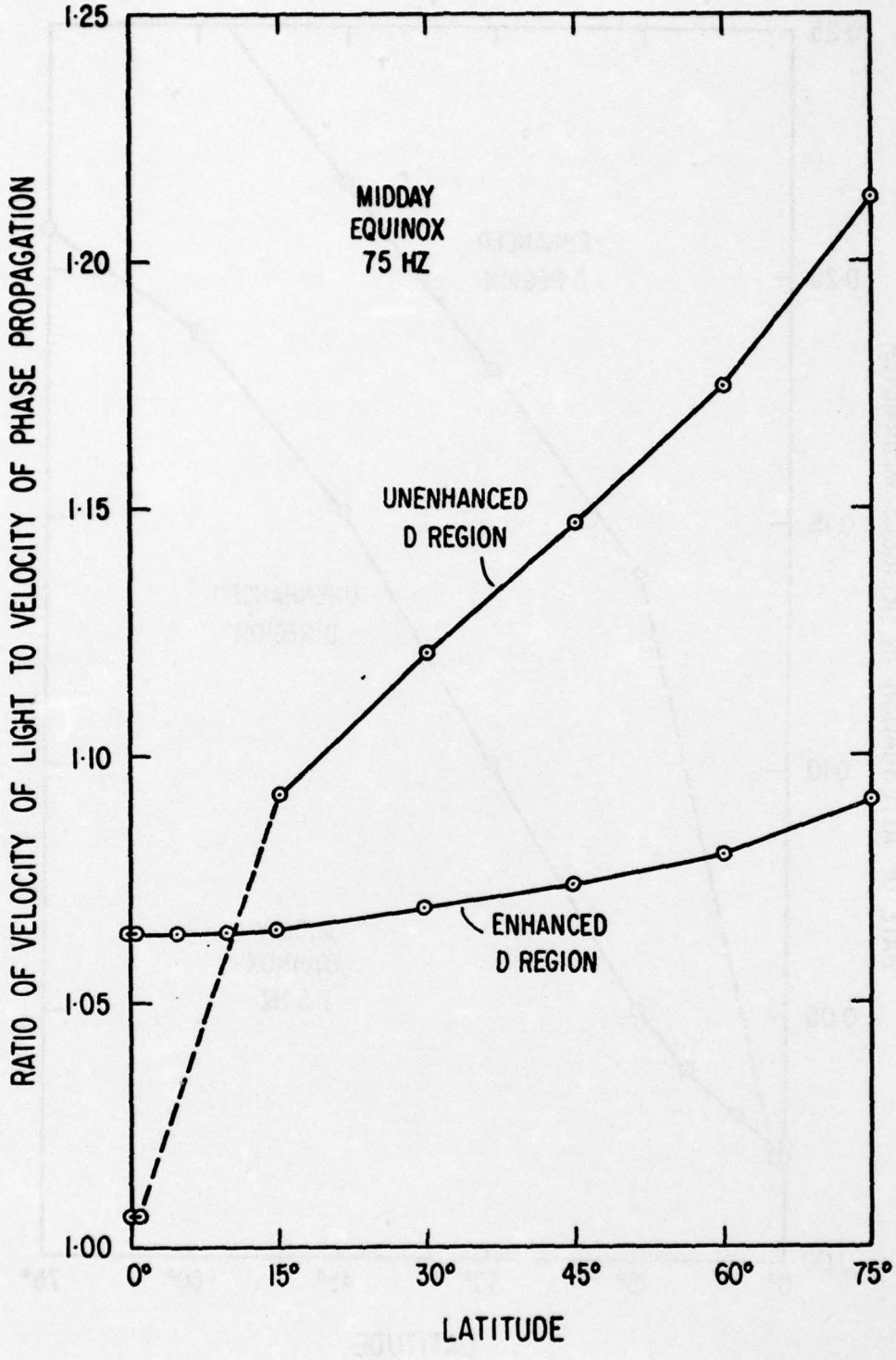

Figure 22a. Illustrating the effect on propagation velocity at 75 hz of increasing the ionization in the day-time D region by a factor of ten.

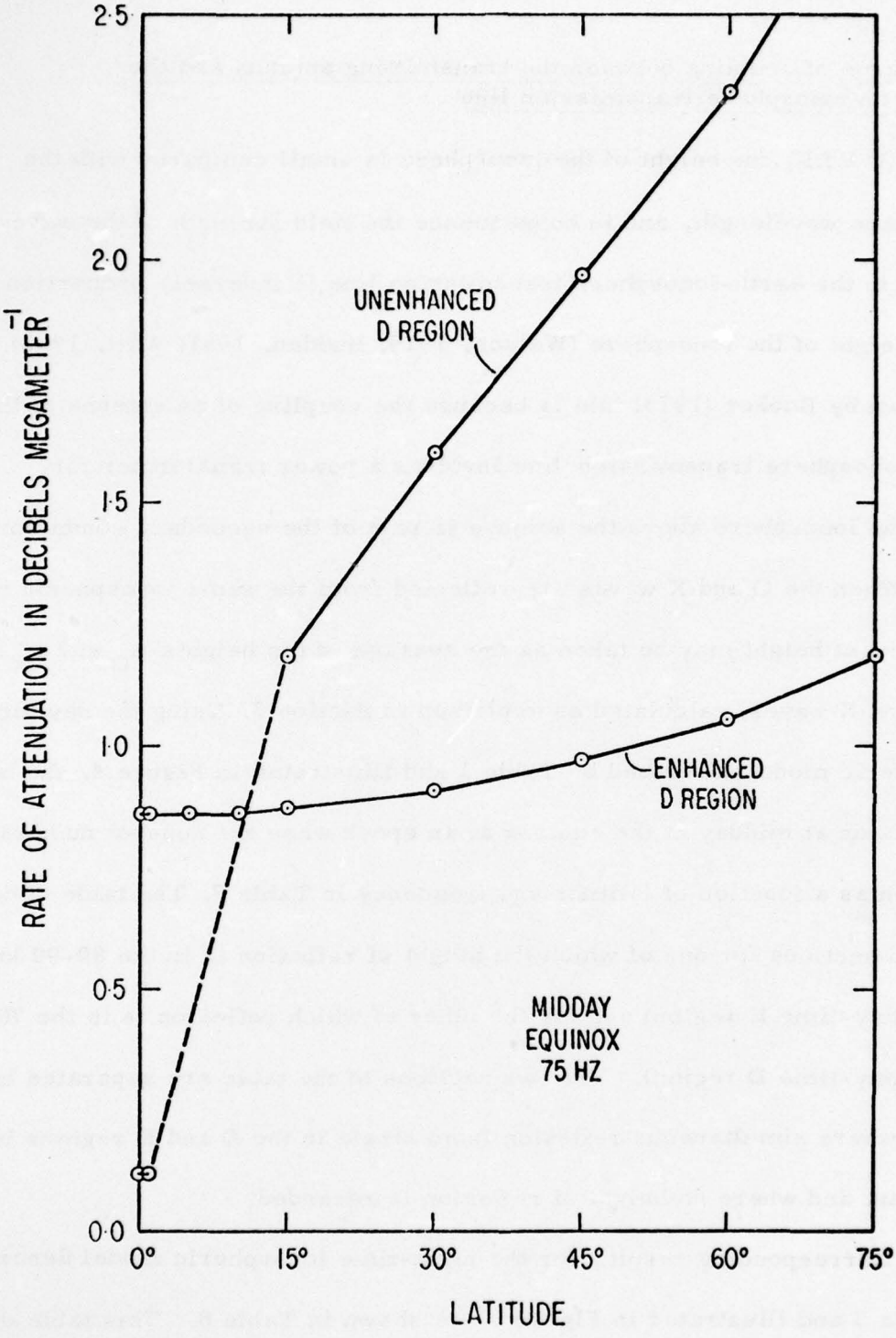

Figure 22b. Illustrating the effect on attenuation rate at 75hz of increasing the ionization in the day-time D region by a factor of ten.

10. Degree of coupling between the transmitting antenna and the earth-ionosphere transmission line

At ELF, the height of the ionosphere is small compared with the free-space wavelength, and in consequence the field strength of the wave excited in the earth-ionosphere transmission line is inversely proportional to the height of the ionosphere (Watson, 1919; Budden, 1961; Wait, 1962). As shown by Booker (1973) this is because the coupling of an antenna to the earth-ionosphere transmission line involves a power transformer for which the ionosphere above the antenna is part of the secondary conductor.

When the O and X waves are reflected from the same ionospheric region, the relevant height may be taken as the average of the heights z_O and z_X for the O and X waves, calculated as explained in Section 3. Using the day-time ionospheric model described by Table 1 and illustrated in Figure 4, the height of reflexion at midday at the equinox at an epoch when the sunspot number is 10 is shown as a function of latitude and frequency in Table 7. The table divides into two sections for one of which the height of reflexion is in the 80-90 km range (day-time E region) and for the other of which reflexion is in the 70-80 km range (day-time D region). The two sections of the table are separated by a band where simultaneous reflexion from strata in the D and E regions is important and where no height of reflexion is recorded.

Corresponding results for the night-time ionospheric model described by Table 3 and illustrated in Figure 6 are shown in Table 8. This table divides into two sections for one of which reflexion is from the main E region above 90 km and for the other of which reflexion is from the sub-E region ledge of ionization below 90 km.

Table 7

Height of reflexion in kilometers
(midday, equinox, sunspot number = 10)

Latitude	Frequency in hertz							
	7.5	15	30	45	60	75	150	300
0^{o}	85	85	85	84	84	84	76	73
15^{o}	85	85	85	--	--	78	76	73
30^{o}	86	86	--	78	78	77	75	72
45^{o}	86	86	--	78	77	76	74	72
60^{o}	86	86	--	78	77	76	74	72
75^{o}	86	86	--	--	78	77	75	73

Table 8

Height of reflexion in kilometers
(night, sunspot number = 10)

Latitude	Frequency in hertz							
	7.5	15	30	45	60	75	150	300
0^{o}	92	91	91	91	91	91	86	85
15^{o}	92	92	91	--	--	86	85	84
30^{o}	92	92	91	--	86	85	85	84
45^{o}	92	92	--	--	85	85	85	84
60^{o}	92	92	--	86	85	85	85	84
75^{o}	92	92	--	86	85	85	85	84
90^{o}	92	92	--	85	85	85	85	84

Table 9

Effect on height of reflexion (km) of enhanced ionization below the E region in polar regions (latitude = 75^{o})

Frequency (hertz)	Day profiles (Figs. 7 & 9)				Night profiles (Figs. 8 & 10)			
	0	1	2	3	0	1	2	3
7.5	86	77	70	65	92	85	83	82
45	--	71	66	62	86	84	82	80
75	77	70	65	61	85	83	82	80

For calculating the degree of coupling between an antenna and the earth-ionosphere transmission line, high accuracy for the height of the ionosphere is not necessary. However, we can see from Tables 7 and 8 that it is desirable to determine whether, for the frequency and location of the transmitter under consideration, the secondary conductor of the coupling transformer is associated with the E region or the D region under day-time conditions, and whether it is associated with the main E region above 90 km or the sub-E region ledge below 90 km under night-time conditions. For a disturbed ionosphere, somewhat greater care is necessary in selecting the ionospheric height relevant for calculating the excitation factor as shown in Table 9.

11. Discussion

In principle, it should be possible to adjust the profiles of electron density shown in Figures 4 and 6 so as to secure agreement between theory and observations. Observations are available of the bandwidth of the Schumann resonances (Balzer and Wagner, 1960; Madden and Thompson, 1965; Galejs, 1972; Jones, 1974), of the attenuation experienced over various propagation paths for a transmitter located in North Carolina and operated on frequencies of 78 and 156 hz (Ginsberg, 1974), for a transmitter located in Wisconsin and operated on frequencies of 45 hz and 75 hz (White and Willim, 1974; Bannister, 1974; Bannister, Williams, Katan and Ingram, 1974; Davis, 1974), and of the radiation from lightning flashes in the ELF band - the "slow trail" of "atmospherics" (Hughes and Theisen, 1970; Hughes

and Gallenberger, 1974; Jones, 1974). All of these observational techniques are challenging, and high accuracy is difficult to achieve. Comprehensive observations over the globe under a wide range of ionospheric conditions have not been made, and simultaneous observations of ionospheric profiles by other methods (such as rockets) are not usually available.

Nevertheless, sufficient observations have been made with sufficient accuracy to detect discrepancies. Attention has already been drawn in Section 5 to the fact that the night-time profiles being proposed for the International Reference Ionosphere appear to be inconsistent with observations of the Schumann resonance, and an alternative model of the night-time ionosphere was tentatively devised in Figure 6. Even with this modified model of the night-time ionosphere the calculated attenuation rates in the earth-ionosphere transmission line at frequencies of 75 hz and above are too high. The same is true for the model of the day-time ionosphere shown in Figure 4 even though this model is in reasonable agreement with what is being proposed for the International Reference Ionosphere.

There is, of course, no difficulty in adjusting the ionospheric profiles so as to improve the agreement with observations of the attenuation-rate in the earth-ionosphere transmission line. Waves of different frequencies in the ELF band are reflected at different ionospheric levels, and consequently the variation of electron density with height can be adjusted so as to accommodate the observed variation with frequency in the rate of attenuation. However, the wisdom of carrying out such an operation of profile adjustment at this time is in doubt.

It should be noted that it is not sufficient to adjust the ionospheric profiles to reproduce the correct variation of attenuation rate with frequency in the ELF band. It is necessary to fit observations in the entire radio spectrum. It is necessary to fit in situ observations. Even in the ELF band, it is necessary to reproduce the correct variation with frequency not only of the attenuation rate but also of the velocity of phase propagation. With some ELF observational techniques, velocity information is unfortunately not available. A desirable technique is one with which both the velocity and the rate of attenuation can be estimated as functions of frequency throughout the ELF band in various parts of the world under various ionospheric conditions, and that can be used in conjunction with simultaneous in situ observations of the ionospheric profiles themselves.

It is premature to attempt detailed adjustment of ionospheric profiles to fit even the limited ELF observations currently available before steps have been taken further to develop the theory presented in paper 1. Figures 15a and b reveal the fact that, over the frequency range 20-60 hz in middle and high latitudes during the day-time, simultaneous reflexion from strata in the D and E regions is a major phenomenon and that, as the frequency drops from about 60 hz to about 20 hz, penetration of the D region takes place, first for the O wave and then for the X wave. Moreover, Figures 19a and b show that a similar phenomenon is likely to take place at night. A theory capable of describing this penetration phenomenon conveniently should be developed so as to facilitate quantitative comparison with observations made at frequencies in the range 20-60 hz.

At frequencies from about 75 hz upwards, day-time reflexion in middle and high latitudes is primarily from the D region. Even so, it is doubtful if the theory developed in paper 1 is good enough for detailed adjustment of ionospheric profiles to fit observations of propagation velocity and attenuation rate in the earth-ionosphere transmission line in the frequency range 75-300 Hz. The theory developed in paper 1 is probably adequate in circumstances when only one reflecting stratum is important, for example, at 7.5 hz. But the theory may not be adequate in the frequency range 75-300 hz for the following reason. The X wave transmitted above the reflecting stratum in the D region is the whistler wave, except close to the equator. This wave suffers some attenuation in the D region but it has not become negligible in the E region. As shown in Figure 14, further reflexion will come into play for the X wave in the E region, and the resulting reflected whistler wave is unlikely to be completely negligible at the level of the primary reflecting stratum in the D region. Even though day-time reflexion is predominantly from the D region in the frequency range 75-300 hz at middle and high latitudes, nevertheless reflexion of the transmitted whistler wave from the E region will modify somewhat the mode calculation for the earth-ionosphere transmission line. This modification is expected to reduce somewhat the rate of attenuation and increase somewhat the value of c/v.

Simultaneous reflexion from strata in the D and E regions is certainly a major phenomenon during the day-time at middle and high latitudes in the frequency range 20-60 hz. This phenomenon is unlikely to become completely negligible at higher frequencies and must be taken into account before detailed agreement between theory and observation can be expected. On the other hand, when such a theory has been developed in convenient form, and when the profiles for the International Reference Ionosphere are sufficiently comprehensive and reliable, there seems to be no reason why useful propagation curves for ELF communications should not be prepared covering most ionospheric conditions.

While the absolute values of the propagation velocities and attenuation rates shown in the diagrams and tables of this paper will require modification for the reasons just stated, it is likely that most of the trends will be preserved. In particular, it should be noted that, for a given frequency, attenuation rates at low latitudes are less than they are at high latitudes, especially during the day-time. It follows that, for the same transmitter arrangements (including the same site geology), the latitude at which an ELF communications transmitter is located has an important bearing on the degree of world-wide coverage that it achieves.

12. Night-time variability of ELF signals from the Wisconsin Test Facility

It has been shown by Bannister, Williams, Katan and Ingram (1976) that, during the night-time but not during the day-time, there are appreciable variations in the signals received in Connecticut from a transmitter in Wisconsin operating on a frequency of about 75 hz. Similar results have been obtained at other receiving sites. Similar results have been obtained at a frequency of about 45 hz (Bannister and Williams, 1975) but on different occasions. Decreases of field-strength up to 5 decibels are reported. It has been hypothesized that these lowered night-time field-strengths are caused by variations in the flux of electrons precipitating in the ionosphere (White, 1972), and this suggestion has been followed up by Imhof, Larson, Reagan and Gaines (1976).

Table 6 shows that a night-time decrease in field-strength cannot be due to a large increase in the ionization density near the base of the ionosphere such as is associated with a polar cap absorption event. Neither can it be due to a large decrease in ionization density such as might correspond to virtual elimination of the sub-E region ledge of ionization in Figure 6. This would cause the plots to the left of the broken sections in Figures 19a and b to extend to higher frequencies without modification, and consequently would improve transmission.

It was found in Section 9 that, when an enhancement of the day-time D region results in reflexion being transferred from the E region to the

D region, the rate of attenuation in the earth-ionosphere transmission line is increased but that, when reflexion is already predominantly from the D region beforehand, enhancement reduces the rate of attenuation. This phenomenon is illustrated by a comparison of Figures 21b and 22b; it is also illustrated in the left half of Table 6. A similar phenomenon can occur at night in association with the sub-E region ledge of ionization, and can be made to appear in the right half of Table 6 by suitable selection of ledge profiles.

In Figure 6 the bottom of the sub-E region ledge of ionization was arbitrarily taken at about 80 km. Moreover, the ionization density associated with the ledge was arbitrarily taken to be about the same as that associated with the D region during the day-time (Figure 4). In fact, the parameters associated with such a sub-E region ledge are largely unknown and are available for adjustment. Reducing the ionization density of the ledge would cause displacement towards higher frequencies in Figures 19a and b of the broken sections of the plots that have to be replaced by double S bends to allow for penetration of the ledge by the O and X waves in succession.

The simple explanation, therefore, of the night-time variability of the signals from the Wisconsin transmitter is in terms of variability in the penetration frequencies of the sub-E region ledge for the O and X waves. This requires some variability in the ionization density associated with the ledge, but nothing resembling the increases associated with polar cap absorption events.

It is likely that, under quiet ionospheric conditions, a sub-E region ledge of ionization exists at night, but with an ionization density and a thickness somewhat less than those shown in Figure 6. Reflexion at 75 hz under the conditions of the Wisconsin experiments was principally from the main E region on quiet nights. A small increase in the ionization density of the ledge caused the primary reflecting stratum at 75 hz to drop to the ledge, with an accompanying increase in the attenuation rate at 75 hz only partially offset by an increase in the degree of coupling of the transmitting antenna to the earth-ionosphere transmission line. A somewhat larger increase in the ionization density of the ledge caused the primary reflecting stratum at 45 hz also to drop to the ledge, with an accompanying increase in the attenuation rate at 45 hz. A further large increase in ionization density at the base of the night-time ionosphere would have caused a substantial decrease in the rate of attenuation, but in fact the ionosphere returned to normal without this happening.

Bibliography

Balser, M., and Wagner, C. 1962a Diurnal power variations of the earth-ionosphere cavity modes and their relationship to world-wide thunderstorm activity, Journal of Geophysical Research 67, 619-625.

Balser, M., and Wagner, C. 1962b On frequency variations of the earth-ionosphere cavity modes, Journal of Geophysical Research 67, 4081-4083.

Banks, P. M., and Kockarts, G. 1973 Aeronomy, Academic Press, New York.

Bannister, P. R. 1974 Far-field extremely low frequency propagation measurements 1970-1972, IEEE Transactions on Communications 22, 468-474.

Bannister, P. R., Williams, F. J., Katan, J. R., and Ingram, R. F. 1974 Night-time variations of extremely low frequency signal strengths in Connecticut, IEEE Transactions on Communications 22, 474-476.

Bannister, P. R., and Williams, F. J. 1975 Naval Underwater Systems Center, Technical Report 4927.

Barr, R. 1972 Some new features of ELF attenuation, Journal of Atmospheric and Terrestrial Physics 34, 411-420.

Berry, L. A., and Davis, R. M. 1976 A statistical model of the lower atmosphere, U. S. Defense Communications Agency, Report C600-TP-76-2.

Booker, H. G.	1973	The ionosphere as the secondary conductor of a transformer at ELF, Radio Science 8, 757-762.
Booker, H. G.	1977	Fitting of multi-region ionospheric profiles of electron density by a single analytic function of height, to be submitted for publication.
Booker, H. G., and Lefeuvre, F.	1977	The relation between ionospheric profiles and ELF propagation in the earth-ionosphere transmission line (1) theory, to be submitted for publication.
Budden, K. G.	1961a	Radio waves in the ionosphere, Cambridge University Press, Cambridge
Budden, K. G.	1961b	The wave-guide mode theory of wave-propagation, Logos Press, London.
Chapman, F. W., and Jones, D. L.	1964	Observations of earth-ionosphere cavity resonances and their interpretation in terms of a two-layer ionospheric model, Radio Science Journal of Research of the National Bureau of Standards 68D, 1177-1185.
Davis, J. R.	1974	The influence of certain ionospheric phenomena on extremely low frequency propagation, IEEE Transaction on Communications 22, 484-492.
Galejs, J.	1972	Terrestrial propagation of long electromagnetic waves, Pergamon Press, New York.

Ginzberg, L. H.	1974	Extremely low frequency propagation measurements along a 4900 km path, IEEE Transactions on Communications 22, 452-457.
Hughes, H. G., and Gallenberger, R. J.	1974	Propagation of extremely low frequency atmospherics over a mixed day-night path, Journal of Atmospheric and Terrestrial Physics 36, 1643-1661.
Hughes, H. G. and Theisen, J. F.	1970	Diurnal variations of the apparent attenuations of ELF atmospherics over two different propagation paths, Journal of Geophysical Research 75, 2795-2801.
Imhof, N. L., Larson, T. R., Reagan, J. B., and Gaines, E. E.	1976	Analysis of satellite data on precipitating particles in coordination with ELF propagation anomalies, Lockheed Palo Alto Research Laboratory Report LMSC-D502063.
Jones, D. L.	1967	Schumann resonances and ELF propagation for inhomogeneous isotropic ionospheric profiles, Journal of Atmospheric and Terrestrial Physics 29, 1037-1044.
Jones, D. L.	1974	Extremely low frequency ionospheric radio propagation studies using natural sources, IEEE Transactions on Communications 22, 477-484.
Large, D. B., and Wait, J. R.	1968	Theory of electromagnetic coupling in the earth-ionosphere cavity, Journal of Geophysical Research 73, 4335-4362.
Madden, T., and Thompson, W.	1965	Low frequency electromagnetic oscillations of the earth-ionosphere cavity, Reviews of Geophysics 3, 211-253.

Mechtly, E. A., and Smith, L. G.	1968	Seasonal variation of the lower ionosphere at Wallops Island during the IQSY, Journal of Atmospheric and Terrestrial Physics 30, 1555-1561.
Mechtly, E. A., Rao Mukunda, M., Skaperdas, D. O., and Smith, L. G.	1969	Latitude variation of the lower ionosphere, Radio Science 4, 517-520.
Mechtly, E. A., and Smith, L. G.	1970	Changes of lower ionosphere electron densities with solar zenith angle, Radio Science 5, 1407-1412.
Mechtly, E. A., Bowhill, S. A., and Smith, L. G.	1972	Changes of lower ionosphere electron concentrations with solar activity, Journal of Atmospheric and Terrestrial Physics 34, 1899-1907.
Mechtly, E. A., and Bilitza, D.	1974	Models of D region density profiles, Institüt für physikalishe Weltraumforschung, Internal report.
Morfi . G.	1976	Determination of effective ionospheric electron density profiles for VLF LF propagation, U.S. Defense Communications Agency, Report C[illegible]50-TR-76-[illegible]
ert, F and pler, W.	1974	Propagation theory lower [illegible] Communications 2[illegible]
r K., Ramakrishnan S., and Bilitza, D.	1975	Preliminary reference electron and [illegible] tures proposed for Reference Ionosphere physikalishe Welt[illegible] Scientific Report [illegible]

Schumann, W. O. 1952a Über die strahlunglosen Eigenschwingungen einer leitenden Kugel, die von einer Luftschicht und einer Ionospharenhulle ungenden ist, Z. Naturforsch. 7A, 149-154.

Schumann, W. O. 1952b Über die Dampfung der elektromagnetischen Eigenschwingungen des Systems Erde-Luft-Ionosphare, Z. Naturforsch. 7A, 250-252.

Schumann, W. O. 1952c Über die Ausbrectung sehr langer elektrischer Wellen um die Erde und die Signale des Blitzes, Nuovo Cimento 9, 1116-1138.

Schumann, W. O., and König, H. 1954 Über die Beobactung von Atmospherics bie geringsten Frequenzen, Naturwiss. 41, 183-184.

Schumann, W. O. 1957 Über elektrische Eigenschwingungen des Hohlraumes Erde-Luft-Atmosphare, erregt durch Blitzenladungen, Z. Angew. Phys. 9, 373-378.

Soboleva

Wait, J. R. 1958 An extension to the mode theory of VLF ionospheric propagation, Journal of Geophysical Research 63, 125-135.

Wait, J. R.	1962	Electromagnetic waves in stratified media, Macmillan, New York.
Watson, G. N.	1919	The transmission of electric waves round the earth, Proceedings of the Royal Society, A95, 546-563.
White, D. P.	1972	ELF propagation measurements (phase III - Fall 1971), MIT Lincoln Laboratory, Technical Note 1972-21.
White, D. P., and Willim, D. K.	1974	Propagation measurements in the extremely low frequency band, IEEE Transactions on Communications 22, 457-467.

Appendix C

Method of describing profiles analytically

30 November 1976

Fitting of multi-region ionospheric profiles of electron density by a single analytic function of height

by

Henry G. Booker
Professor of Applied Physics
University of California, San Diego*

Abstract

A single analytic function of height is devised that has the flexibility required to represent simultaneously the principal features of the D, E, F_1 and F_2 regions of the ionosphere. Such a function, free of mathematical singularities, is essential for obtaining satisfactory wave-solutions to ionospheric problems using methods more exact than the phase-integral (WKB) approximation. The method is applicable to profiles of atmospheric parameters besides electron density.

---

*Supported by the U.S. Office of Naval Research under Contract N00014-75-C-0959.

1. Introduction.

The need for standard profiles of electron density and of other ionospheric parameters has been recognized for some time. A committee of URSI and COSPAR is currently at work preparing such profiles, and a preliminary report has been issued (Rawer, Ramakrishnan and Bilitza, 1975). The present author was recently interested in using the proposed profiles for a problem in radio wave propagation that required a treatment more precise than the phase-integral (or WKB) approximation. Difficulty was encountered with the RRB profiles on account of the discontinuities of slope that they contain.

The fact that ionospheric profiles with discontinuous derivatives give trouble in handling "exact" wave-solutions was first encountered by Hartree (1929). Discontinuities in derivatives cause spurious partial reflections, and if more than one level of reflection is involved, spurious interference phenomena are introduced. These simultaneously complicate the calculations and lead to effects that usually have to be disregarded for a realistic ionosphere. Exact wave-solutions are hardly worth calculating for any profile that contains discontinuities, even discontinuities in low order derivatives; such wave-solutions are inexact no matter how much mathematical exactness is lavished on their development. Profiles used for exact wave-solutions should always be analytic functions of height.

While this has been known for a long time, the practical difficulty has been to think of a reasonable analytic function of height that has the flexibility necessary to represent simultaneously the principal features of the D, E, F_1 and F_2 regions. It is almost certainly for this reason that Rawer, Ramakrishnan and Bilitza chose to fit together several different analytic functions to form a composite profile having discontinuities of slope. Nevertheless such profiles are inconvenient and undesirable for discussion of many wave propagation problems.

It is the objective of this paper to devise a single analytic function of height that possesses the necessary flexibility to represent the entire profile

of electron density in the ionosphere from the bottom side of the D region to the top side of the F_2 region. The satisfaction of this long-standing need is far simpler than has hitherto been supposed. Different sections of the overall profile may be initially described by different functions, and these functions may then be strung together into a single analytical function of height by using exponential functions to fade one profile gradually out and fade the next profile gradually in. Almost any functions may be used to describe the individual sections initially. However, because of the exponential character of many atmospheric processes, it is convenient, and for a number of purposes desirable, also to use the exponential function to describe the individual sections of the overall profile. In this way we arrive at the following procedure.

2. Method

If the electron density N varies exponentially with height z and if the scale height is H, then

$$\frac{1}{N}\frac{dN}{dz} = H^{-1} \tag{1}$$

Let us consider initially a skeleton profile in which N varies exponentially with z, but the scale height changes from H_1 to H_2 at a height a. If this happens abruptly, then

$$\begin{cases} \frac{1}{N}\frac{dN}{dz} = H_1^{-1}, & z < a \qquad (2) \\ \frac{1}{N}\frac{dN}{dz} = H_2^{-1}, & z > a \qquad (3) \end{cases}$$

A profile involving this behavior is undesirable because of the discontinuity in slope at z = a. Let us therefore arrange for the logarithmic derivative on the left hand sides of Equations (2) and (3) to change continuously from H_1^{-1} to H_2^{-1} as z increases through a, and to do so without involving discontinuities in higher

order derivatives. This may be achieved by writing

$$\frac{1}{N}\frac{dN}{dz} = H_1^{-1} + \frac{H_2^{-1} - H_1^{-1}}{1 + \exp\{-(z-a)/h\}} \tag{4}$$

where h is a scale that controls the interval of height over which the transition in slope takes place.

Equation (4) reduces to Equation (2) if z is appreciably less than a - h and to Equation (3) if z is apprecibly greater than a + h. The bulk of the transition in the logarithmic derivative from H_1^{-1} to H_2^{-1} takes place between the levels a - h and a + h, and the transition is smooth in all derivatives. The quantity h may be described as the smoothing scale appropriate to the transition at the level z = a.

This idea may be extended to incorporate any number of transition levels $z_1, z_2, \ldots, z_m$, with different smoothing scales $h_1, h_2, \ldots, h_m$ at the various transitions. We then start with a skeleton profile such that

$$\left.\begin{aligned}
&\frac{1}{N}\frac{dN}{dz} = H_{01}^{-1}, && z < z_1 \\
&\frac{1}{N}\frac{dN}{dz} = H_{12}^{-1}, && z_1 < z < z_2 \\
&\cdots\cdots\cdots\cdots\cdots\cdots && \\
&\frac{1}{N}\frac{dN}{dz} = H_{m-1,\,m}^{-1} && z_{m-1} < z < z_m \\
&\frac{1}{N}\frac{dN}{dz} = H_{m,\,m+1}^{-1} && z > z_m
\end{aligned}\right\} \tag{5}$$

where $H_{n,\,n+1}$ is the scale height of the skeleton profile in the height interval $z_n < z < z_{n+1}$. If we now apply smoothing scales $h_1, h_2, \ldots$ at the transition levels $z_1, z_2, \ldots$ respectively, we obtain

$$\frac{1}{N}\frac{dN}{dz} = H_{01}^{-1} + \sum_{n=1}^{m} \frac{H_{n,\,n+1}^{-1} - H_{n-1,\,n}^{-1}}{1 - \exp\{-(z-z_n)/h_n\}} \tag{6}$$

Integration with respect to z then gives

$$\ln \frac{N}{N_0} = H_{01}^{-1} (z - z_0) + \sum_{n=1}^{m} (H_{n,\,n+1}^{-1} - H_{n-1,\,n}^{-1}) h_n \ln \frac{1 + \exp\{(z-z_n)/h_n\}}{1 + \exp\{(z_0-z_n)/h_n\}} \quad (7)$$

where N_0 is the electron density at a reference height z_0. Equation (7) may also be written

$$N = N_0 \exp\left[\frac{z-z_0}{H_{01}} + \sum_{n=1}^{m}\left(\frac{h_n}{H_{n,\,n+1}} - \frac{h_n}{H_{n-1,\,n}}\right) \ln \frac{1 + \exp\{(z-z_n)/h_n\}}{1 + \exp\{(z_0-z_n)/h_n\}}\right] \quad (8)$$

The profile of electron density presented in Equation (8) is an analytic function of height at all levels. There are no discontinuities of N or of any of its derivatives. This analytic profile tends to the skelton profile shown in Equations (5) as the smoothing scales h_1, h_2, ... tend to zero. The character of the analytic profile in Equation (8) may be controlled by adjusting the following 3m + 2 parameters:

(i) the transition heights $z_1, z_2, \ldots, z_m$,

(ii) the scale-heights $H_{01}, H_{12}, \ldots, H_{m,m+1}$ of the skeleton profile for the height ranges $z < z_1, z_1 < z < z_2, \ldots, z > z_m$ respectively,

(iii) the smoothing scales $h_1, h_2, \ldots, h_m$ for the transition heights $z_1, z_2, \ldots, z_m$ respectively, and

(iv) either N_0 or z_0.

It is clear that Equation (8) constitutes a profile of electron density that possesses considerable flexibility and yet is a fully analytic function of height at all levels.

3. Application

We need to investigate whether the analytic profile of electron density presented in Equation (8) has adequate flexibility to represent practical ionospheric profiles without involving an unreasonably large number of adjustable parameters.

It will be convenient to draw profiles in a form that shows $\log_{10} N$ as a function of z. We therefore rewrite Equation (7) in the form

$$\log_{10} N = \log_{10} N_0 + A_{01}(z - z_0) + \sum_{n=1}^{m} (A_{n,\,n+1} - A_{n-1,\,n})\{f(z - z_n, B_n) - f(z_0 - z_n, B_n)\} \quad (9)$$

where

$$f(z, B) = B^{-1} \ln\{1 + \exp(Bz)\} \quad (10)$$

In Equation (9) the quantities $A_{01}, A_{12}, \ldots, A_{m,\,m+1}$ are the slopes of the skeleton profile of $\log_{10} N$ versus z in the height-ranges $z < z_1$, $z_1 < z < z_2$, $\ldots, z > z_m$ respectively, while $B_1, B_2, \ldots, B_m$ are the reciprocals of the smoothing scales $h_1, h_2, \ldots, h_m$ for the transition heights $z_1, z_2, \ldots, z_m$ respectively.

It may be noted that, as $z \to -\infty$, the function $f(z, B)$ tends to zero. On the other hand, as $z \to +\infty$, $f(z, B)$ behaves as z. For computational purposes it is convenient to rewrite Equation (10) as

$$f(z, B) = \begin{cases} B^{-1} \ln\{1 + \exp(Bz)\}, & z < 100B^{-1} \quad (11) \\ z, & z \geq 100B^{-1} \quad (12) \end{cases}$$

This avoids use in the computer of numbers larger than e^{100} while avoiding fractional errors larger than $(100\, e^{100})^{-1}$.

Figure 1 shows two skeleton profiles consisting of linear segments in a plot of $\log_{10} N$ versus z. Electron density is measured in m^{-3} and height in km. After smoothing in accordance with Equation (9), one curve is intended to reproduce an illustrative day-type profile of electron density and the other an illustrative night-type profile. Eight transition points have been used in Figure 1 for the day-type profile and six for the night-type profile. Hence m = 8 in Equation (9) for the day-type profile, and m = 6 for the night-type profile. Associated with each transition level, a pair of numbers are shown in brackets in Figure 1. These are the cartesian coordinates of the transition point, the first number being an assumed value of $\log_{10} N$ at the point and the second an assumed value of z. The number following the bracketed pair, and preceded by a $\pm$ sign, is the assumed

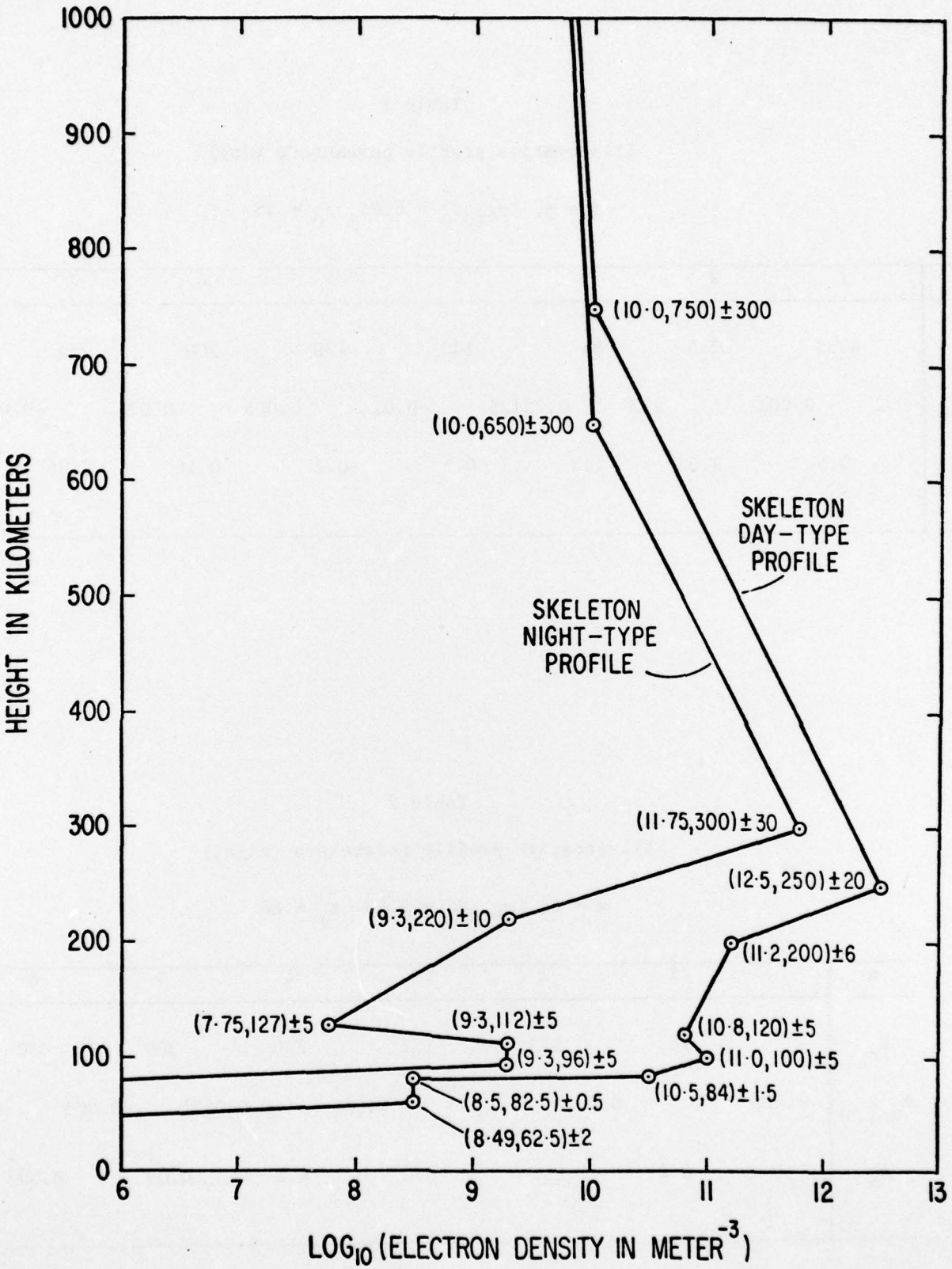

Figure 1: Skeleton profiles of electron density. Pairs of numbers in brackets are cartesian coordinates of a transition point. The number following the $\pm$ sign is the smoothing scale for the transition point in km.

Table 1

Illustrative profile parameters (day)

$m = 8$, $\log_{10} N_0 = 6.93$, $z_0 \approx 55$

n	1	2	3	4	5	6	7	8
z_n	62.5	82.5	84	100	120	200	250	750
$A_{n-1,n}$	0.2	0.001	1.3	0.03125	-0.01	0.005	0.026	-0.005	-0.0005
B_n	0.5	2.0	1.5	0.2	0.2	0.16	0.05	0.003

Table 2

Illustrative profile parameters (night)

$m = 6$, $\log_{10} N_0 = 5.53$, $z_0 = 80$

n	1	2	3	4	5	6
z_n	96	112	127	220	300	6[illegible]
$A_{n-1,n}$	0.225	0.0	-0.103	0.016	0.030625	-0.005	-0.0005
B_n	0.2	0.2	0.2	0.1	0.03	0.003

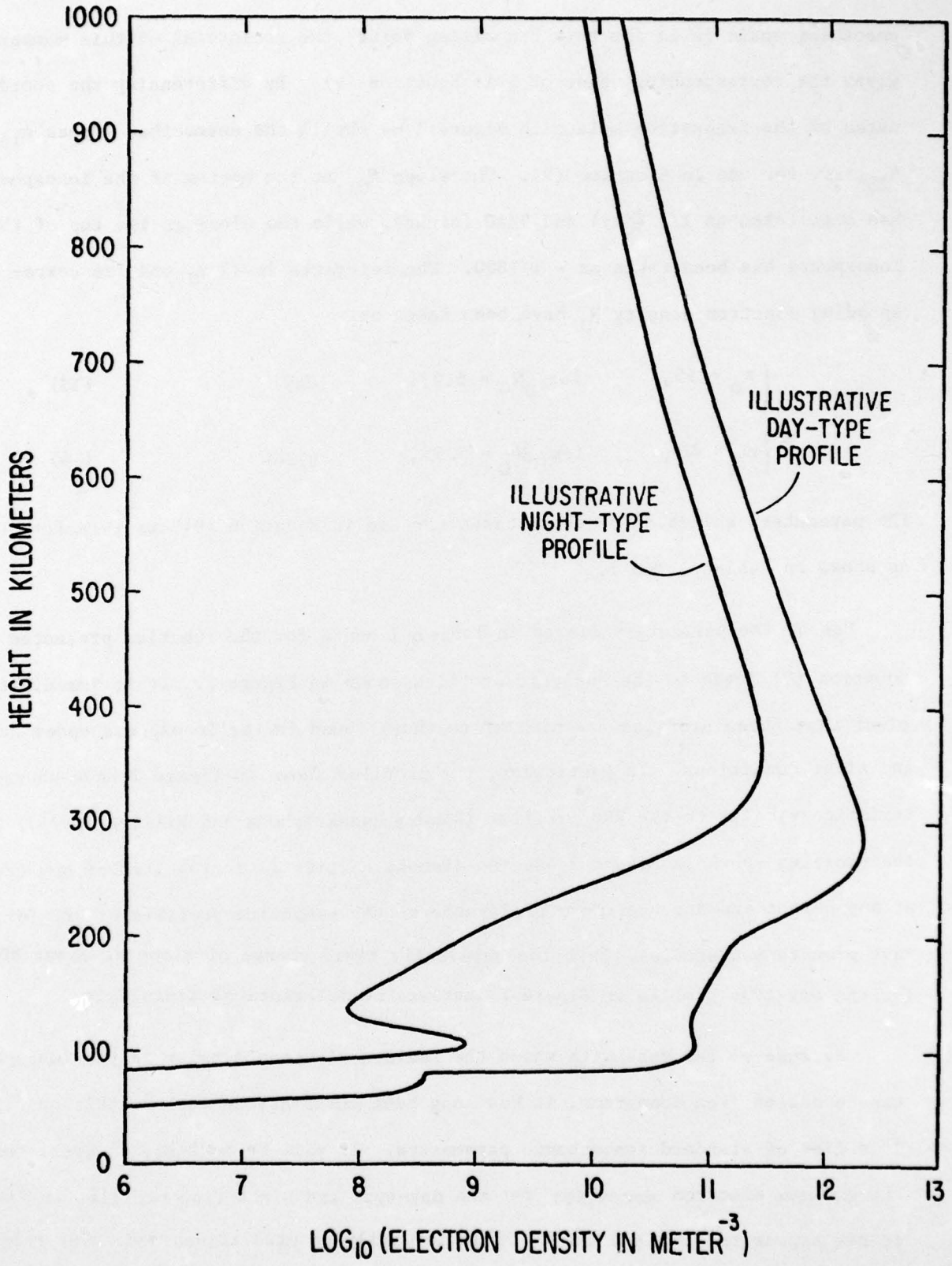

Figure 2: Analytic profiles of electron density derived from the skeleton profiles in Figure 1 in accordance with Equation (9) using the parameters listed in Tables 1 and 2.

smoothing scale in km for this transition point; the reciprocal of this number gives the corresponding value of B in Equation (9). By differencing the coordinates of the transition points in Figure 1 we obtain the unsmoothed slopes A_{12}, A_{23}, ... for use in Equation (9). The slope A_{01} at the bottom of the ionosphere has been taken as 1/5 (day) and 9/40 (night), while the slope at the top of the ionosphere has been taken as - 1/1800. The reference level z_0 and its corresponding electron density N_0 have been taken as:

$$\begin{cases} z_0 = 55, & \log_{10} N_0 = 6.93, \quad \text{day} \end{cases} \tag{13}$$

$$\begin{cases} z_0 = 80, & \log_{10} N_0 = 5.53, \quad \text{night} \end{cases} \tag{14}$$

The parameters selected on these bases for use in Equation (9) are therefore as shown in Tables 1 and 2.

Use of the parameters listed in Tables 1 and 2 for the function presented in Equation (9) leads to the analytic profiles shown in Figure 2. It is immediately clear that these profiles are similar to those found in the ionosphere under day and night conditions. In particular, the profiles shown in Figure 2 have characteristics similar to the RRB profiles (Rawer, Ramakrishnan and Bilitza, 1975). But the profiles shown in Figure 2 have no discontinuities in derivatives of any order at any height and are therefore preferable to the composite profiles of RRB for wave propagation studies. Even the physically rapid change of slope at about 80 km for the day-type profile in Figure 2 involves no mathematical singularity.

Because of the ease with which the maximum electron density in the ionosphere can be scaled from ionograms, it has long been customary to include this quantity in a list of standard ionospheric parameters. It will be noticed, however, that the maximum electron densities for the day-type and night-type profiles in Figure 2 do not appear in Tables 1 and 2. This is easily changed if desired. The reference height z_0 is at our disposal; we may choose z_0 as the height of maximum electron

density, and N_0 is then the value of the maximum electron density. If this is done, the values for N_0 and z_0 in Tables 1 and 2 are changed to:

$$\begin{cases} \log_{10} N_0 = 12.32, \quad z_0 = 287 \text{ km, day} & (15) \\ \log_{10} N_0 = 11.44, \quad z_0 = 364 \text{ km, night} & (16) \end{cases}$$

These changes in Tables 1 and 2 cause no changes in the profiles depicted in Figure 2.

Any method of fitting standard ionospheric profiles to the ionosphere must, in practice, be applied to actual observations of electron density as a function of height. For fitting the profile presented in Equation (9) to such observations the following procedure can be adopted:

(i) Present the observations in a diagram of $\log_{10} N$ versus z.

(ii) Use any convenient pair of corresponding values of $\log_{10} N$ and z for $\log_{10} N_0$ and z_0.

(iii) Approximate the relationship between $\log_{10} N$ and z with rectilinear segments as shown in Figure 1, using tangents near points of inflexion as far as possible.

(iv) Estimate visually the smoothing scales required at the various transition points.

(v) Substitute the resulting parameters into Equation (9), and exhibit the corresponding analytic profile on the cathode-ray screen of a computer.

(vi) Where necessary, readjust parameters by trial and error so as to make the profile on the screen match the observations.

By this procedure analytic profiles that constitute reasonable fits to given observational profiles can easily be derived.

4. Conclusion

It is recommended that any method adopted for specifying standard ionospheric profiles be based on the use of a single analytic function usable at all ionospheric heights rather than on a composite of several functions, one for each region or sub-region with discontinuities in derivatives at the junctions. Use of a single analytic function of height is desirable aeronomically and is

essential for properly deriving exact wave solutions to ionospheric problems. It also facilitates use of the concept of complex height, which simplifies a number of wave propagation problems.

In particular, the analytic function presented in Equation (9) has the necessary flexibility to represent a multi-region ionosphere without employing an unreasonably large number of parameters. When the profile of electron density employed in a wave propagation problem is described in this way, the solution may be quickly reprogrammed for a different profile merely by changing the values of some of the parameters listed in Tables 1 and 2.

Bibliography

Hartree, D.R.	1929	The propagation of electromagnetic waves in a stratified medium, Proc. Camb. Phil. Soc., 25, 97.
Rawer, K., Ramakrishnan, S., and Bilitza, D.	1975	Preliminary reference profiles for electron and ion densities and temperatures proposed for the International Reference Ionosphere, Institut für physikalishe Weltraumforschung, Scientific Report W.B.2.